OF COLLEGE ENGINEERING

VIRGINIA POLYTECHNIC INSTITUTE AND STATE UNIVERSITY

BLACKSBURG, VIRGINIA

(NASA-CR-176428) THERMODYNAMIC EVALUATION OF TRANSONIC COMPRESSOR ROTORS USING THE FINITE VOLUME APPROACH Annual Report, 20 Dec. 1984 - 19 Dec. 1985 (Virginia Polytechnic Inst. and State Univ.) 118 p
N86-16220
G3/07 05267
Unclas

Annual Report on NASA Grant No. NAG 3-593

Thermodynamic Evaluation of Transonic Compressor Rotors Using the Finite Volume Approach

for the period
12/20/84 - 12/19/85

by
John Moore
Professor of Mechanical Engineering
Principal Investigator

Stephen Nicholson
Instructor
and
Joan G. Moore
Research Associate

Grantee Institution -

NASA Lewis Research Center
21000 Brookpark Road
Cleveland, Ohio 44135

Turbomachinery Research Group

Report No. JM/85-11

Mechanical Engineering Department
Virginia Polytechnic Institute and State University
Blacksburg, Virginia 24061

Abstract

Summer research at NASA Lewis Research Center gave the opportunity to incorporate new control volumes in the Denton 3-D finite-volume time-marching code. For duct flows, the new control volumes require no transverse smoothing and this allows calculations with large transverse gradients in properties without significant numerical total pressure losses.

The summer research also pointed to possibilities for improving the Denton code to obtain better distributions of properties through shocks. Much better total pressure distributions through shocks are obtained when the interpolated effective pressure, needed to stabilize the solution procedure, is used to calculate the total pressure. This simple change largely eliminates the undershoot in total pressure downstream of a shock. Overshoots and undershoots in total pressure can then be further reduced by a factor of 10 by adopting the effective density method, developed at VPI&SU, rather than the effective pressure method. Use of a Mach number dependent interpolation scheme for pressure then removes the overshoot in static pressure downstream of a shock.

The stability of interpolation schemes used for the calculation of effective density is analyzed and a Mach number dependent scheme, the M&M formula, is developed. This formula combines the advantages of the correct perfect gas equation for subsonic flow with the stability of 2-point and 3-point interpolation schemes for supersonic flow.

DEVELOPMENT OF THE FINITE-VOLUME TIME MARCHING METHOD FOR IMPROVED SHOCK CAPTURING AND REDUCED NUMERICAL LOSSES

by

John Moore, Stephen Nicholson and Joan G. Moore

Part 1. Summer Work at NASA Lewis Research Center - Inviscid Flow Calculations Using the Denton Code.

Part 2. 1-D Stability Analysis of Density-Pressure Relations Used in the Computation of Transonic Flow.

Part 3. 1-D Computational Tests of Shock Capturing Using Pressure Interpolation Formulae to Calculate Effective Density.

CONTENTS: PART 1
SUMMER WORK AT NASA LEWIS RESEARCH CENTER
INVISCID FLOW CALCULATIONS USING THE DENTON CODE

PART 1

SUMMER WORK AT NASA LEWIS RESEARCH CENTER

INVISCID FLOW CALCULATIONS USING THE DENTON CODE

1.1 NEW CONTROL VOLUMES IN THREE DIMENSIONS

A new control volume has been introduced (1) which allows the calculation of transonic flow in ducts using the finite-volume method without the smoothing of flow properties that is usually needed(2). Previous work(1) using these new control volumes has been limited to two dimensions. The first part of the work at NASA Lewis this summer was to extend these new control volumes to three-dimensional flow calculations. This was thought important since the three-dimensional version of the Denton finite-volume code is the one typically used at NASA.

An example of a typical new three dimensional control volume is shown in Fig. 1. The locations of control volume boundaries are specified in the input data and the control volume surfaces are constructed from this information. Once the control volume boundaries are known then the grid points are placed in the middle of the upstream and downstream faces of the control volume. The fluxes through the transverse faces of the control volume needed for the continuity and momentum balances are determined from interpolated properties using the nodes adjacent to the face. Fig. 2 shows two adjacent control volumes of different sizes. The procedure for calculating the properties to

be used in calculating the fluxes on the common boundary(face I) can be shown in the following way. For face I, any property, X, is determined from the average of the property at points A and B, where the values of the properties X_A and X_B are determined by linearly interpolating between the values of the property at nodes 1 and 2, and between the values of the property at nodes 3 and 4, respectively.

Assuming that face II corresponds to a solid boundary, the values of a property at points C and D are determined by linear extrapolation using the values of the property at nodes 1 and 2, and 3 and 4 ; respectively. For the present calculations, only the pressure needs to be calculated at the solid boundaries since the fluxes of mass are set equal to zero through these solid boundaries.

Additional adjustments were made to NASA's finite volume code to allow the calculation of cascade geometries with the new control volumes . Fig. 3 shows a two dimensional projection of a typical grid system up to the leading edge of a cascade blade. Note that a grid point is not located along the periodic boundary when the new control volumes are used . The computational domain extends from the lower periodic boundary to the upper periodic boundary. The missing calculation points outside the computational domain are replaced by the corresponding points adjacent to the other periodic boundary. For the calculations made this summer the leading and trailing edges were modeled as shown in Fig.4.

1.2 SAJBEN'S DIFFUSER CALCULATIONS USING THE NEW CONTROL VOLUMES

Sajben's diffuser(3) was used as a test case to test the effect which the new control volumes have on the calculation of transonic flow. The results from calculations using NASA's current finite-volume code are used for comparison.

The geometry and grid used in the calculations are shown in Fig. 5. There were 34 axial grid points and 10 equally spaced radial grid points. The current NASA code requires input in x-r-θ coordinates. This requires that the two dimensional nozzle geometry be input either in the x-θ coordinates or in the x-r coordinates. Both were used successfully. The current calculations are made essentially two dimensional by inputing the coordinates of the diffuser at a very large radius (900 m.) in x-r coordinates. The calculations begin at x/h=-3.6 and end at x/h=7.9, where h is the throat height. The inlet total pressure is 135 kPa and the inlet total temperature is 300 K. The exit static pressure is 108 kPa. The gives a P_{exit}/Pt_{inlet}=0.800. With these conditions, one dimensional isentropic flow gives a shock with an upstream Mach number of 1.495 at the location marked in Fig. 5. Multigridding is used to improve the convergence speed. A copy of the input file used for these calculations is in Appendix A.

Fig. 6 shows a comparison of bottom flat wall static pressures obtained using the old control volumes and using the new control volumes("old" will refer to the type of control volumes used in NASA's current finite volume code and "new" will refer to the type of control volumes shown in Fig. 1). A one

dimensional analytical calculation was made for the Sajben diffuser geometry using the above specified boundary conditions. Fig. 6 includes the static pressure distribution of this one-dimensional calculation for comparison with the numerical solutions. The agreement is good except through the shock.

1.3 EVALUATION OF TOTAL PRESSURE IN THE DENTON CODE

Fig. 7 shows a comparison of the calculated bottom flat wall total pressures and the one dimensional analytical solution . Both calculations show overshoots and a large undershoot in total pressure in the region through the shock. The exit total pressures, however, are essentially the same for both the calculations and are close to the one-dimensional analytical solution.

The overshoots and undershoots in total pressure arise because the pressure used in the momentum equation, an interpolated effective pressure, is not used to calculate the total pressure. The current code uses the thermodynamic pressure, determined from the ideal gas equation of state, to evaluate the total pressure.

Because of the way that the effective pressure is calculated in NASA's current finite-volume code, the shock is smeared out over several grid points. One byproduct of this smearing is that the maximum Mach number before the shock shown in the calculations is lower that the one dimensional value (1.385 and 1.433 compared with 1.495) and should therefore not be used to predict the total pressure loss across the shock. However the

total pressure loss through the shock agrees well between the one dimensional solution and the calculation. Pt_{exit}/Pt_{inlet} from the one-dimensional solution was .9304 . This compares well with the computed value of .931 using the new control volumes and reasonably well with the value of .934 using the old control volumes.

The effective pressure is used to stabilize the calculation procedure and reduces overshoots and undershoots in static pressure and Mach number through the shock. From Fig. 7, it was seen that the local total pressure undershoots considerably because of this but that the net total pressure loss through the shock is calculated with good accuracy. If the local total pressure is calculated from the effective pressure rather than the thermodynamic pressure then the total pressure is much better behaved as can be seen in Fig. 8. This demonstrates the advantage of being consistent by choosing the pressure for use in evaluating the total pressure to be the same as the pressure used in the momentum equation. Since the effective pressure is equal to the thermodynamic pressure at the exit the value of the calculated Pt_{exit}/Pt_{inlet} is still .931. Fig. 9 shows a comparison of the effective pressure and the thermodynamic pressure for this test case . Perhaps the effective pressure should be considered the best representation of the "actual" static pressure.

It was attempted to remove the pressure inconsistency brought about in the transonic calculations by the way that the effective pressure is calculated. The program currently uses Eqs. 2-4 given in Table 1 to calculate the effective pressure, and for the

Table 1 Effective Pressure Calculation

Pressure Interpolation

$$FUP = 1.7 \tag{1}$$

$$A = (FUP-1.)*\left(\frac{\rho_{I+1} - \rho_{I-1}}{\rho_I}\right) \tag{2}$$

$$0.0 \leq A \leq 0.9$$

$$CFP_I = (1.-RF)*CFP_I + RF*(1.-A)*.333*(P_{I-1} - P_{I+2}) \tag{3}$$

where RF= 0.02 to 0.05 typically and CFP is updated every 5 iterations

$$PEFF_I = P_{I+1} + CFP_I \tag{4}$$

In the limit when convergence is reached,

$$PEFF_I = P_{I+1} + (1.-A)*0.333*(P_{I-1} - P_{I+2})$$

Relaxation to Ideal Gas

$$CFP_I = (1.-RF)*CFP_I + RF*(P_I - P_{I+1}) \tag{5}$$

$$PEFF_I = P_{I+1} + CFP_I \tag{6}$$

in the limit when convergence is reached,

$$PEFF_I = P_I$$

calculations in Figs. 5-9 the parameter FUP was set equal to 1.7 (Eq. 1). If Eqs. 5-6 are used instead, as the solution approaches a steady state the thermodynamic pressure would equal the effective pressure. But this procedure causes large overshoots in the static pressure as can be seen in Fig. 10. The solution also did not converge and the static pressures shown in Fig. 10 are after 2200 iterations. Many different ways of applying equations 5-6 were tried for the transonic case but none of them got rid of the overshoot problem. However, equations 5 and 6 could be used to obtain a stable solution if the Mach number throughout the duct remained subsonic.

1.4 THE INFLUENCE OF TRANSVERSE SMOOTHING ON A STEP PROFILE IN A STRAIGHT DUCT

Transverse smoothing is required in the current Denton method with the old control volumes because there are more grid points across the duct (unknowns) than there are control volumes (equations). Smoothing formulae are used to add non-physical "extra equations". Two forms of transverse smoothing are used in the Denton code; these are linear smoothing, described in Table 2, and non-linear smoothing, described in Table 3 and Fig. 11. This transverse smoothing of properties causes numerical viscosity to be introduced into the solution when large gradients in the properties are seen across the duct.

For the Sajben diffuser test case, there are no large gradients of properties across the duct so you would expect little numerical viscosity. This lack of significant numerical

Table 2 Linear Smoothing of Flow Properties

$$D(J) = (1.-SF)*D(J)+\frac{SF}{2.}*(D(J+1)+D(J-1))$$

the variable D at node J is smoothed using this equation. The smoothing factor is SF, typically 0.01 - 0.02. The variables are updated and then smoothed. The variables that are smoothed are ρ, ρV_x, ρV_r, $\rho r V_\theta$, and ρe.

Table 3 Procedure for Non-Linear Smoothing

1) an average value of a property D is determined from the neighboring nodes using linear interpolation. AVG(J) (see equation 1 Fig. 11)

2) the difference between the actual and average value of a property D at a node is determined and assigned the variable name CURVE(J) (see equation 2 Fig. 11)

3) a variable SCURVE is determined from the average of the variable CURVE from the neighboring nodes. (see equation 3 Fig. 11)

4) the variable D at node I is smoothed using equation 4 in Fig. 11 . The smoothing factor is SF, typically 0.01-0.02.

5) this non-linear smoothing procedure results in no smoothing added to linearly or parabolically varying properties.

viscosity is seen by the agreement between the calculations made using the new control volumes without smoothing and old control volumes with smoothing(see Fig. 6 and 7). As a severe test case, calculations were made for a step profile in inlet properties in a straight duct. The geometry can be seen in Fig. 12. A step inlet profile of total pressure is specified. The total pressure at the centerline is 135 kPa and the total pressure is reduced to 120 kPa ($Pt_{side}/Pt_{centerline}$=0.889) at the sides(see Fig. 13) . The exit static pressure in the duct is 108 kPa ($0.8*Pt_{centerline}$).

Fig. 14 shows Mach number profiles at three axial locations along the duct for the case where linear smoothing was used (with SF=0.02) . The inlet step profile(x=0.0m) is quickly altered into a parabolic type profile(x=4.0m). This parabolic profile then changes relatively little until the end of the duct (x=21.0m). Fig. 15 presents the total pressure distribution along the duct. The step profile causes an almost step change in the total pressure at the beginning of the duct and then the total pressure decreases as in a viscous flow. Fig. 16 compares the Mach number profiles at the end of the duct for calculations using linear smoothing (SF=0.02) and non-linear smoothing (SF=0.02). Non-linear smoothing did not improve the profile.

Additional calculations were made using the same boundary conditions as above but using the new control volumes and no smoothing. Fig. 17 compares the inlet Mach number and exit Mach number profiles for this case . The improvement over the previous results is dramatic. The total pressure distribution has also improved especially along the centerline of the duct as can be

seen in Fig. 18. These results show conclusively that the numerical scheme used to calculate flows with large transverse gradients in properties, like those seen in turbulent boundary layers, must not have smoothing of properties in the transverse direction.

1.5 SHOCK LOSSES IN AN INCLINED DIFFUSER

One of the possible sources of inaccuracy in the calculation of total pressure in transonic compressor calculations is due to the possibility of smoothing through the shock due to a inclined flow path. In the Sajben diffuser calculations for Figs. 6-10 the property gradients across the duct were not large and transverse smoothing did not add noticeable numerical viscosity into the calculations. However, if the diffuser were inclined at an angle, the shock would become oblique to the grid and would introduce large transverse gradients in properties there. Fig. 19 shows Sajben's diffuser inclined at an angle of 40 degrees with respect to the horizontal axis. This geometry would cause a normal shock to cross about 4 transverse grid lines. The Sajben geometry used previously(see Fig. 5) has been extended with constant area sections added on to the inlet and exit of the duct. The same inlet and exit boundary conditions were specified as in the previous Sajben diffuser calculations. The input file used in these calculations is in Appendix A.

The effective pressures along the flat wall are plotted in Fig. 20 for the old and new control volumes, with and without smoothing respectively. The wall pressures using the new control

volumes were determined by linearly extrapolating from the interior points. The effective pressures for the old control volumes are displaced downstream of the effective pressures using the new control volumes. Fig. 21 presents the total pressures along the bottom wall calculated using the effective pressures. The exit total pressures are approximately the same(0.941 for new C.V. and 0.944 for old C.V.) for both calculations but the local total pressures from the calculation using the new control volumes are better behaved. In both cases, however, the exit total pressure ratios of 0.941 and 0.944 are different from the exit total pressure of 125.7 kPa (Pt_{exit}/Pt_{inlet}=0.931) calculated for the horizontal Sajben diffuser.

Further comparisons of the inclined and horizontal results, using the old and new control volumes, are shown in Figs. 22,23,24,and 25. The minimum static pressure for the inclined calculations is greater than that obtained from the horizontal calculations. The total pressure behavior is also poorer for the inclined calculations when compared with the horizontal solution. The total pressure losses through the shock for the inclined calculations are approximately 15% less than those for the horizontal calculations. The oscillations in total pressure at the exit of the inclined diffuser (with the old control volumes) are perhaps the result of the long thin control volumes that are seen there.

It was difficult to obtain a converged solution for the inclined geometry with either control volume. So the results presented here are after 1000 iterations. At this point in the calculations the maximum error in mass flow rate with the old

control volumes is 0.2% and the maximum change in axial velocity was .00009 of the mean flow velocity. For the new control volumes, the corresponding error is 0.2% and the corresponding change is .00019.

1.6 EFFECTIVE DENSITY CALCULATIONS

The method presented in reference 1 uses a different procedure to update the pressure and density. The pressure is updated directly from the continuity error and then the density is updated using the ideal gas equation of state. This procedure was necessary because of the multi-volume approach used in the boundary layer region. This updating procedure was also implemented in the three dimensional version of the finite volume code at NASA Lewis.

If the density is updated in the calculations such that the effective density becomes the actual density at a node the same overshoot phenomena in static pressure and Mach number appears here as did when the effective pressure was used (see Fig. 10). The solution would also not converge. Therefore an effective density which does not use the actual pressure at a node, but uses an interpolated pressure, is used and is described in Table 4. This effective density reduces the overshoot problem and results in a stable solution. The following results use this effective density. Just as the interpolation procedure before introduced an inconsistency between the thermodynamic and effective pressures, the ideal gas equation of state is not satisfied completely when the effective density is used.

Table 4 Effective Density Calculation

$$CFP_I = (1.-RF)*CFP_I + RF/3.*(P_{I+1} - P_{I-2}) \qquad (1)$$

$$\rho_{I+1} = \frac{(P_I + CFP_I)}{R*T_{I+1}} \qquad (2)$$

in the limit when convergence is reached

$$\rho_{I+1} = \frac{P_I + \frac{P_{I+1}-P_{I-2}}{3}}{RT_{I+1}}$$

Fig. 26 compares the bottom flat wall static pressures for calculations of transonic flow in Sajben's diffuser (Fig. 5) using the effective pressure method and the effective density method with the same boundary conditions as in our previous test cases and the new control volumes (the effective pressure is shown for the effective pressure method) . Fig. 27 compares the total pressures for these two cases. The effective density method gives a much more uniform total pressure upstream and downstream of the shock; there are no overshoots in total pressure when the effective density method is used.

To obtain a stable solution using the effective density, it was found necessary to assume a constant total temperature rather than use the energy equation in its full form. It may be that an interaction between the continuity error and the energy equation was responsible for this instability.

1.7 CASCADE GEOMETRIES

Some additional calculations were made, using the new control volumes and the effective pressure method, on some simple cascade geometries. The purpose of these runs was to check out the periodicity condition and the treatment of the leading and trailing edges which were discussed earlier. The geometries are shown in Figs. 28 and 29. The inlet total pressure was 101.352 kPa, the inlet total temperature was 288.166 K, and the exit static pressure was 85.44 kPa. Fig. 30 shows the Mach numbers calculated along grid lines which are closest to the pressure and

suction surfaces. A copy of the input data is in Appendix A.

The only difficulty encountered in these cascade flows was a problem with the flow properties oscillating at the inlet about some mean value between adjacent grid points. This was due to the periodicity condition and the absence of smoothing to damp out these oscillations. This problem was found to occur only when there were an even number grid points across the inlet. An odd number of transverse grid points seems to decouple the odd-even oscillations.

1.8 CALCULATIONS FOR AN INLET GUIDE VANE

Fig. 31 shows the geometry and grid for an inlet guide vane that was my final test for the summer work. The total pressures along the streamline closest to the suction surface are presented in Fig. 32. The new control volumes are used for both calculations, one uses the effective pressure method and one uses the effective density method. The total pressure distributions in Fig. 32 , which use the new control volumes ,can be compared with the results ,from the Denton code using the old control volumes, shown in Fig. 33. Both the calculations using the effective pressure method have large oscillations in total pressure around the leading edge whereas the calculations using effective density method give better total pressure behavior. The effective density method is much better at calculating the total pressure than the effective pressure method even when the effective pressure is used to calculate the total pressure as was done for the results shown in Fig. 32 .

Figs. 34 and 35 present Mach numbers along grid lines through the inlet guide vane for calculations using the effective density method with the new control volumes and the effective pressure method with the old control volumes ,respectively . It was found necessary to use a small amount of smoothing(SF=0.005), even using the new control volumes ,for this inlet guide vane. This need for smoothing is perhaps the result of an incorrect treatment of the pressure at the trailing edge.

SUMMARY

The work at NASA Lewis Research Center involved using and modifying the Denton finite-volume time-marching code. The results can be summarized as follows.

1. The new control volumes developed at V.P.I. & S.U. can be extended to a three dimensional geometry. For duct flows the new control volumes require no transverse smoothing.

2. The results for Sajben's diffuser were essentially the same for both control volumes.

3. If the effective pressure is used to calculate the total pressure the total pressures are much better behaved through the shock.

4. Even though the total pressure is incorrectly calculated

in the shock, the overall total pressure loss through the duct is calculated accurately.

	Pt_{exit}/Pt_{inlet}
A. One dimensional solution	0.9304
B. Old control volumes	0.934
C. New control volumes	0.931

5. An interpolated effective pressure is needed to stabilize the solution.

6. For calculations where large transverse gradients in properties are observed, transverse smoothing cannot be used if an accurate solution is to be expected.

7. The new control volumes with no transverse smoothing allow calculations with large transverse gradients in properties without significant numerical total pressure losses.

8. Good convergence was not obtained for the inclined Sajben with either control volume.

9. Calculations which use the effective density method,

developed at V.P.I. & S.U., rather than an effective pressure method give a much more uniform total pressure upstream and downstream of the shock. Overshoots and undershoots were a factor of 10 smaller with the effective density method.

1.10 REFERENCES

1) Nicholson, S. and Moore,J.,"Extension of a Finite Volume Method to Laminar and Turbulent Flow," V.P.I.&S.U. Turbomachinery Research Group Report No. JM/85-6, June 1985.

2) Denton, J.D.,"An Improved Time Marching Method for Turbomachinery Calculations," ASME Paper 82-GT-239.

3) Bogar, T.J., Sajben, M. and Kroutil, J.C.,"Characteristic Frequency and Length Scales in Transonic Diffuser Flow Oscillations," AIAA Paper 81-1291.

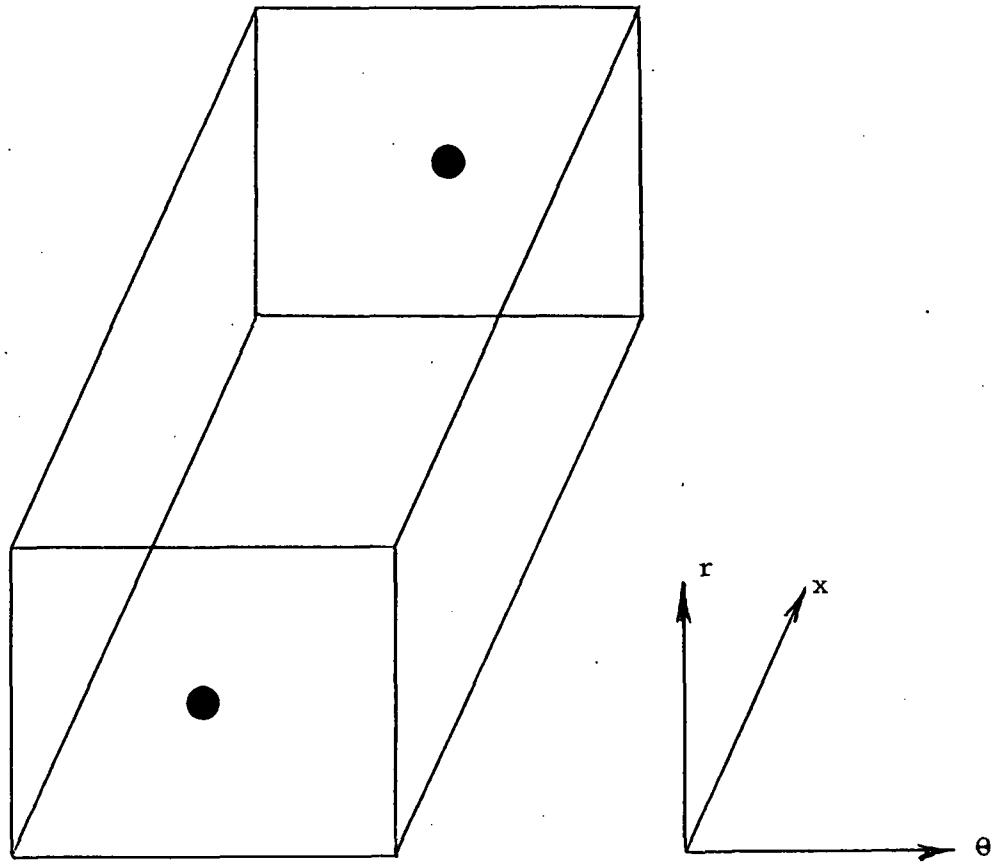

Fig. 1 New Control Volumes in Three Dimensions

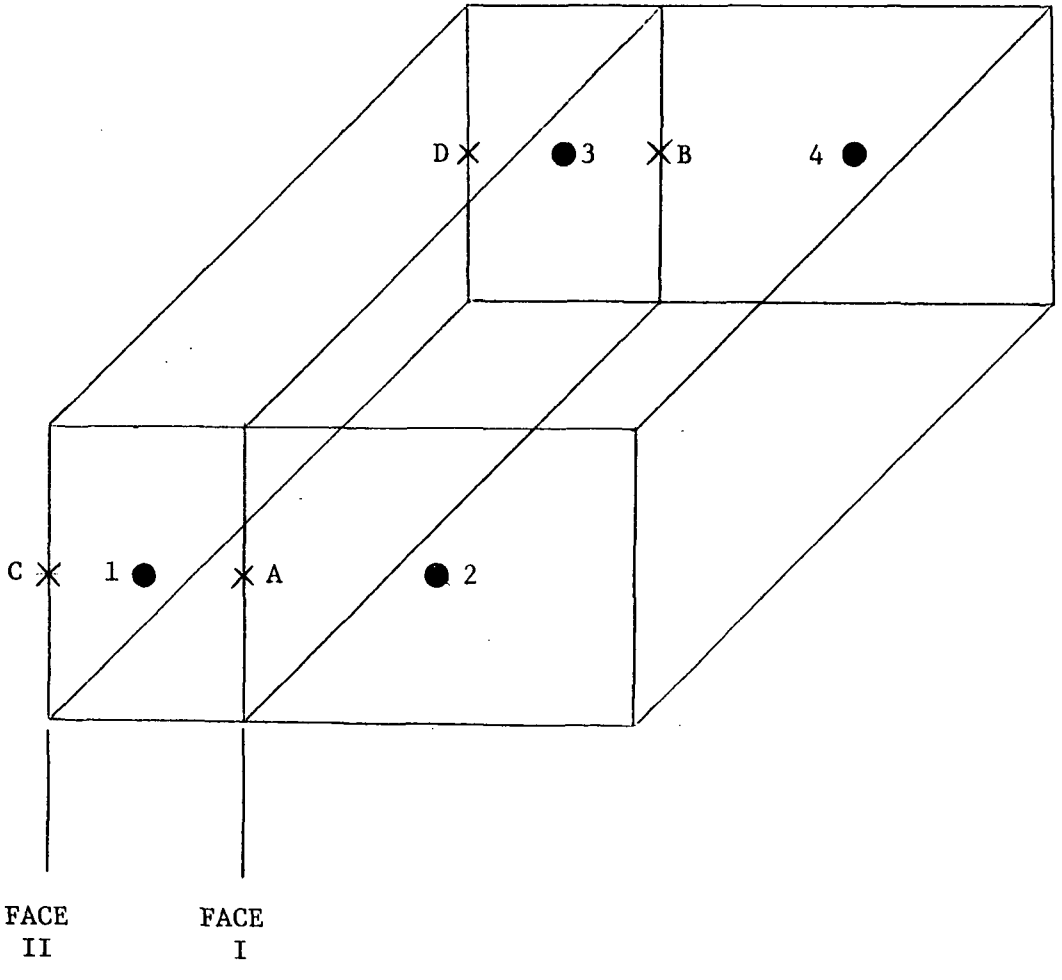

Fig. 2 New Control Volumes in Non-Uniform Grid

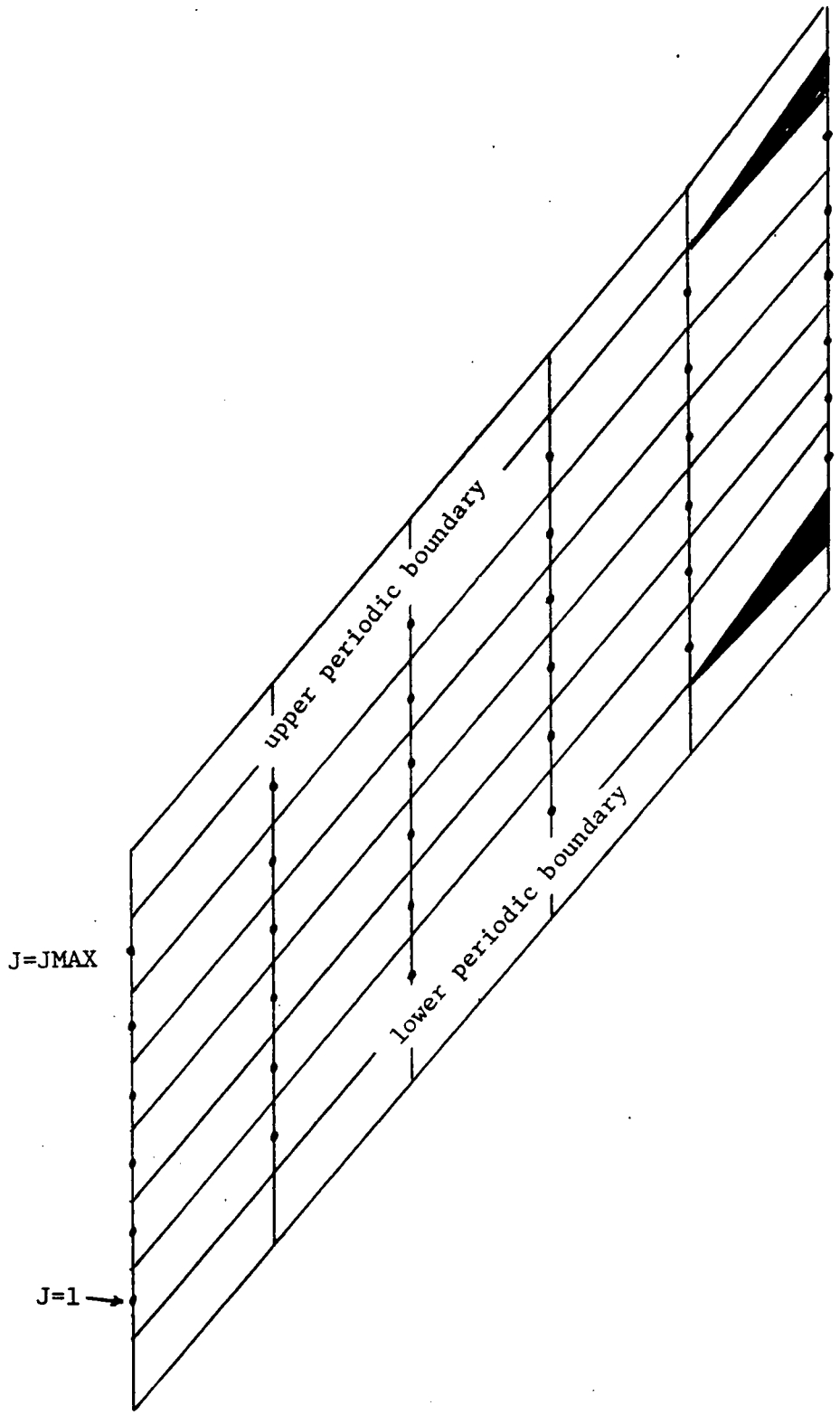

Fig. 3 Periodicity Condition

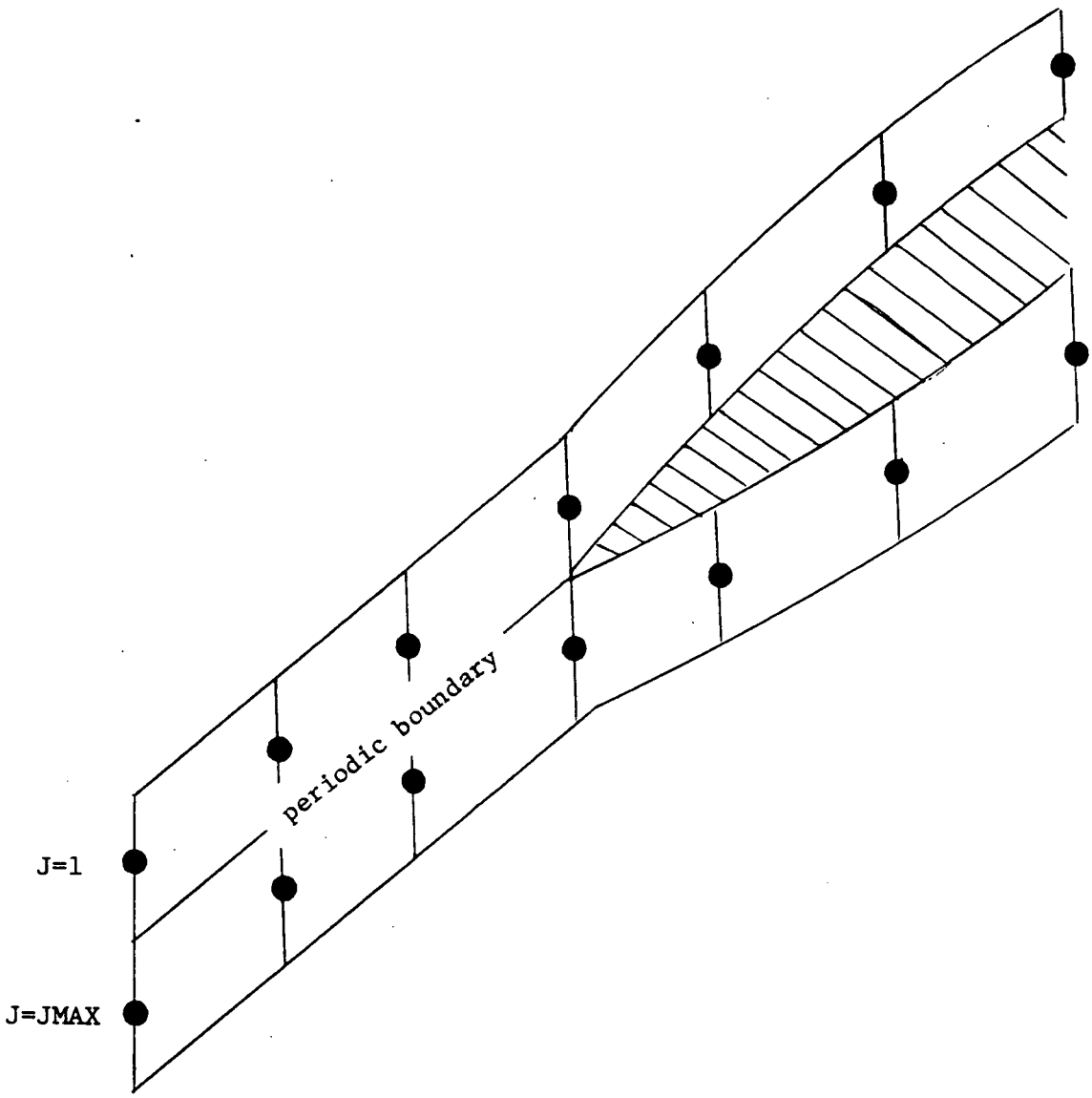

Fig. 4 Leading Edge Treatment

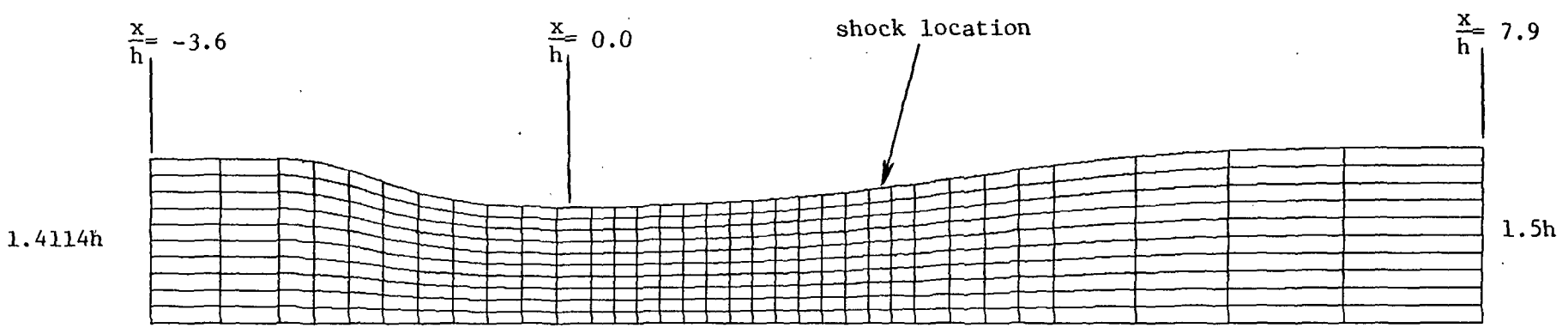

Fig. 5 Geometry and Grid for Sajben's Diffuser Calculations

FIG. 6 FLAT WALL STATIC PRESSURES
FOR SAJBEN DIFFUSER
NEW VS OLD CONTROL VOLUMES

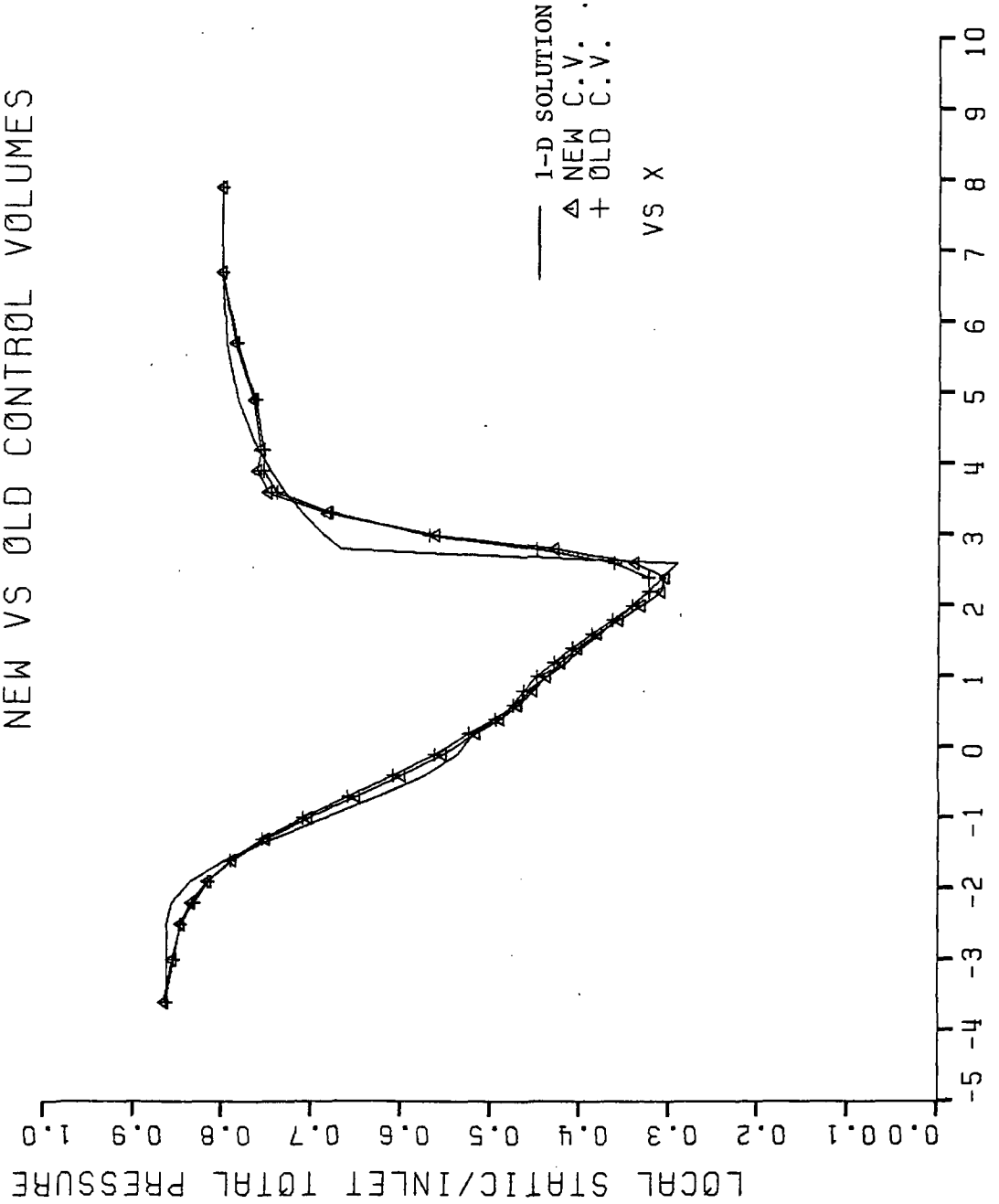

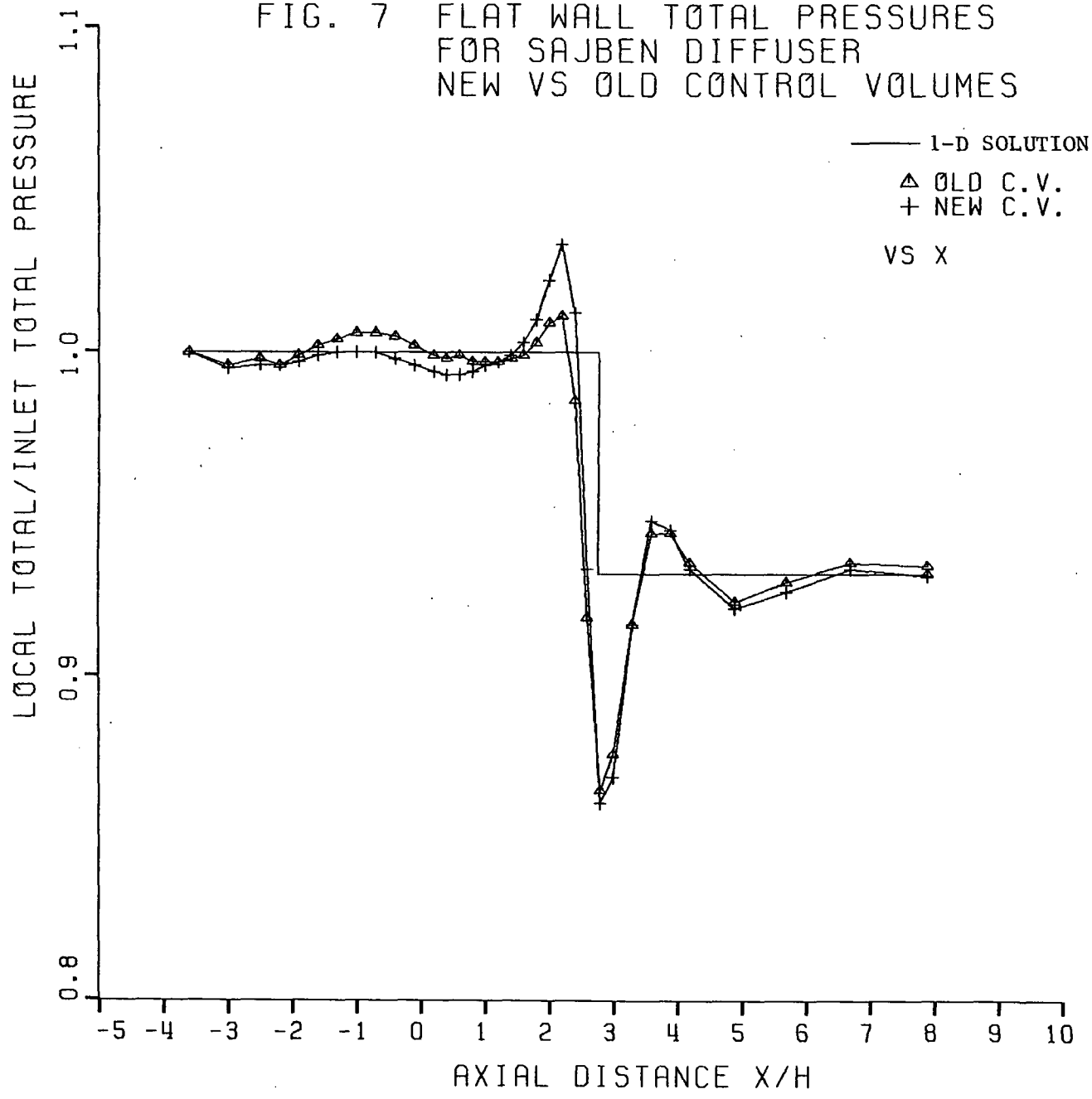
FIG. 7 FLAT WALL TOTAL PRESSURES
FOR SAJBEN DIFFUSER
NEW VS OLD CONTROL VOLUMES
1-D SOLUTION
OLD C.V.
NEW C.V.
VS X
LOCAL TOTAL/INLET TOTAL PRESSURE
1.1
1.0
0.9
0.8
-5 -4 -3 -2 -1 0 1 2 3 4 5 6 7 8 9 10
AXIAL DISTANCE X/H

FIG. 8 FLAT WALL TOTAL PRESSURE FOR SAJBEN DIFFUSER COMPARED WITH THAT OBTAINED FROM THE EFFECTIVE PRESSURE NEW CONTROL VOLUMES

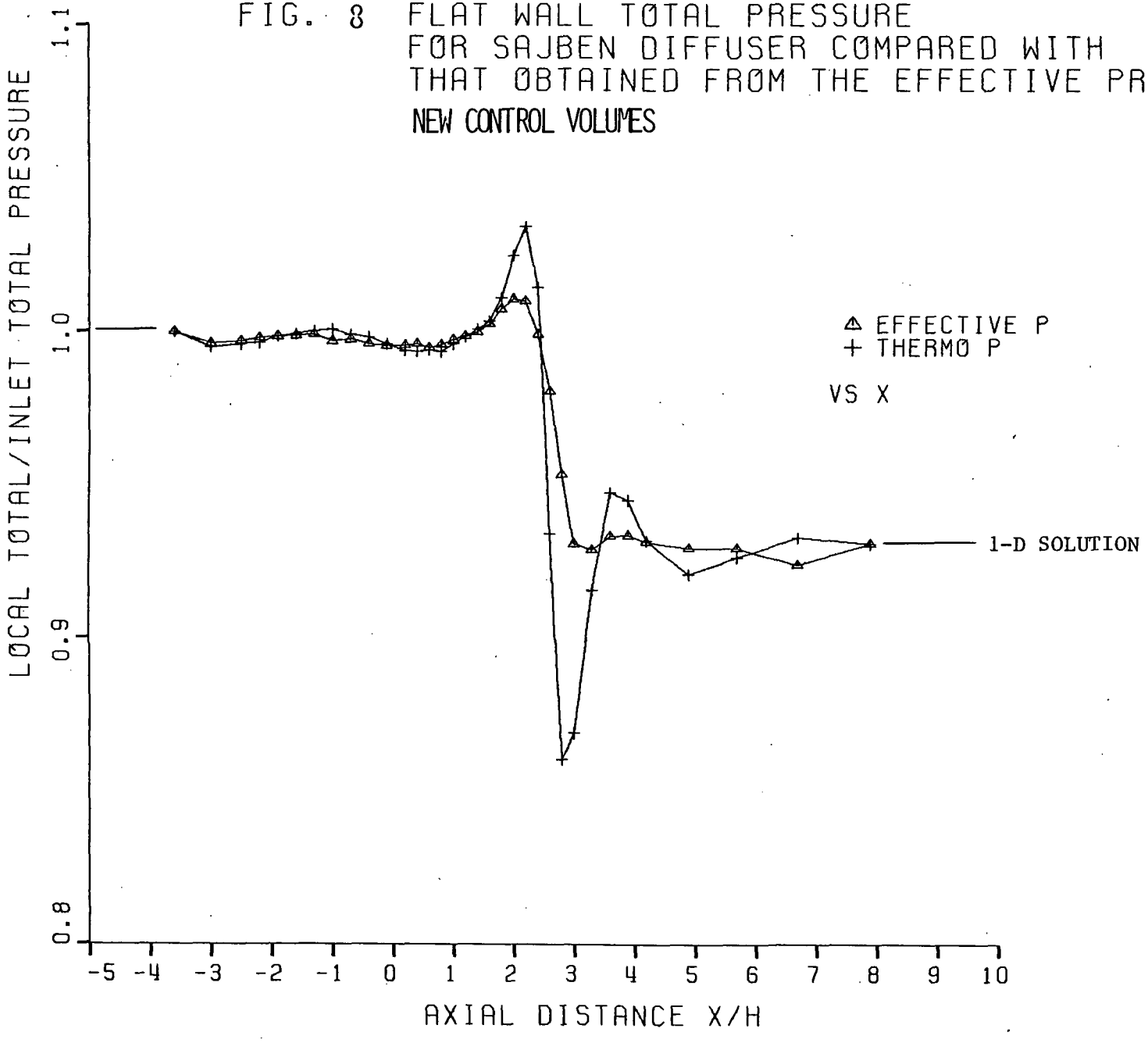

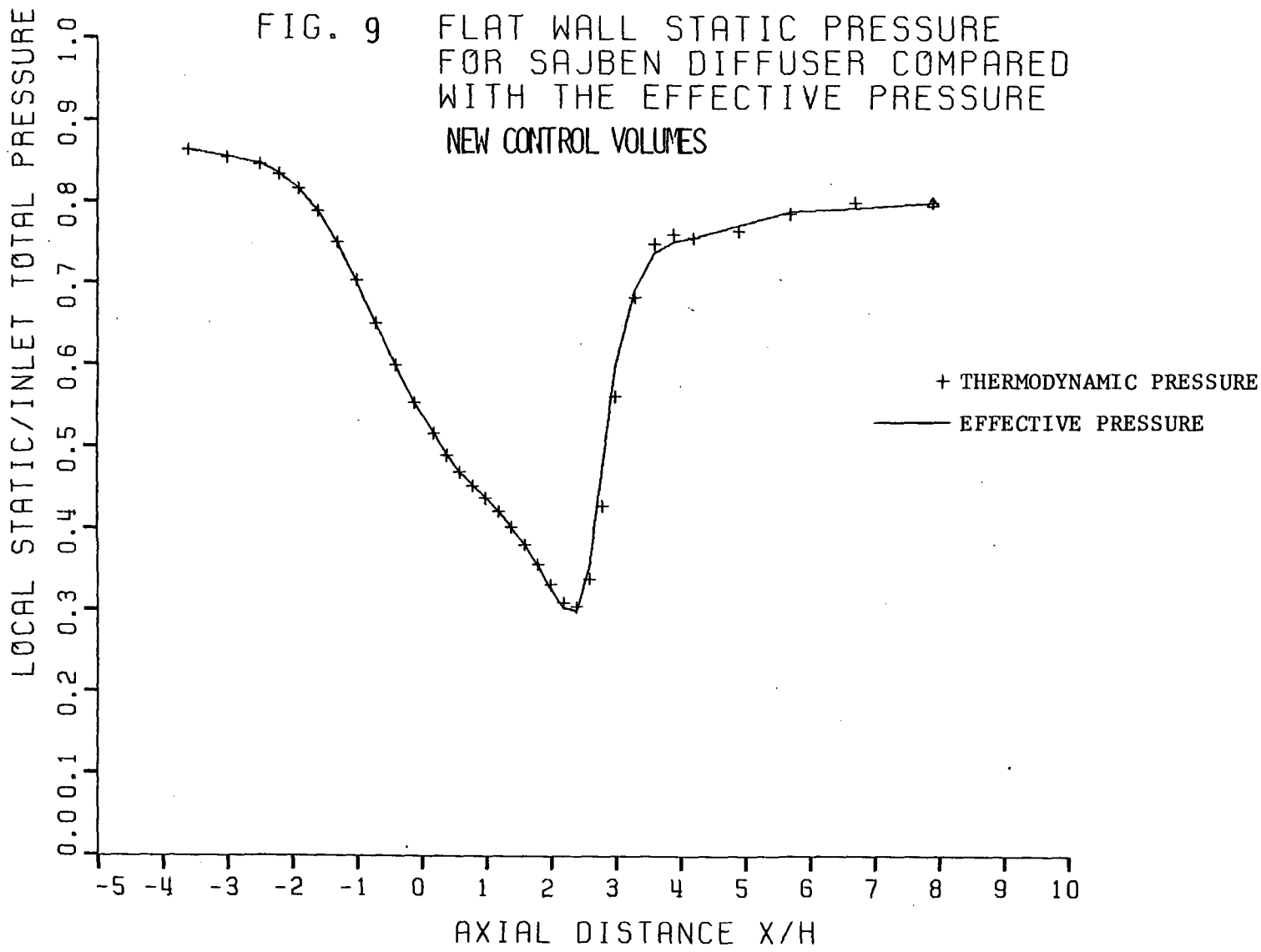
FIG. 9 FLAT WALL STATIC PRESSURE FOR SAJBEN DIFFUSER COMPARED WITH THE EFFECTIVE PRESSURE
NEW CONTROL VOLUMES
LOCAL STATIC/INLET TOTAL PRESSURE
0.0 0.1 0.2 0.3 0.4 0.5 0.6 0.7 0.8 0.9 1.0
-5 -4 -3 -2 -1 0 1 2 3 4 5 6 7 8 9 10
AXIAL DISTANCE X/H
+ THERMODYNAMIC PRESSURE
EFFECTIVE PRESSURE

FIG. 10 FLAT WALL STATIC PRESSURE FOR SAJBEN DIFFUSER WITH AND WITHOUT PRESSURE INTERPOLATION

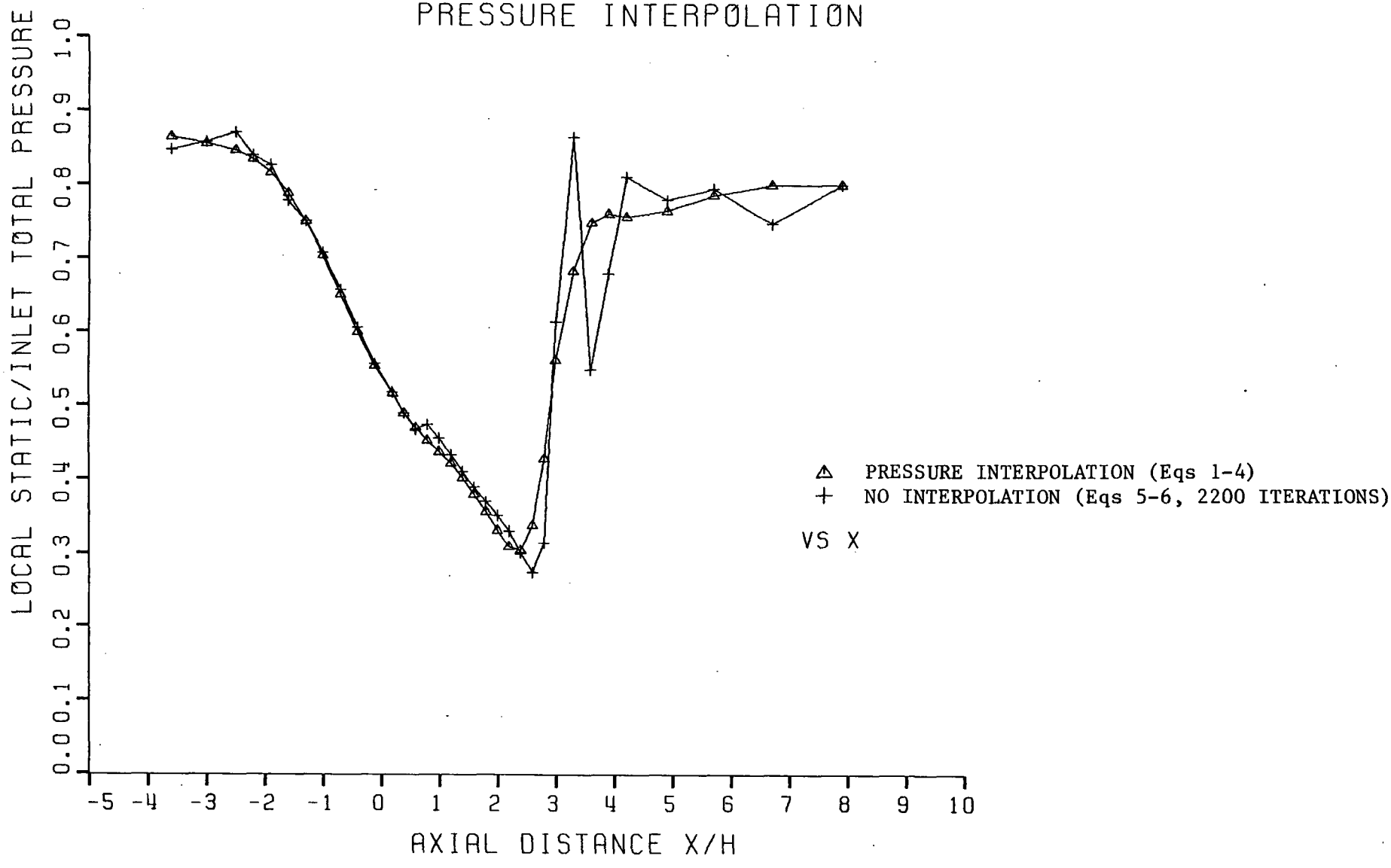

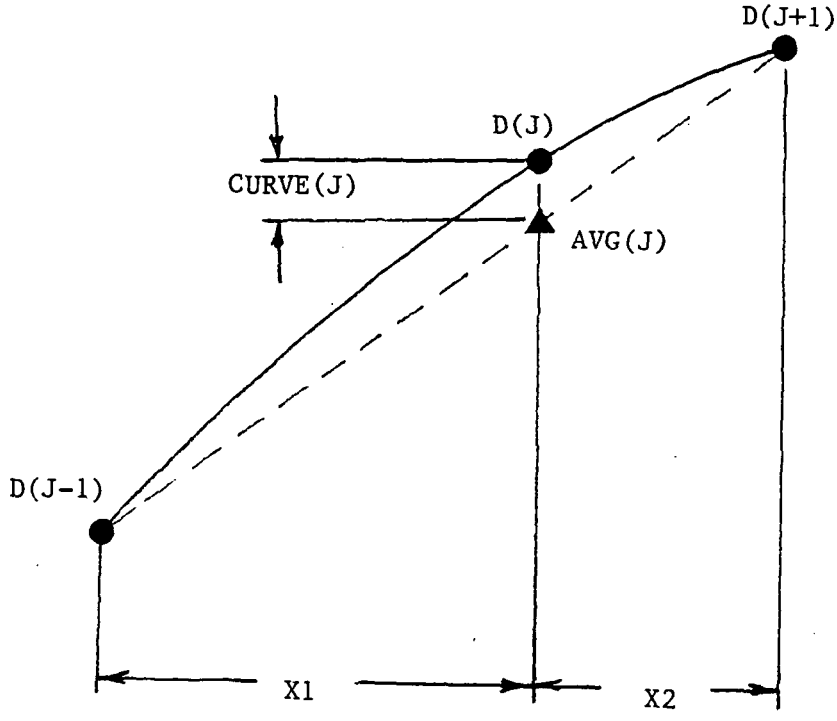

FU(J)= X2/(X1+X2)

FD(J)= X1/(X1+X2)

1) AVG(J)=FD(J)*D(J+1)+FU(J)*D(J-1)

2) CURVE(J)=D(J)-AVG(J)

3) SCURVE(J)=FU(J)*CURVE(J-1)+FD(J)*CURVE(J+1)

4) D(J)= (1.-SF)*D(J)+SF*(AVG(J)+SCURVE(J))

Fig. 11 Non-Linear Smoothing

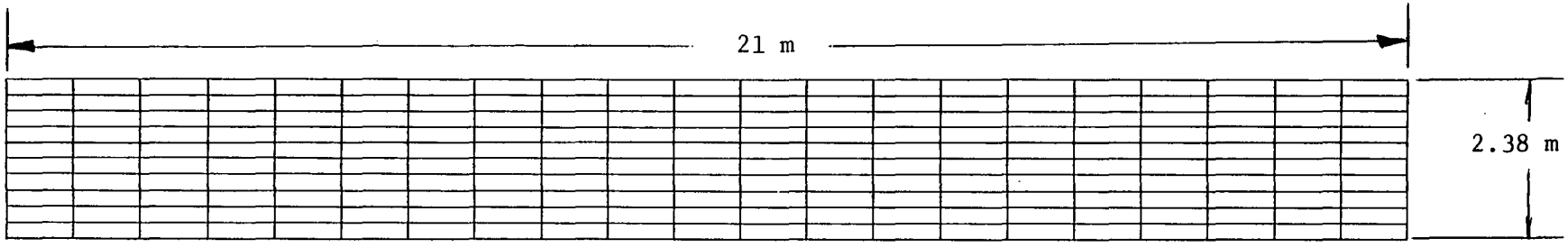

Fig. 12 Geometry and Grid Used For Step Profile

FIG. 13 INLET TOTAL PRESSURE PROFILE

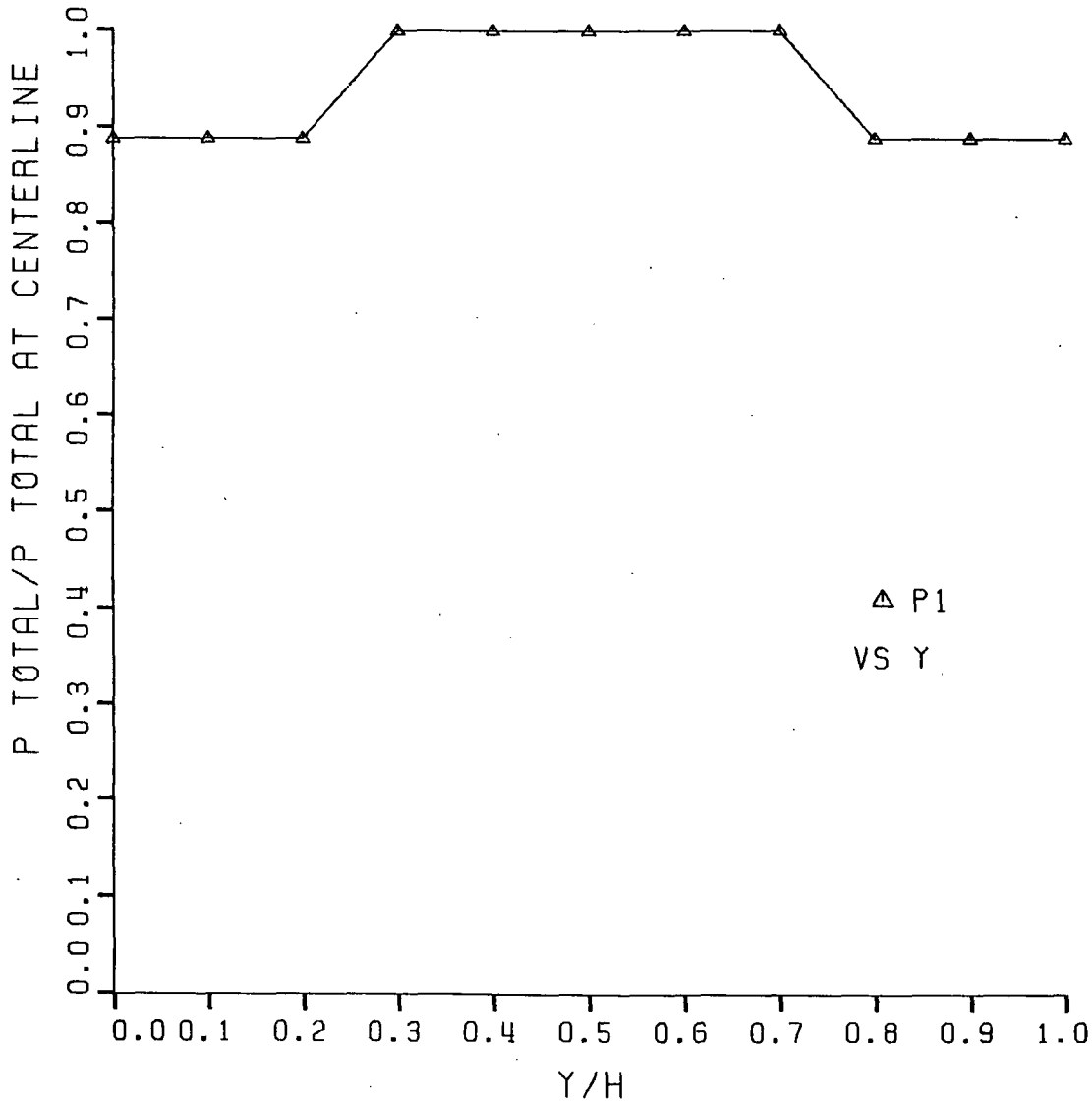

FIG. 14 LINEAR SMOOTHING APPLIED TO STEP PROFILE

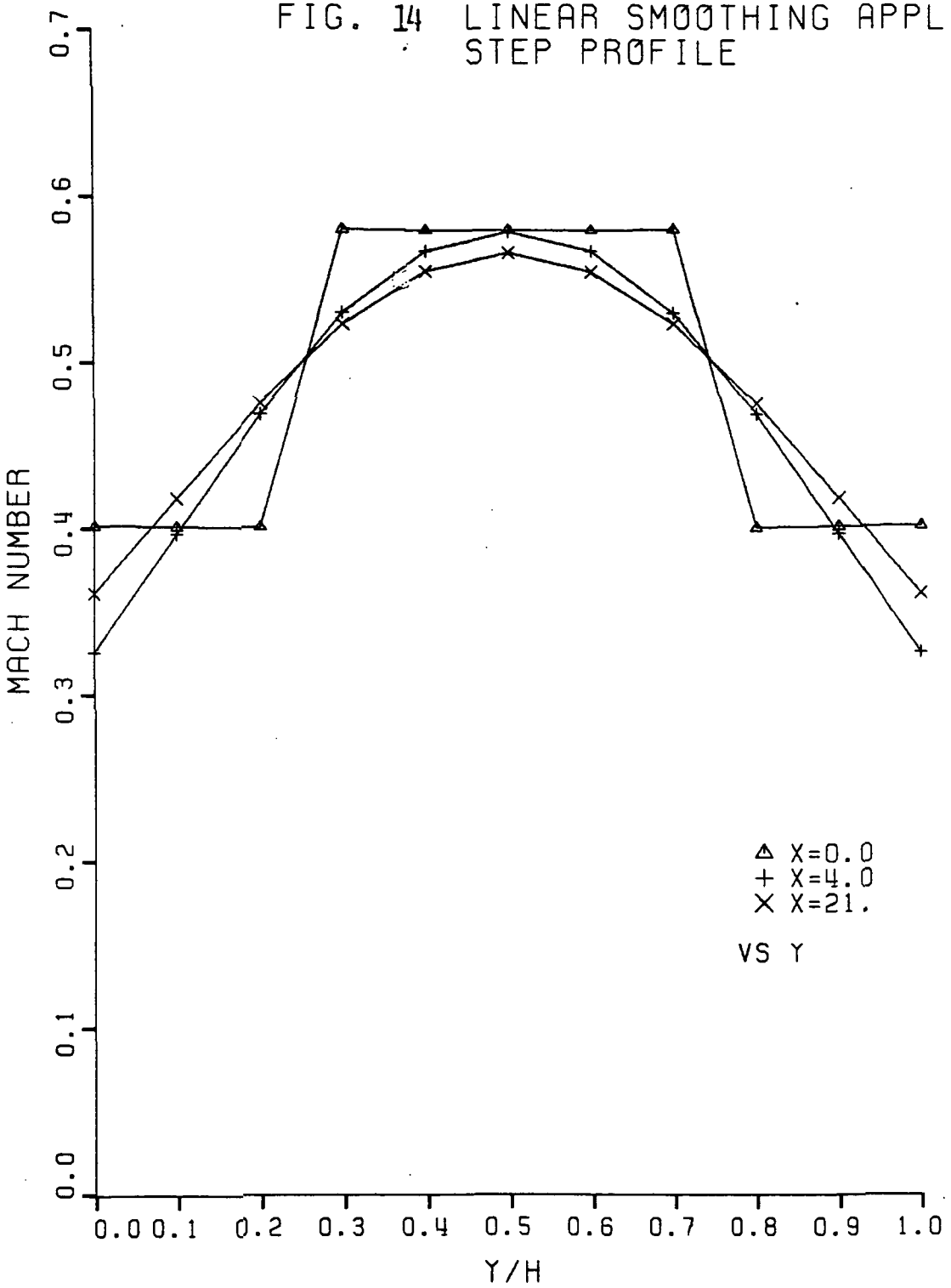

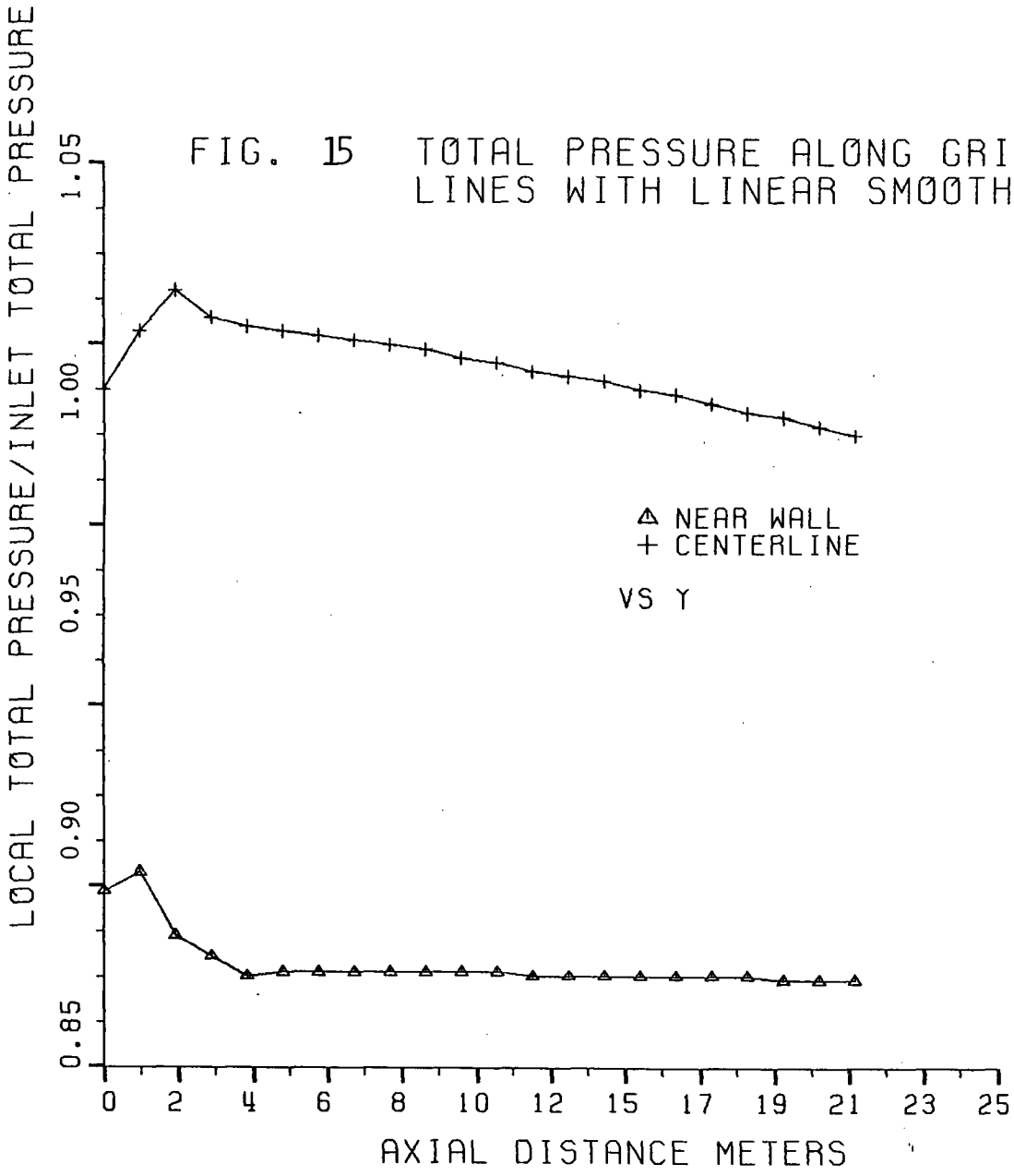
FIG. 15 TØTAL PRESSURE ALØNG GRID LINES WITH LINEAR SMØØTHING
LØCAL TØTAL PRESSURE/INLET TØTAL PRESSURE
1.05
1.00
0.95
0.90
0.85
Δ NEAR WALL
+ CENTERLINE
VS Y
0
2
4
6
8
10
12
15
17
19
21
23
25
AXIAL DISTANCE METERS

FIG. 16 NØN-LINEAR AND LINEAR SMØØTHING EXIT MACH NUMBER PRØFILE COMPARISØNS

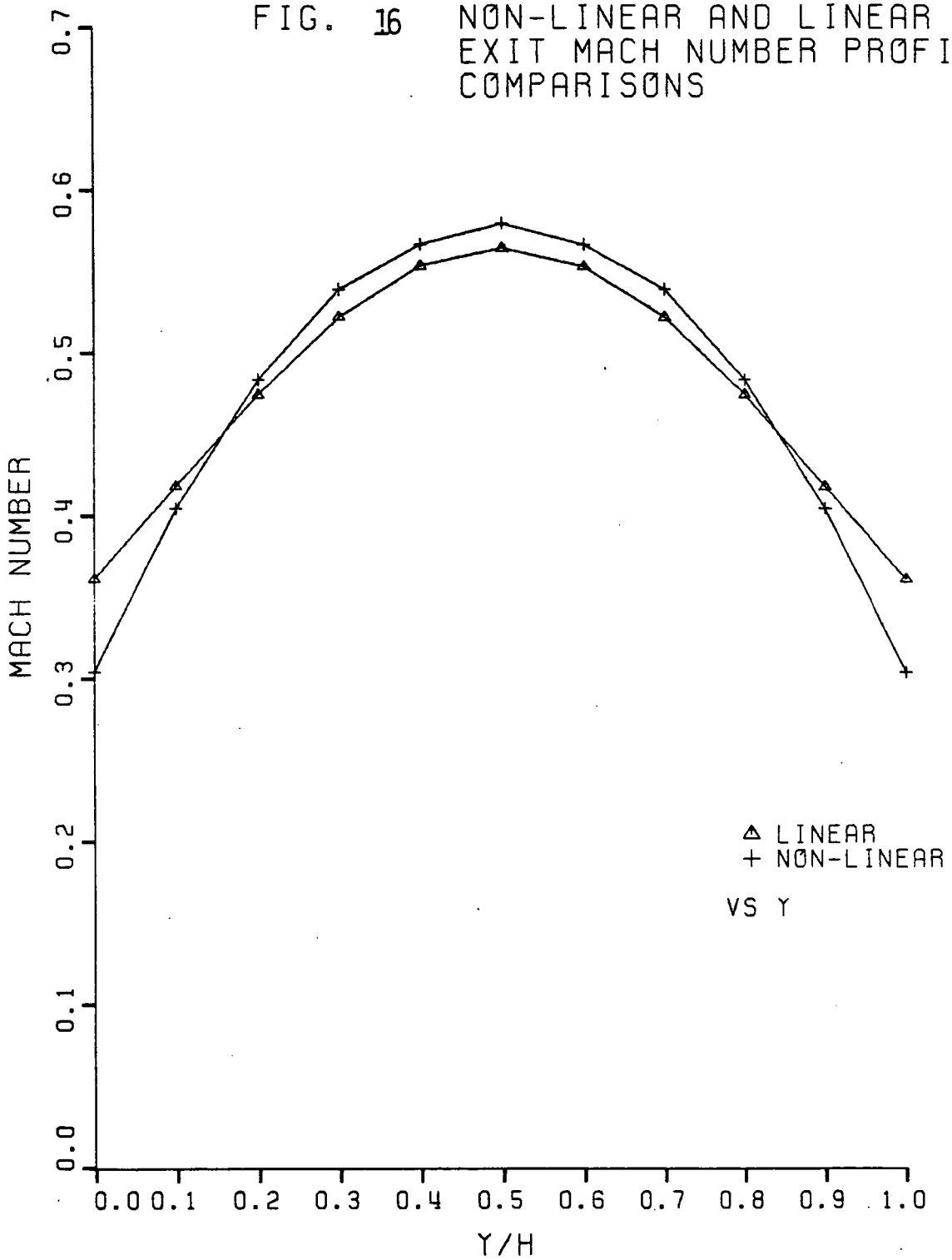

FIG. 17 NO SMOOTHING - NEW CONTROL VOLUMES
MACH NUMBER PROFILES
AT INLET AND EXIT

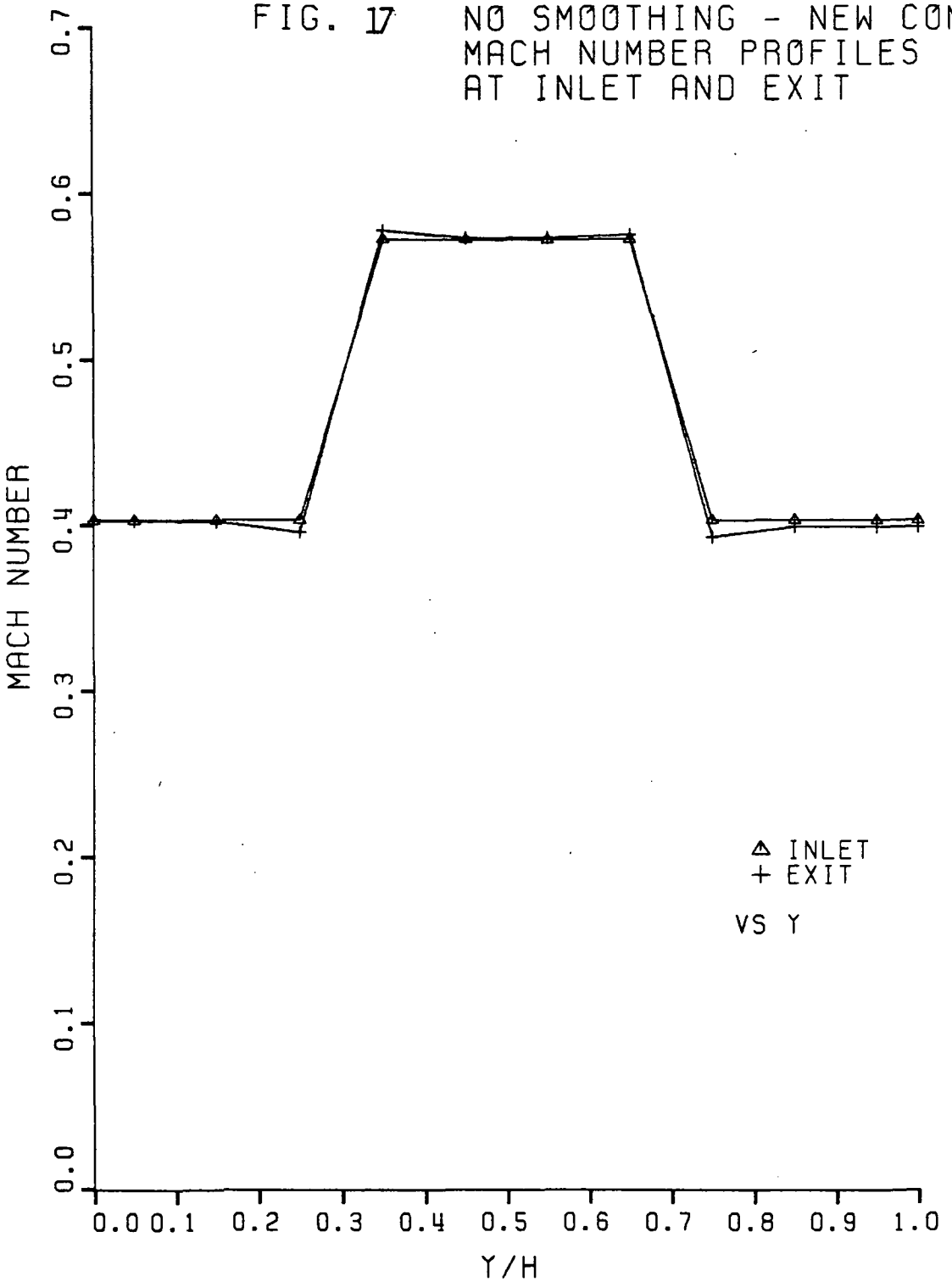

FIG. 18 NO SMOOTHING - NEW CONTROL VOLUMES
TOTAL PRESSURE ALONG GRID LINES

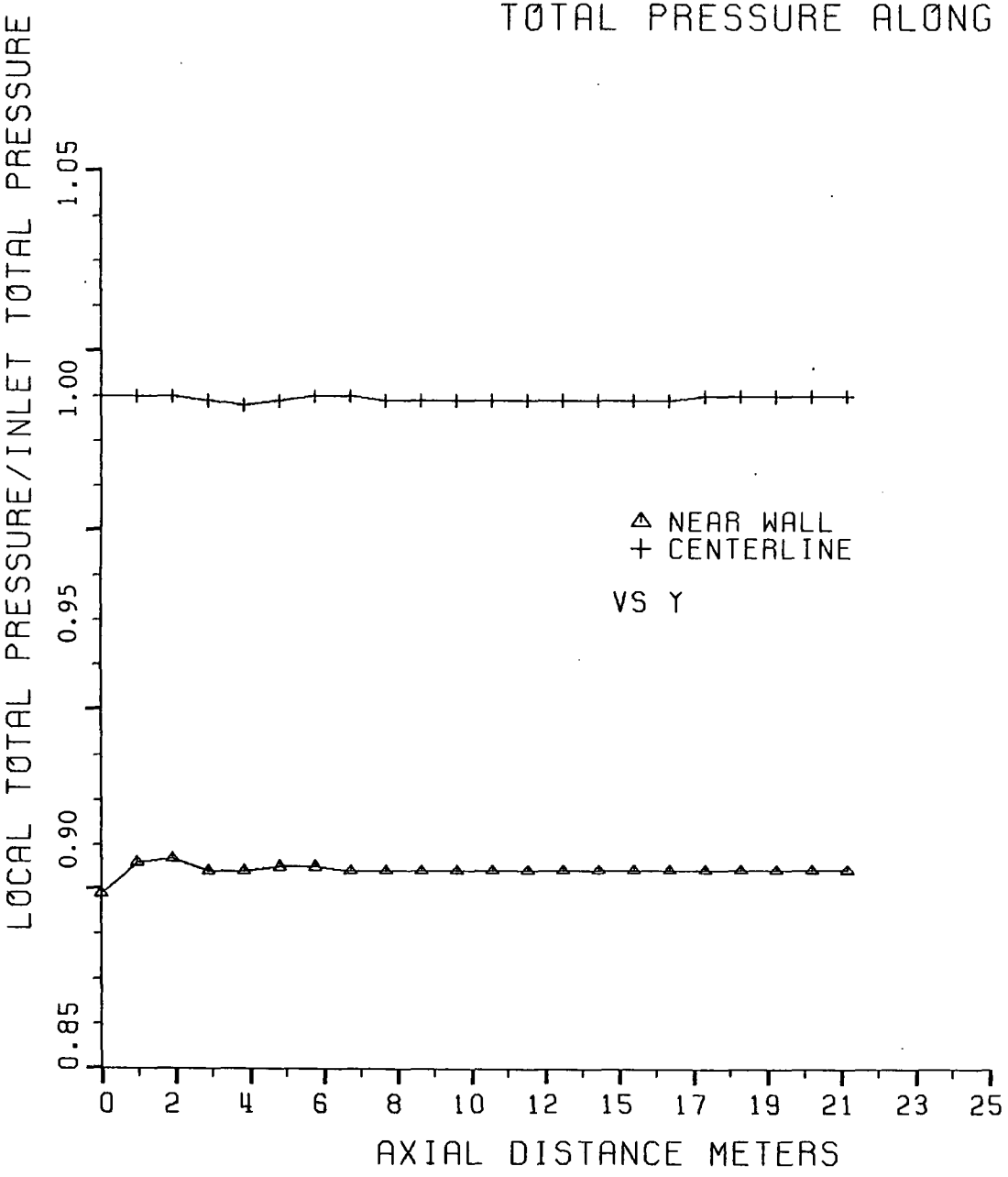

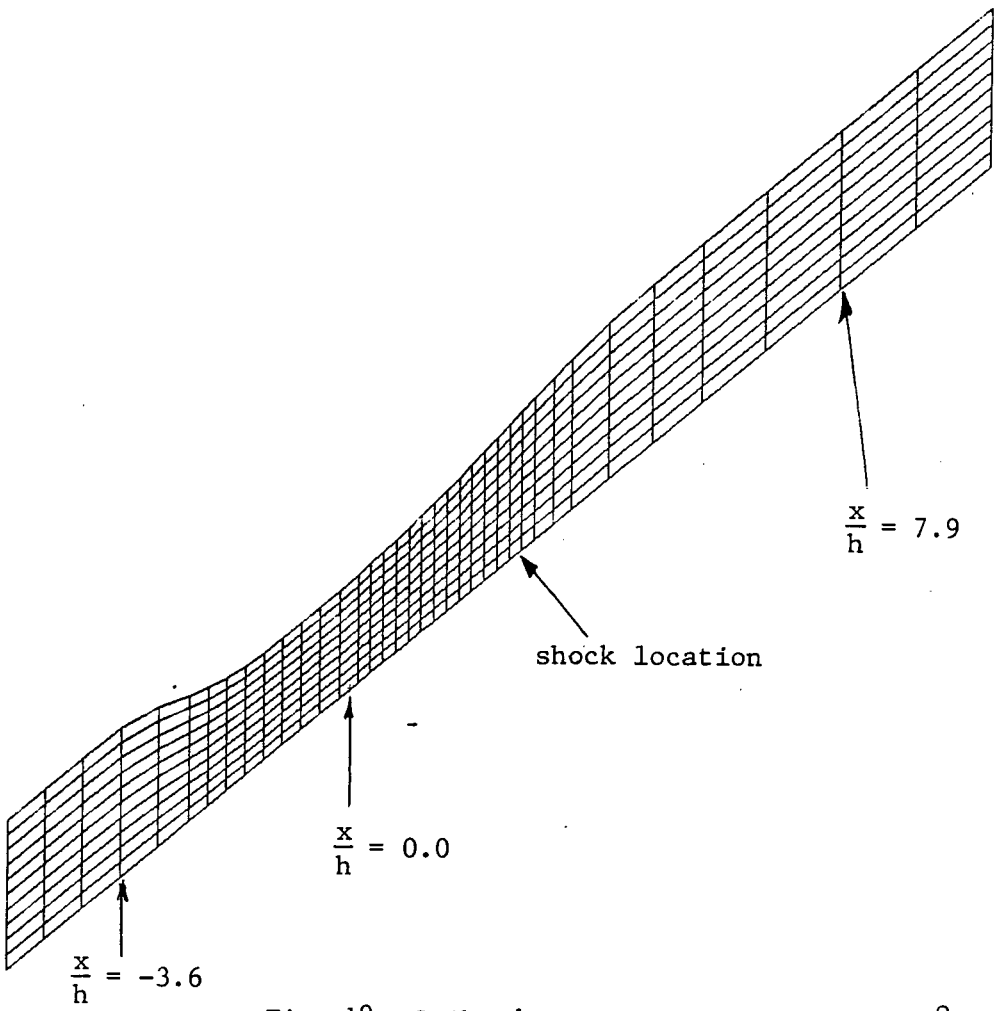

Fig. 19 Sajben's Diffuser Inclined at 40° Angle

FIG. 20 FLAT WALL STATIC PRESSURE FOR INCLINED SAJBEN DIFFUSER NEW VS OLD CONTROL VOLUMES

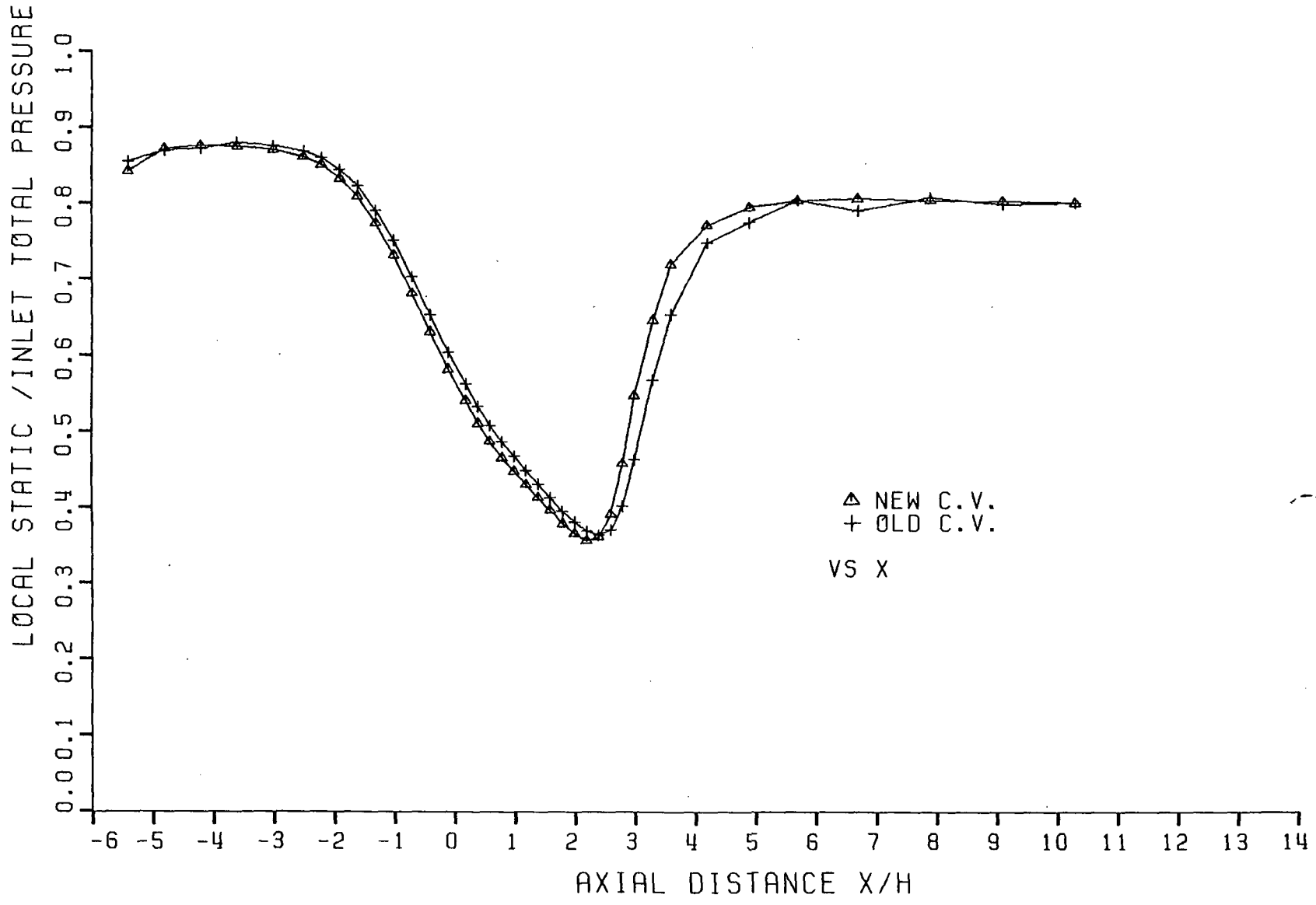

FIG. 21 FLAT WALL TOTAL PRESSURE
FOR INCLINED SAJBEN DIFFUSER
NEW VS OLD CONTROL VOLUMES

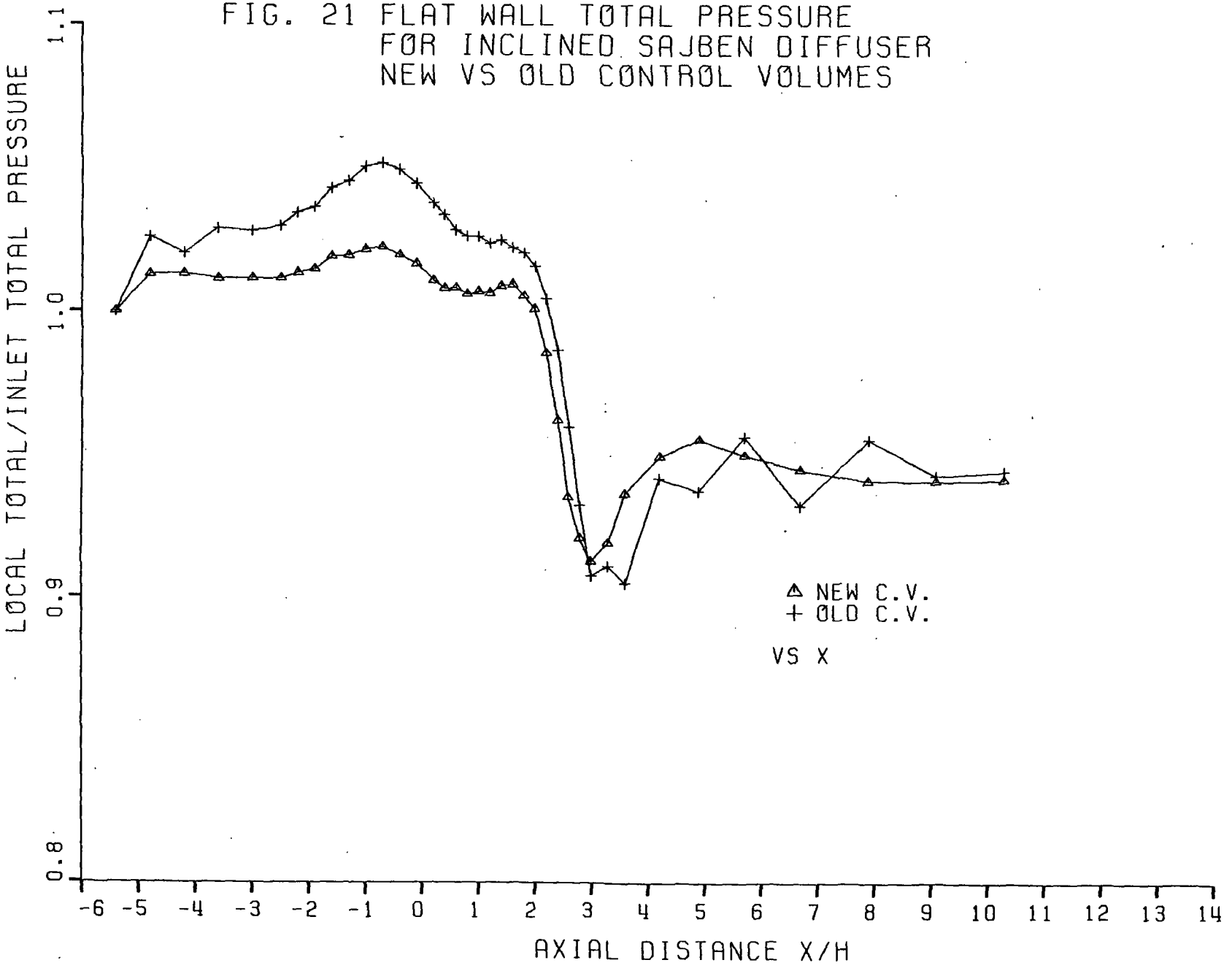

FIG. 22 FLAT WALL STATIC PRESSURE
FOR SAJBEN DIFFUSER-OLD CONTROL VOLUMES
HORIZONTAL AND INCLINED

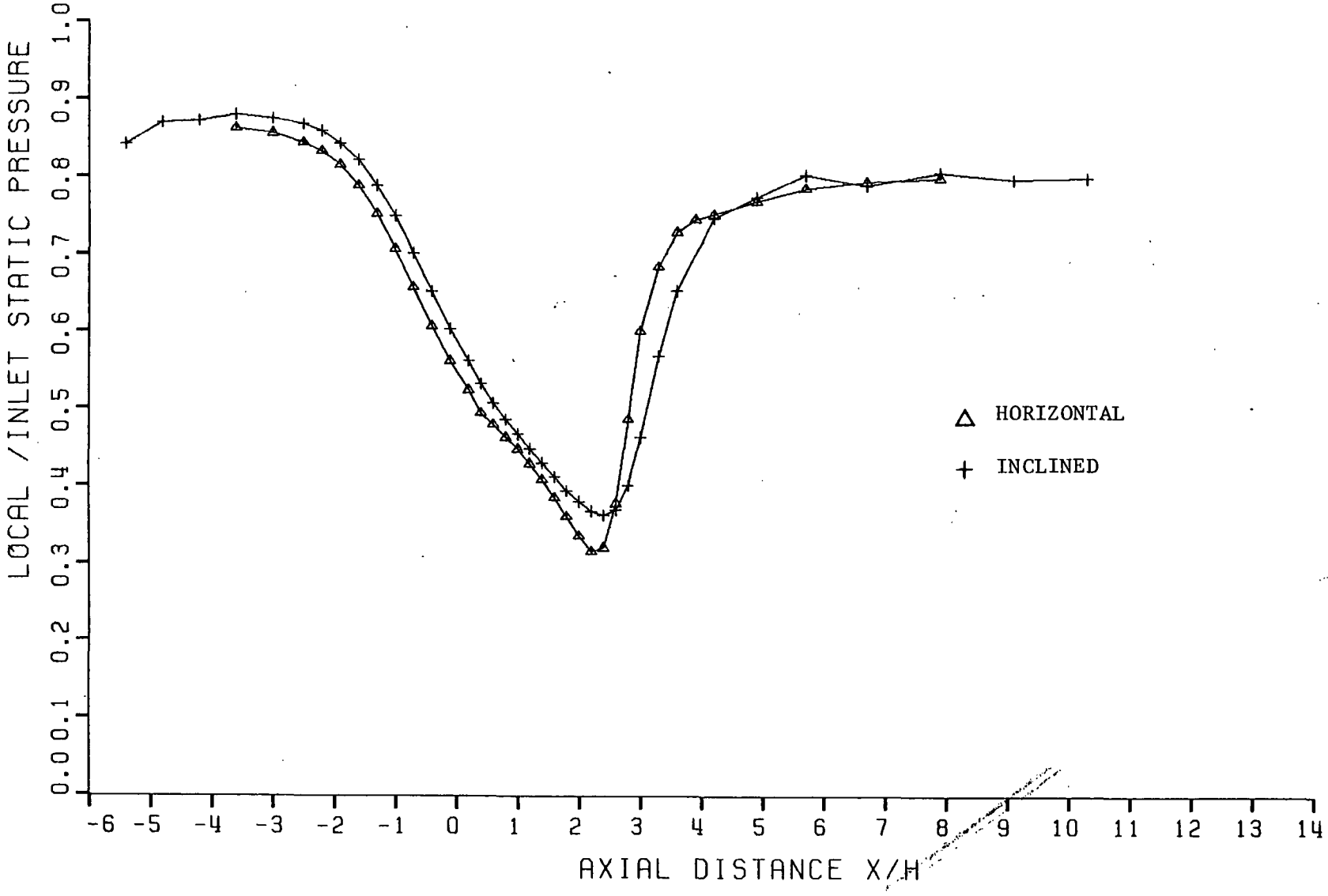

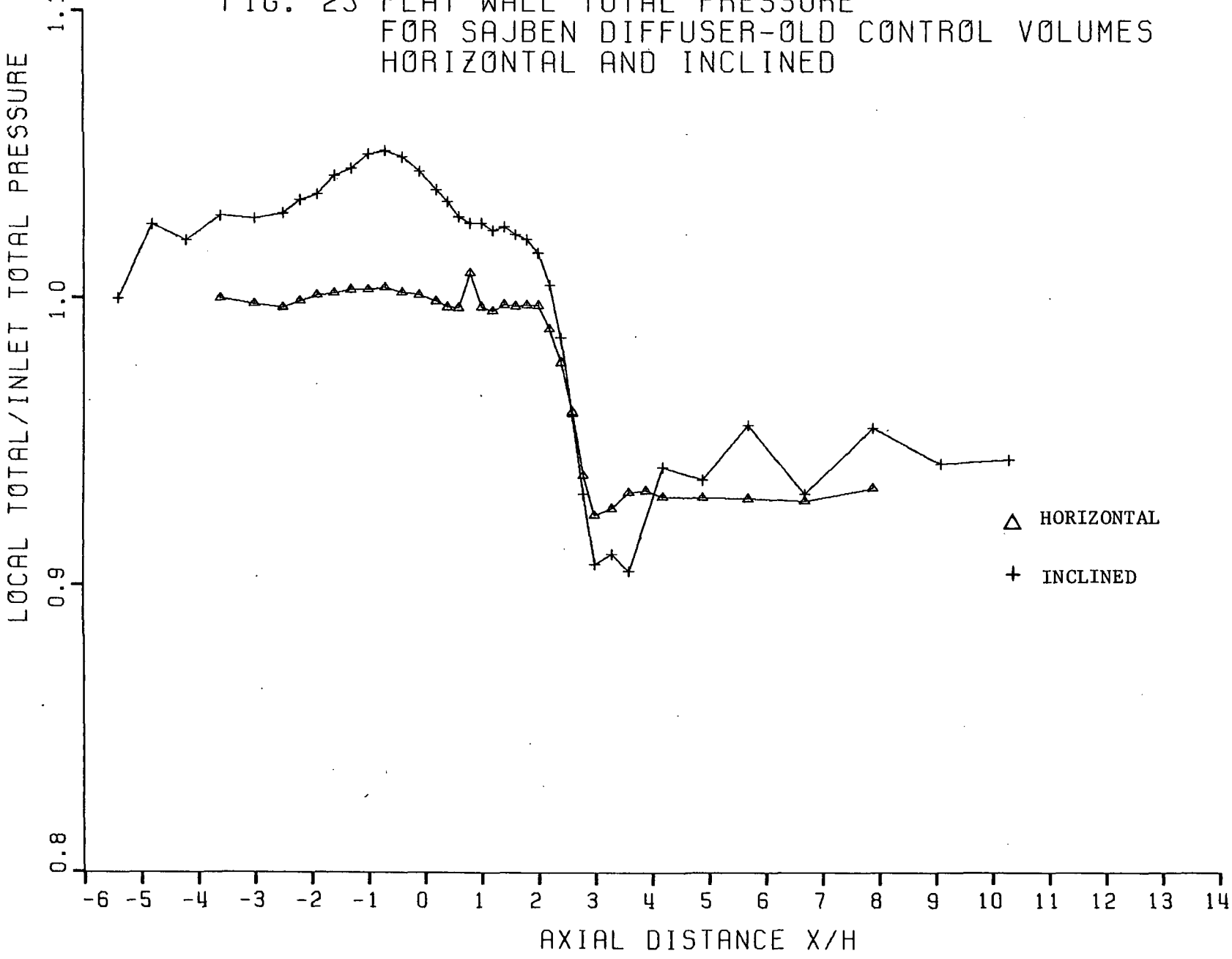
FIG. 23 FLAT WALL TOTAL PRESSURE
FOR SAJBEN DIFFUSER-OLD CONTROL VOLUMES
HORIZONTAL AND INCLINED
LOCAL TOTAL/INLET TOTAL PRESSURE
1.1
1.0
0.9
0.8
-6 -5 -4 -3 -2 -1 0 1 2 3 4 5 6 7 8 9 10 11 12 13 14
AXIAL DISTANCE X/H
HORIZONTAL
INCLINED

FIG. 24 FLAT WALL STATIC PRESSURE
FOR SAJBEN DIFFUSER-NEW CONTROL VOLUMES
HORIZONTAL AND INCLINED

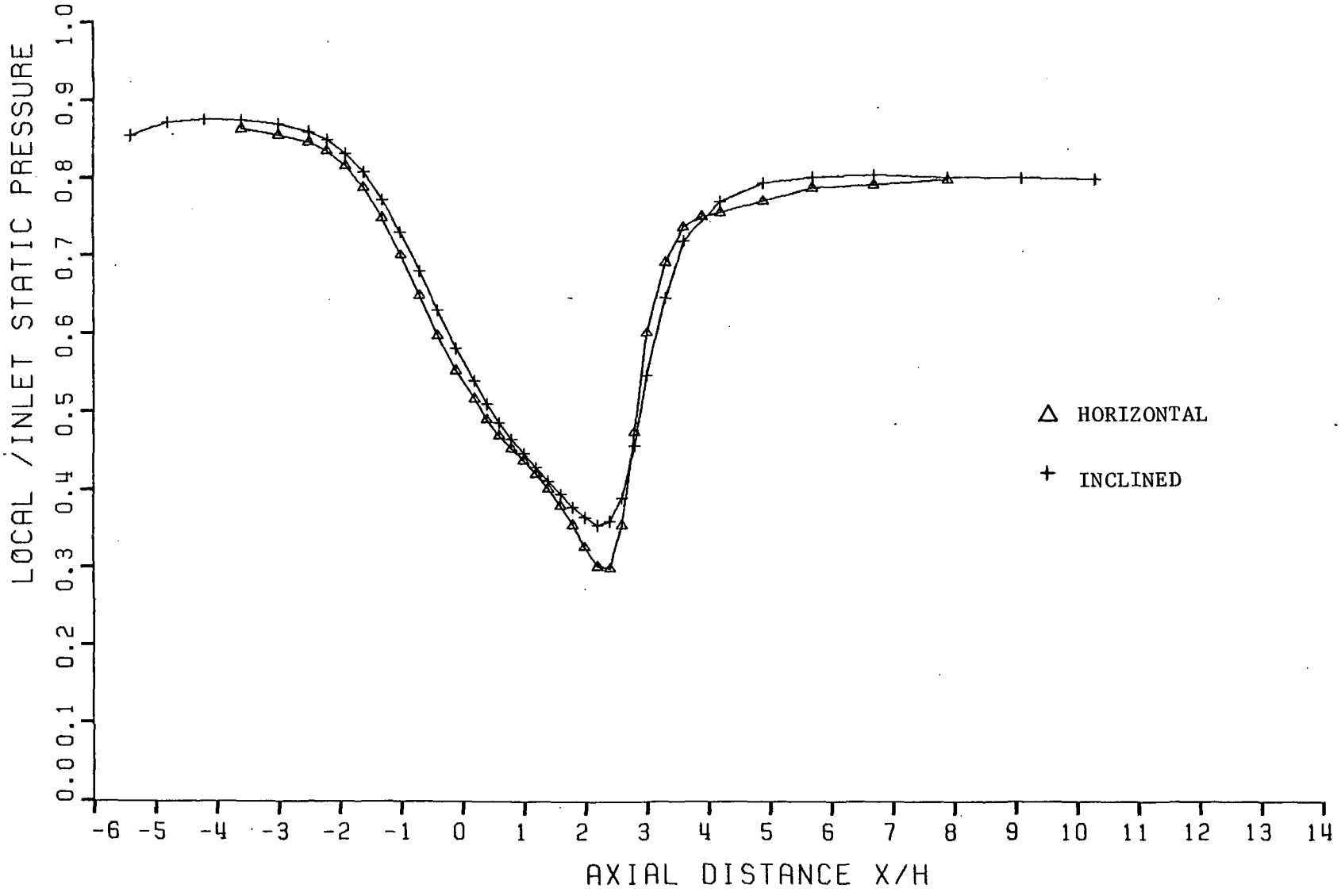

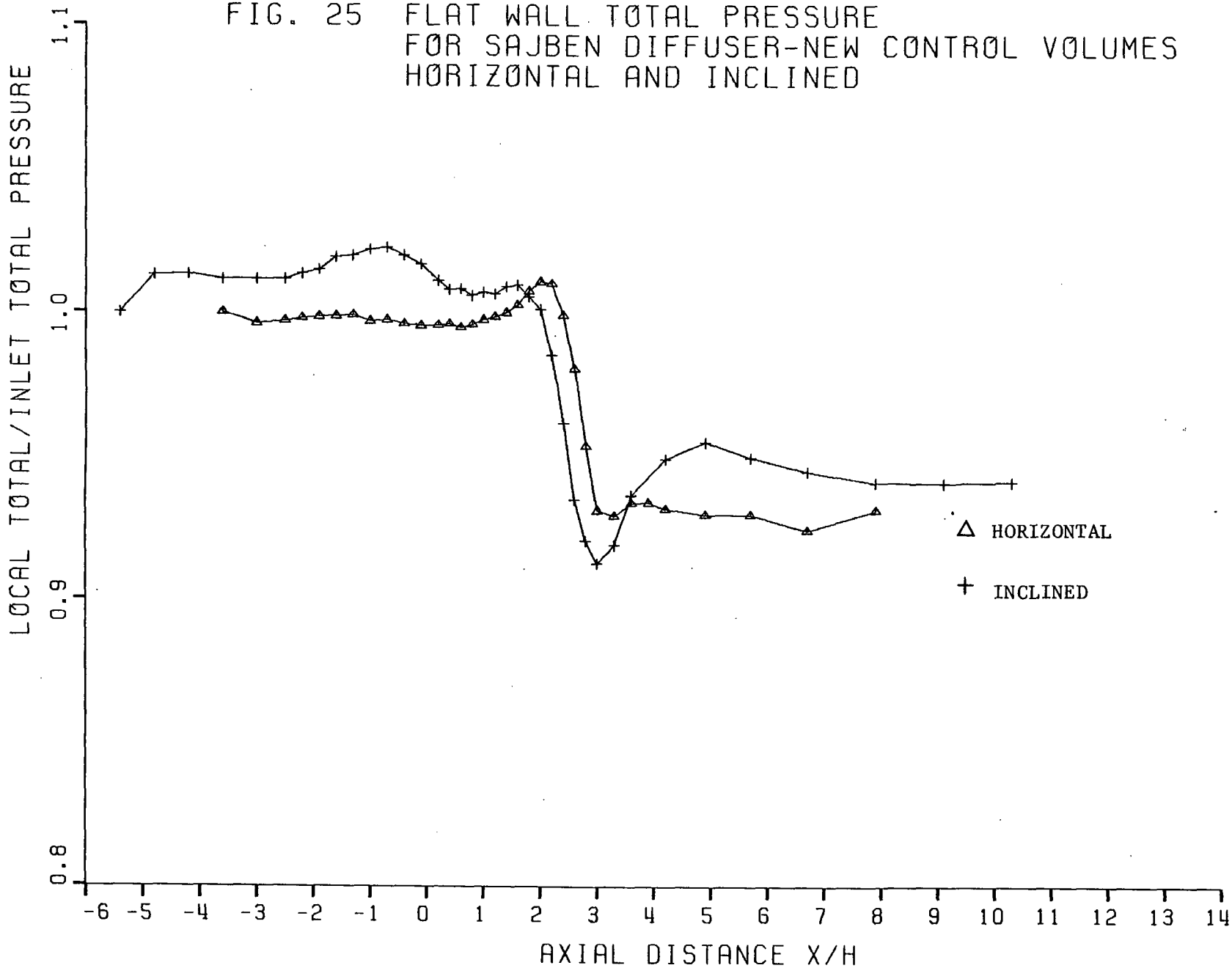
FIG. 25 FLAT WALL TOTAL PRESSURE
FOR SAJBEN DIFFUSER-NEW CONTROL VOLUMES
HORIZONTAL AND INCLINED
LOCAL TOTAL/INLET TOTAL PRESSURE
1.1
1.0
0.9
0.8
-6 -5 -4 -3 -2 -1 0 1 2 3 4 5 6 7 8 9 10 11 12 13 14
AXIAL DISTANCE X/H
HORIZONTAL
INCLINED

FIG. 26 FLAT WALL STATIC PRESSURE FØR SAJBEN DIFFUSER EFFECTIVE PRESSURE VS EFFECTIVE DENSITY METHØD

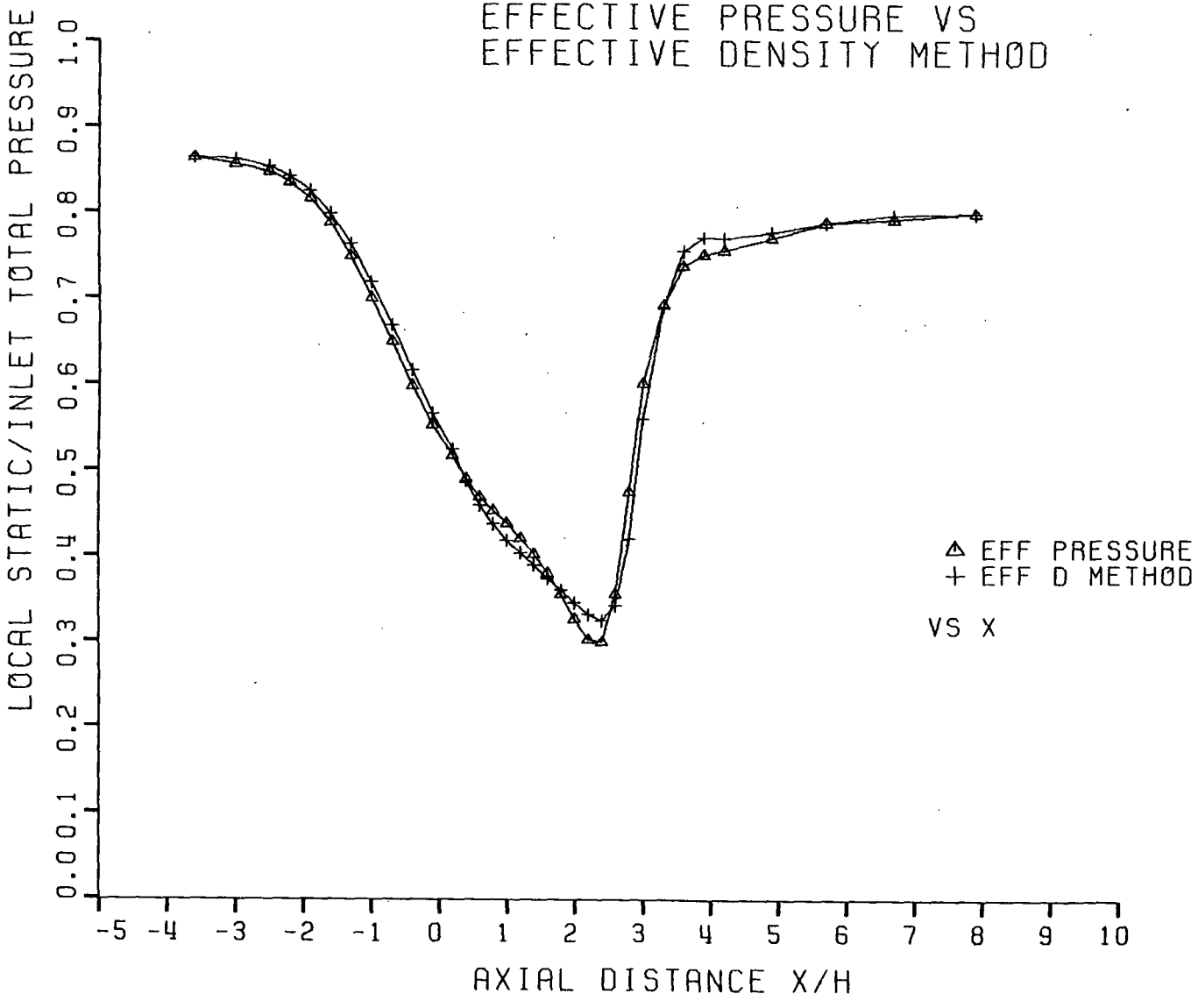

FIG. 27 FLAT WALL TOTAL PRESSURES FOR SAJBEN DIFFUSER EFFECTIVE PRESSURE METHOD VS EFFECTIVE DENSITY METHOD

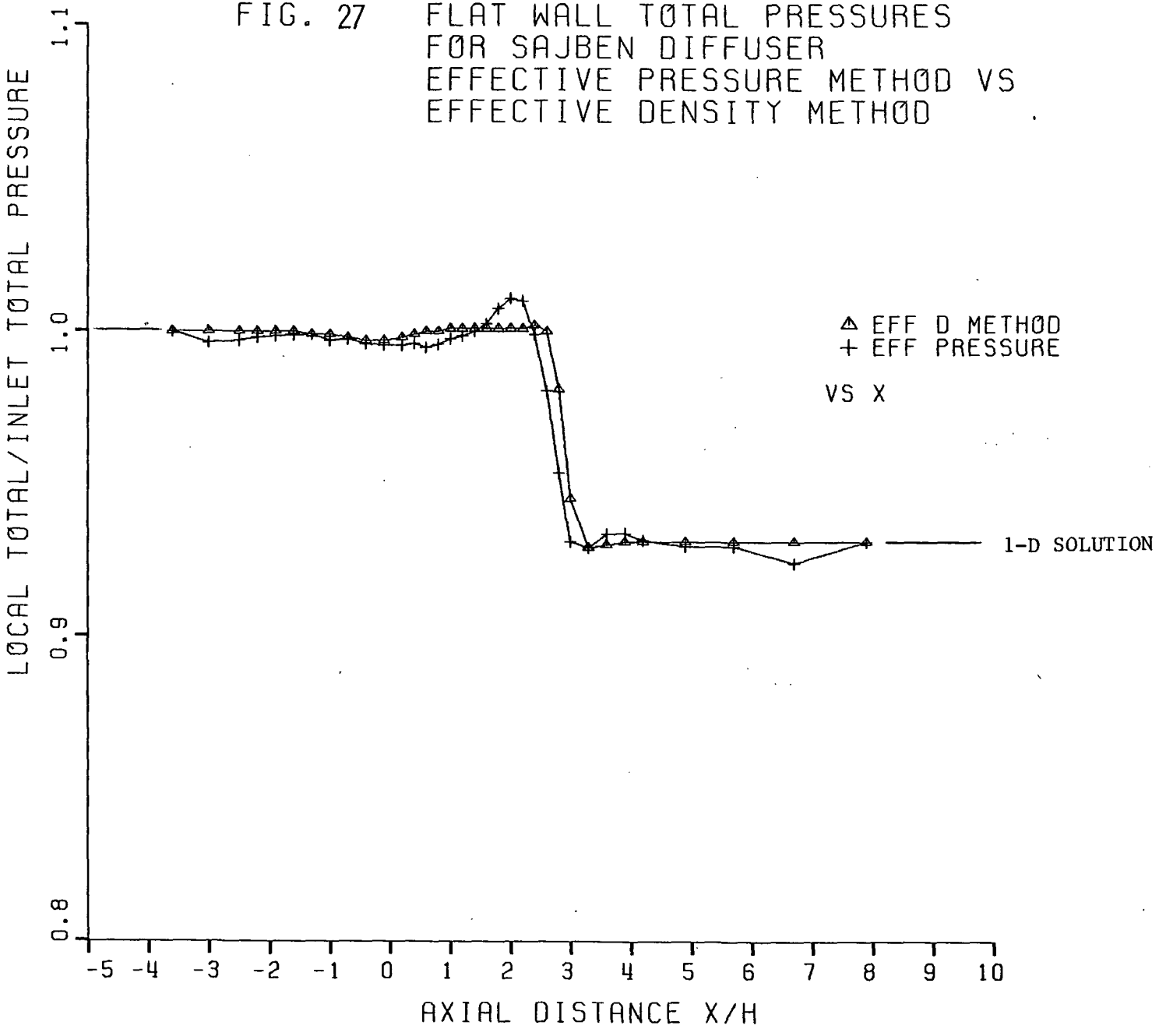

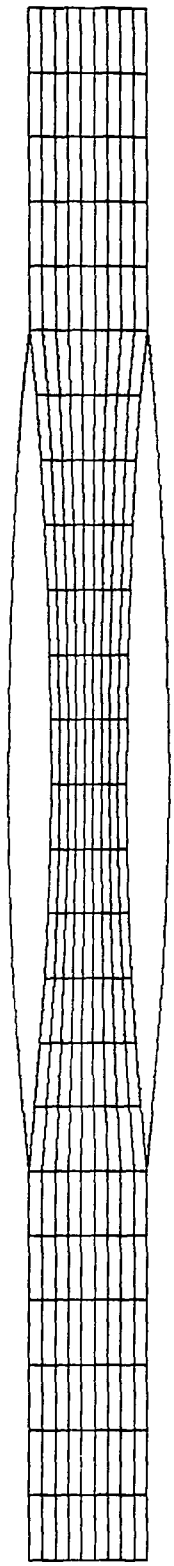

Fig. 28 Straight Cascade Geometry

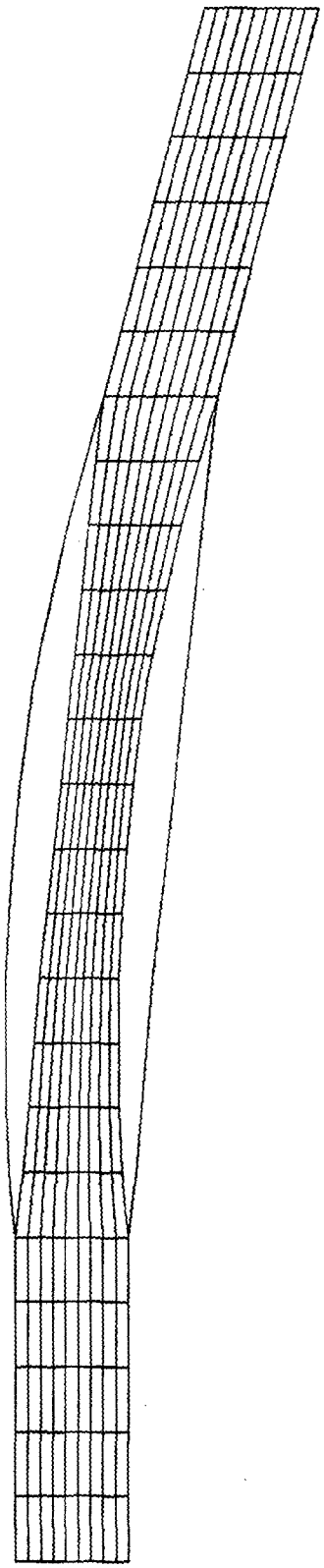

Fig. 29 Curved Cascade Geometry

FIG. 30 MACH NUMBER FOR THE 15 DEGREE CASCADE

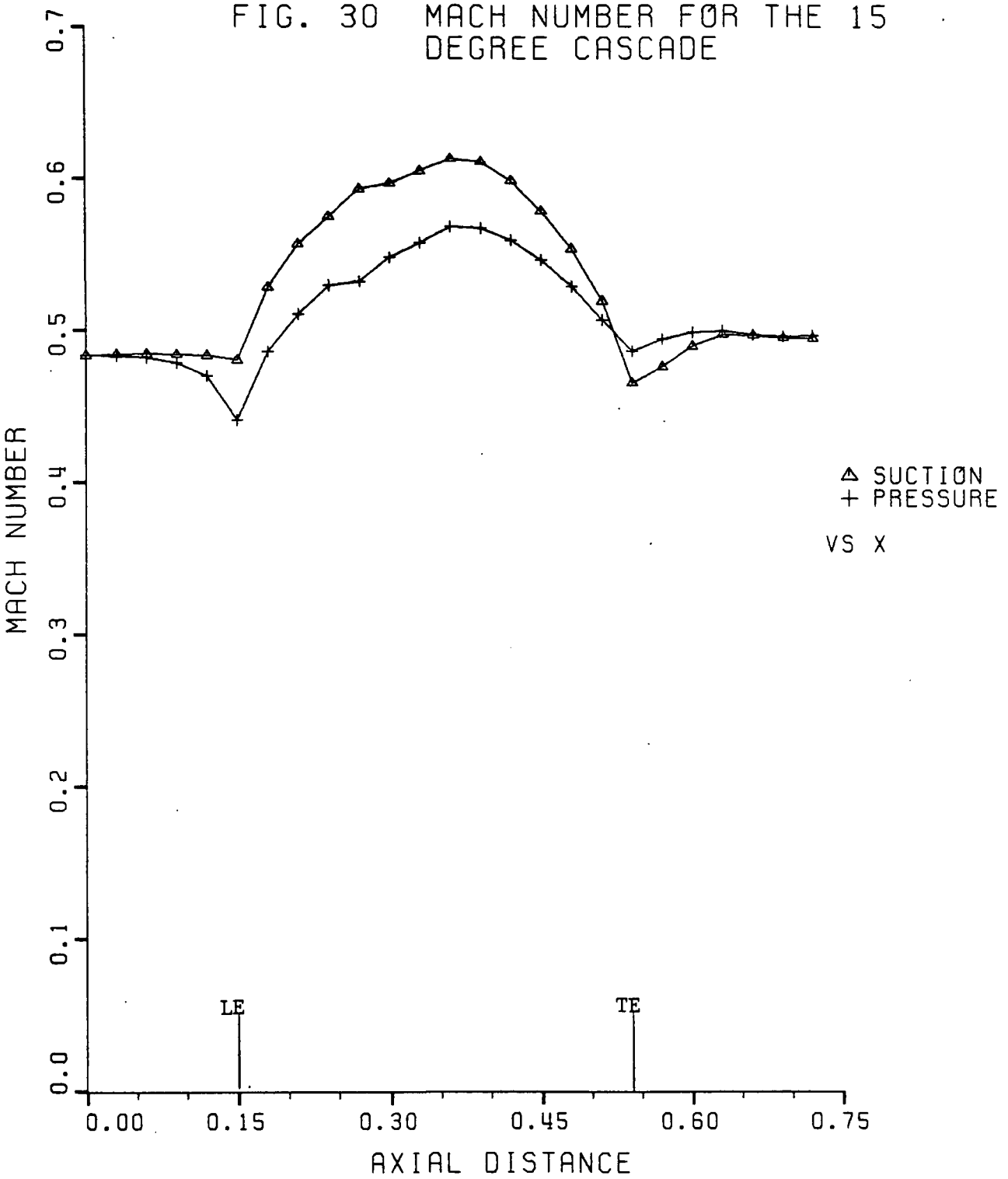

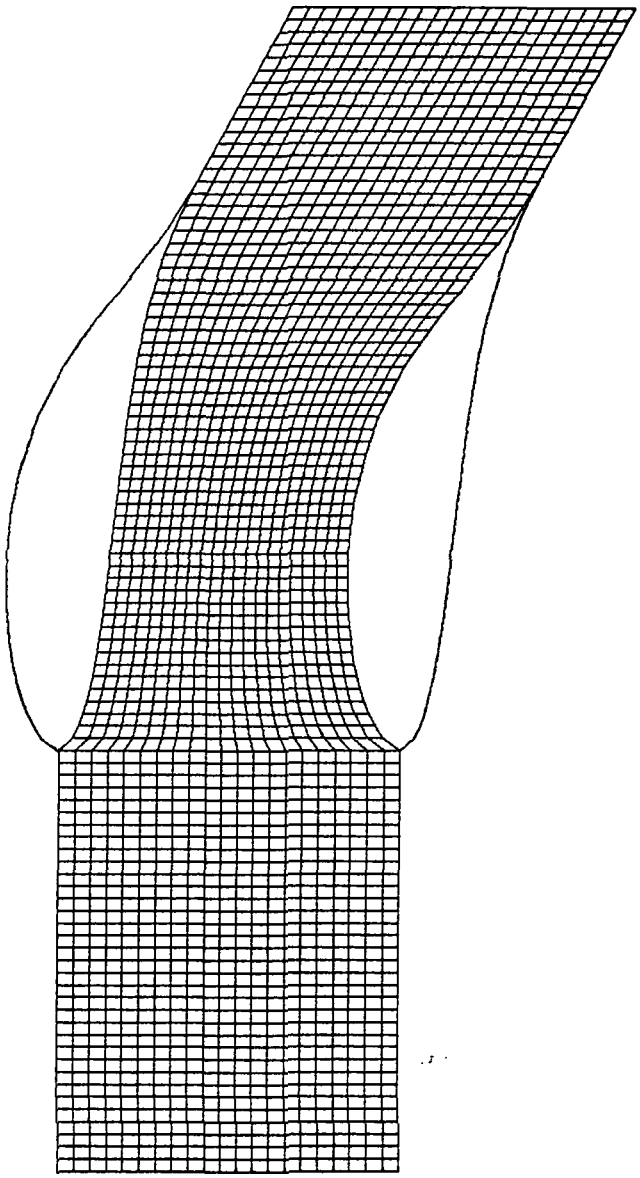

Fig. 31 Inlet Guide Vane Geometry

FIG. 32 TOTAL PRESSURE FOR INLET GUIDE VANE
EFFECTIVE PRESSURE VS EFFECTIVE DENSITY
NEW CONTROL VOLUMES

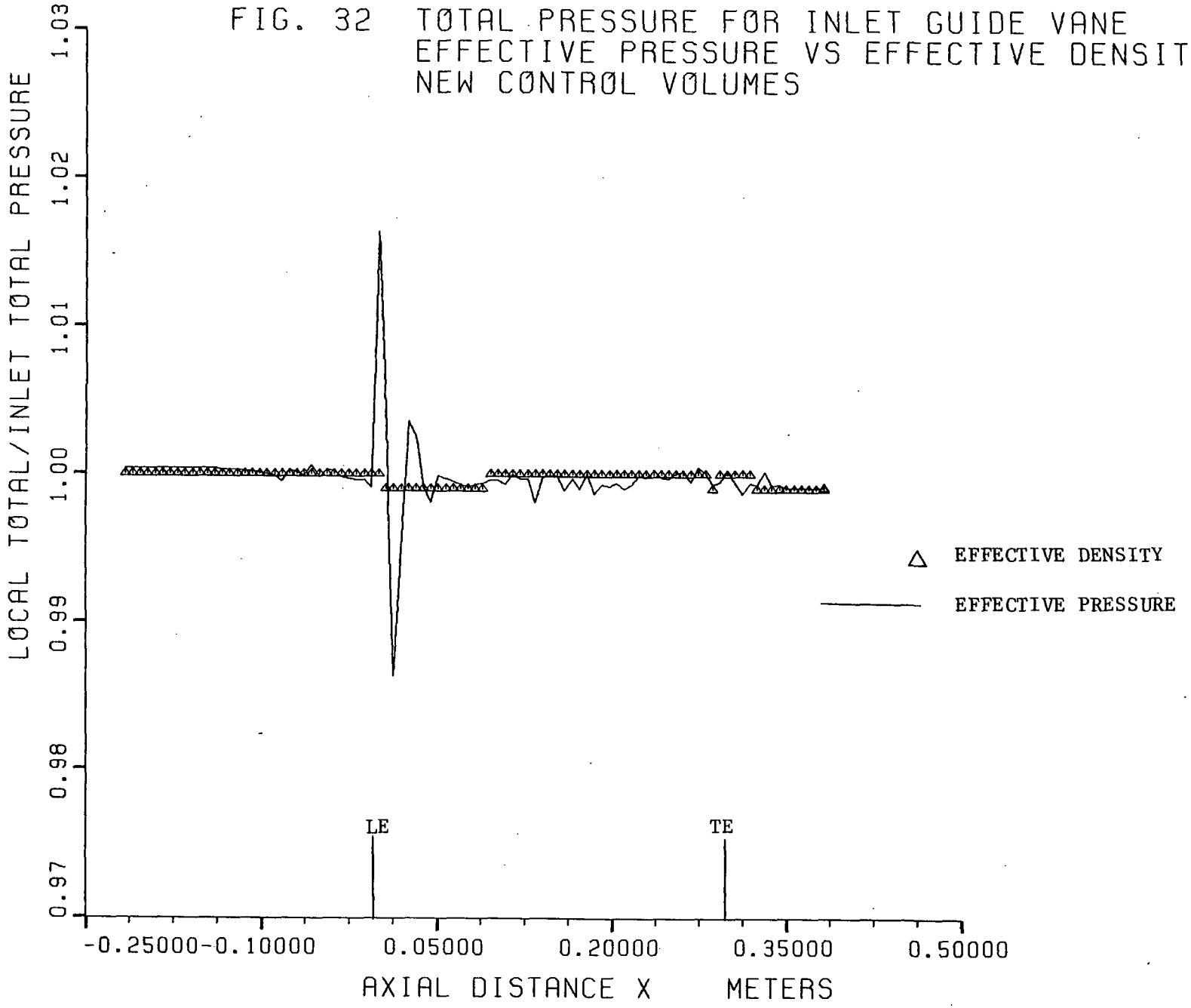

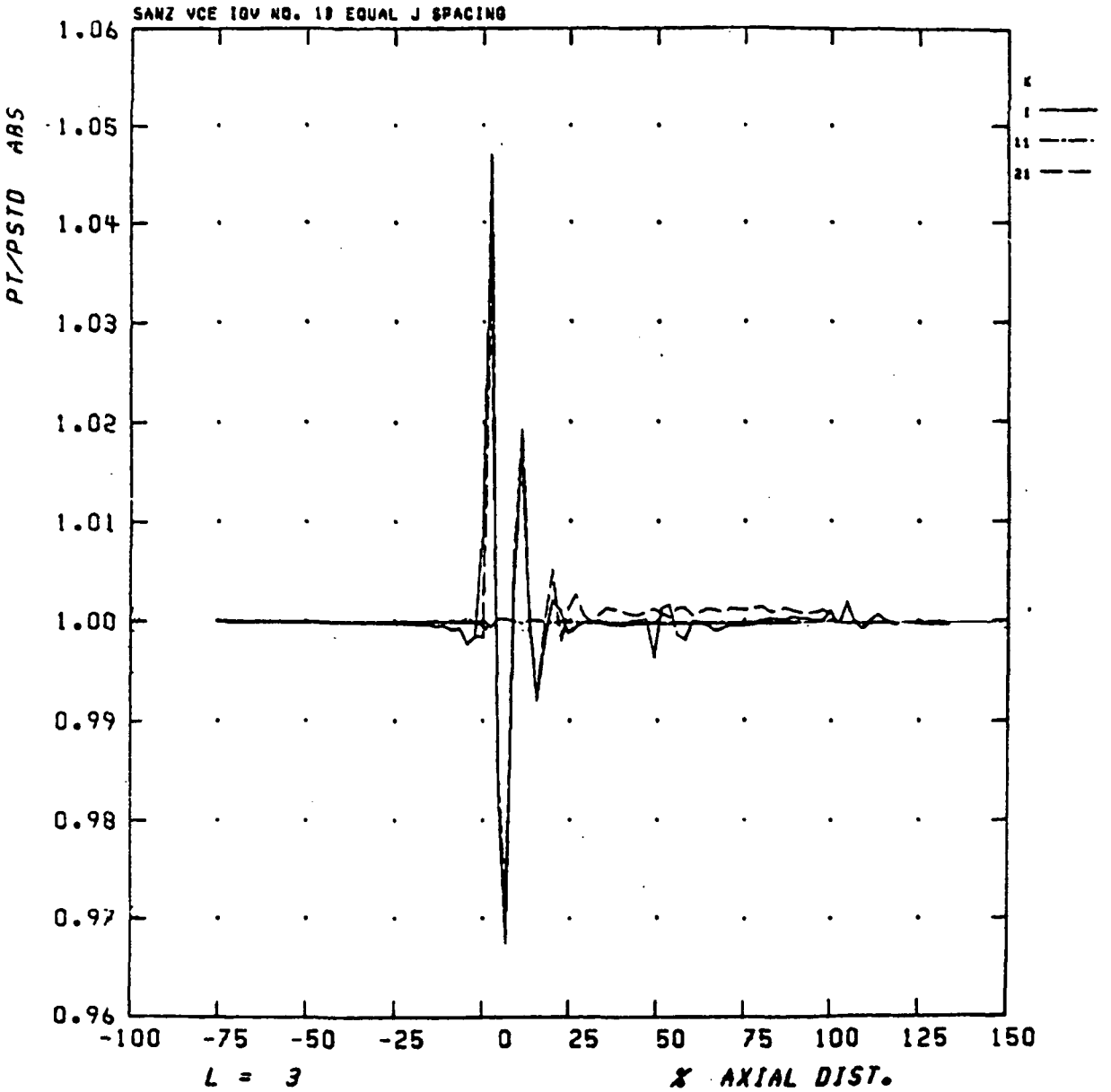

Fig. 33 Total Pressure Distribution for Inlet Guide Vane Using Old Control Volumes

FIG. 34 MACH NUMBER FØR INLET GUIDE VANE

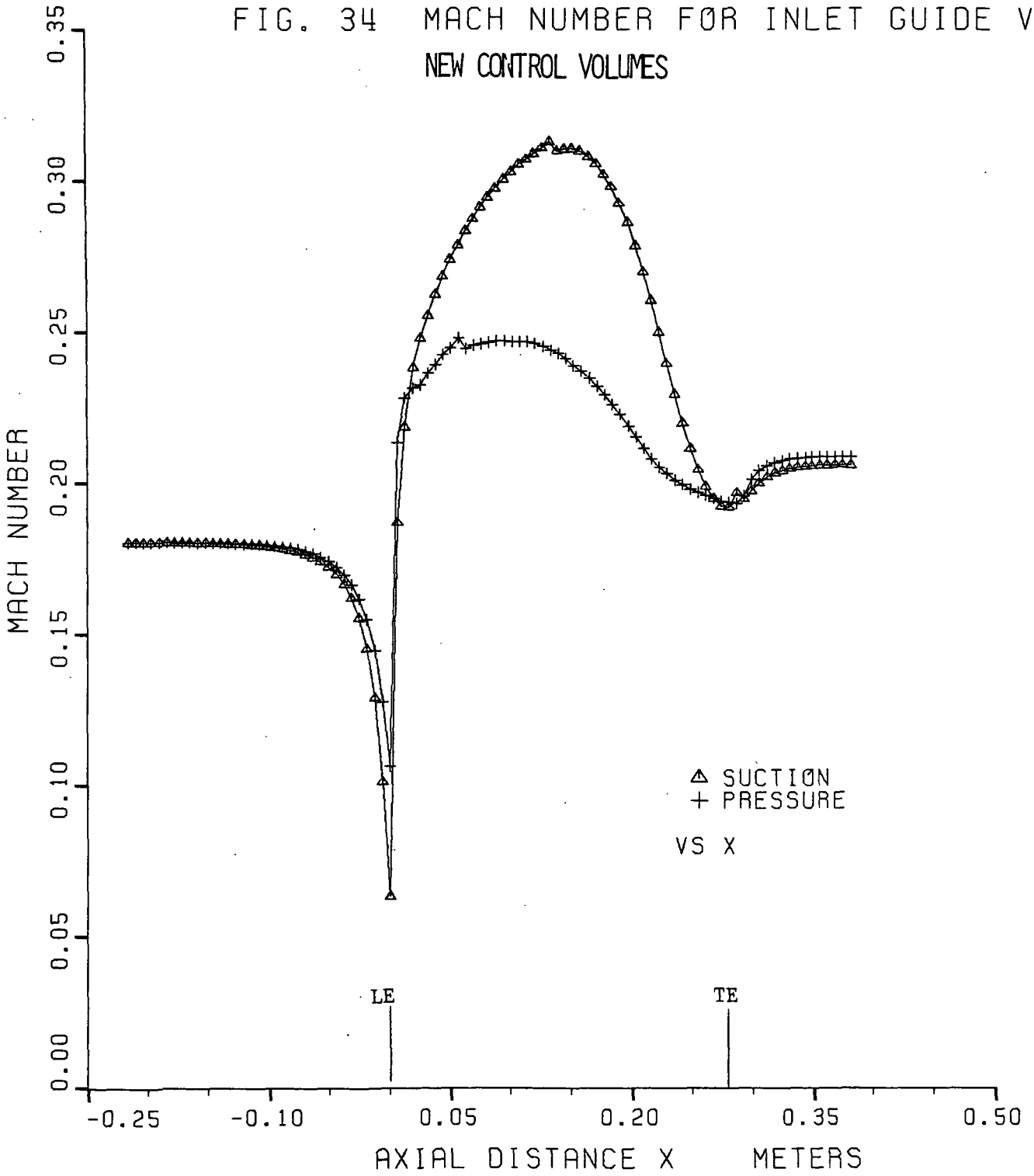

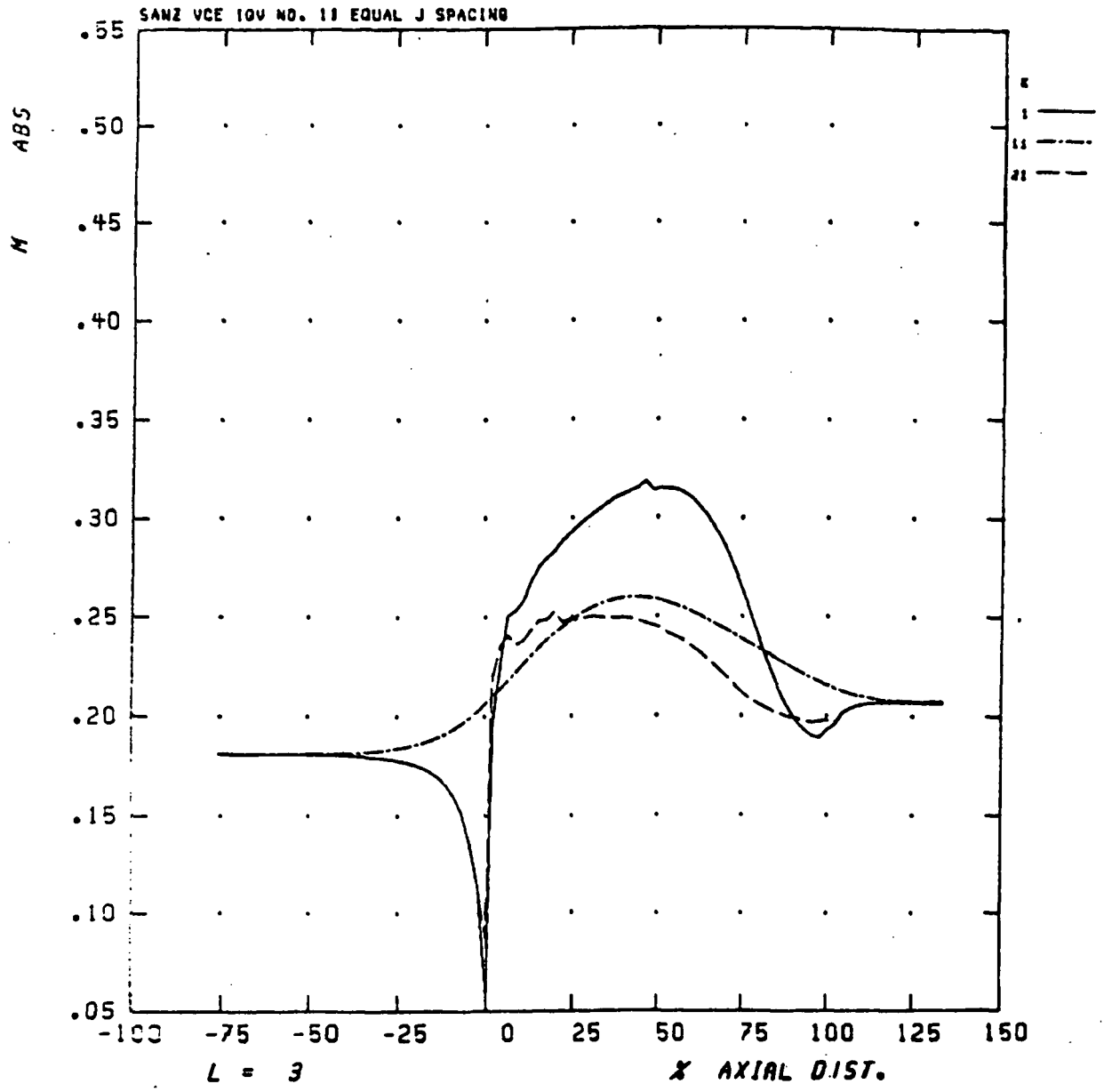

Fig. 35 Mach Number Distribution for Inlet Guide Vane Using Old Control Volumes

Appendix A

Input Files for Summer Calculations

Input File for Sajben's Diffuser

```
7   34   11 2376 2000    4   30    3    0    0    0
1    2    1    1    1    0    0    0
2    3    2
  1.0000
 -3.6000     -3.0000     -2.5000     -2.2000     -1.9000     -1.6000     -1.3000     -1.0000
 -0.7000     -0.4000     -0.1000      0.2000      0.4000      0.6000      0.8000      1.0000
  1.2000      1.4000      1.6000      1.8000      2.0000      2.2000      2.4000      2.6000
  2.8000      3.0000      3.3000      3.6000      3.9000      4.2000      4.9000      5.7000
  6.7000      7.9000
  1.0000
  0.0000      0.0000      0.0000      0.0000      0.0000      0.0000      0.0000      0.0000
  0.0000      0.0000      0.0000      0.0000      0.0000      0.0000      0.0000      0.0000
  0.0000      0.0000      0.0000      0.0000      0.0000      0.0000      0.0000      0.0000
  0.0000      0.0000      0.0000      0.0000      0.0000      0.0000      0.0000      0.0000
  0.0000      0.0000
  1.0000
  0.0000      0.0000      0.0000      0.0000      0.0000      0.0000      0.0000      0.0000
  0.0000      0.0000      0.0000      0.0000      0.0000      0.0000      0.0000      0.0000
  0.0000      0.0000      0.0000      0.0000      0.0000      0.0000      0.0000      0.0000
  0.0000      0.0000      0.0000      0.0000      0.0000      0.0000      0.0000      0.0000
  0.0000      0.0000
  1.0000
900.0000    900.0000    900.0000    900.0000    900.0000    900.0000    900.0000    900.0000
900.0000    900.0000    900.0000    900.0000    900.0000    900.0000    900.0000    900.0000
900.0000    900.0000    900.0000    900.0000    900.0000    900.0000    900.0000    900.0000
900.0000    900.0000    900.0000    900.0000    900.0000    900.0000    900.0000    900.0000
900.0000    900.0000
  1.0000
 -3.6000     -3.0000     -2.5000     -2.2000     -1.9000     -1.6000     -1.3000     -1.0000
 -0.7000     -0.4000     -0.1000      0.2000      0.4000      0.6000      0.8000      1.0000
  1.2000      1.4000      1.6000      1.8000      2.0000      2.2000      2.4000      2.6000
  2.8000      3.0000      3.3000      3.6000      3.9000      4.2000      4.9000      5.7000
  6.7000      7.9000
  1.0000
  0.0000      0.0000      0.0000      0.0000      0.0000      0.0000      0.0000      0.0000
  0.0000      0.0000      0.0000      0.0000      0.0000      0.0000      0.0000      0.0000
  0.0000      0.0000      0.0000      0.0000      0.0000      0.0000      0.0000      0.0000
  0.0000      0.0000      0.0000      0.0000      0.0000      0.0000      0.0000      0.0000
  0.0000      0.0000
  1.0000
  0.0000      0.0000      0.0000      0.0000      0.0000      0.0000      0.0000      0.0000
  0.0000      0.0000      0.0000      0.0000      0.0000      0.0000      0.0000      0.0000
  0.0000      0.0000      0.0000      0.0000      0.0000      0.0000      0.0000      0.0000
  0.0000      0.0000      0.0000      0.0000      0.0000      0.0000      0.0000      0.0000
  0.0000      0.0000
  1.0000
900.7057    900.7057    900.7057    900.6954    900.6580    900.6068    900.5613    900.5295
900.5114    900.5023    900.5000    900.5000    900.5012    900.5034    900.5057    900.5091
900.5137    900.5193    900.5262    900.5330    900.5421    900.5512    900.5614    900.5728
900.5853    900.5978    900.6171    900.6375    900.6568    900.6762    900.7147    900.7421
900.7500    900.7500
  1.0000
 -3.6000     -3.0000     -2.5000     -2.2000     -1.9000     -1.6000     -1.3000     -1.0000
 -0.7000     -0.4000     -0.1000      0.2000      0.4000      0.6000      0.8000      1.0000
  1.2000      1.4000      1.6000      1.8000      2.0000      2.2000      2.4000      2.6000
  2.8000      3.0000      3.3000      3.6000      3.9000      4.2000      4.9000      5.7000
  6.7000      7.9000
```

```
1.0000
0.0000      0.0000      0.0000      0.0000      0.0000      0.0000      0.0000      0.0000
0.0000      0.0000      0.0000      0.0000      0.0000      0.0000      0.0000      0.0000
0.0000      0.0000      0.0000      0.0000      0.0000      0.0000      0.0000      0.0000
0.0000      0.0000      0.0000      0.0000      0.0000      0.0000      0.0000      0.0000
0.0000      0.0000
1.0000
0.0000      0.0000      0.0000      0.0000      0.0000      0.0000      0.0000      0.0000
0.0000      0.0000      0.0000      0.0000      0.0000      0.0000      0.0000      0.0000
0.0000      0.0000      0.0000      0.0000      0.0000      0.0000      0.0000      0.0000
0.0000      0.0000      0.0000      0.0000      0.0000      0.0000      0.0000      0.0000
0.0000      0.0000
1.0000
901.4114    901.4114    901.4114    901.3909    901.3159    901.2136    901.1227    901.0591
901.0227    901.0045    901.0000    901.0000    901.0023    901.0068    901.0114    901.0182
901.0273    901.0386    901.0523    901.0659    901.0841    901.1023    901.1227    901.1455
901.1705    901.1955    901.2341    901.2750    901.3136    901.3523    901.4295    901.4841
901.5000    901.5000
1004.6400     1.4000      0.3000      0.0200      0.0000      0.0000      0.0200      1.7000
25.0000       0.0000      0.2500      1.0000      0.0000
110000.0000 110000.0000 108000.0000 108000.0000   0.0000      0.0000
135000.0000 135000.0000 135000.0000 135000.0000 135000.0000 135000.0000 135000.0000 135000.0000
135000.0000 135000.0000 135000.0000
300.0000    300.0000    300.0000    300.0000    300.0000    300.0000    300.0000    300.0000
300.0000    300.0000    300.0000
0.0000      0.0000      0.0000      0.0000      0.0000      0.0000      0.0000      0.0000
0.0000      0.0000      0.0000
200.0000    200.0000    200.0000    200.0000    200.0000    200.0000    200.0000    200.0000
200.0000    200.0000    200.0000
0.0000      0.0000      0.0000      0.0000      0.0000      0.0000      0.0000      0.0000
0.0000      0.0000      0.0000
0.0000      0.0000      0.0000      0.0000      0.0000      0.0000      0.0000      0.0000
0.0000      0.0000      0.0000
1.0000      1.0000      1.0000      1.0000      1.0000      1.0000      1.0000      1.0000
1.0000      1.0000
1.0000      1.0000      1.0000      1.0000      1.0000      1.0000
 5000 5000 5000 5000 5000
0 1 1 1 1 0 0 0 0 0 1 0 0
1 1 1 1 1 1 1 1 1 1 1 1
    0    0    0    1   16
```

Input File for Inclined Sajben's Diffuser

```
4    38    11 2376 1000     4    34     2     0     0     0
1     2     1    1    1     0     0     0
3     3     2
   1.0000
   0.0000       0.4596       0.9193       1.3789       1.8385       2.2215       2.4513       2.6812
   2.9110       3.1408       3.3706       3.6004       3.8302       4.0600       4.2899       4.4431
   4.5963       4.7495       4.9027       5.0559       5.2091       5.3623       5.5155       5.6687
   5.8219       5.9752       6.1284       6.2816       6.4348       6.6646       6.8944       7.3540
   7.8903       8.5031       9.2691      10.1884      11.1076      12.0269
   1.0000
   0.0000       0.0000       0.0000       0.0000       0.0000       0.0000       0.0000       0.0000
   0.0000       0.0000       0.0000       0.0000       0.0000       0.0000       0.0000       0.0000
   0.0000       0.0000       0.0000       0.0000       0.0000       0.0000       0.0000       0.0000
   0.0000       0.0000       0.0000       0.0000       0.0000       0.0000       0.0000       0.0000
   0.0000       0.0000       0.0000       0.0000       0.0000       0.0000
   1.0000
   0.0000       0.0000       0.0000       0.0000       0.0000       0.0000       0.0000       0.0000
   0.0000       0.0000       0.0000       0.0000       0.0000       0.0000       0.0000       0.0000
   0.0000       0.0000       0.0000       0.0000       0.0000       0.0000       0.0000       0.0000
   0.0000       0.0000       0.0000       0.0000       0.0000       0.0000       0.0000       0.0000
   0.0000       0.0000       0.0000       0.0000       0.0000       0.0000
   1.0000
 900.0000     900.3857     900.7713     901.1570     901.5427     901.8641     902.0569     902.2498
 902.4426     902.6354     902.8283     903.0211     903.2139     903.4068     903.5996     903.7282
 903.8567     903.9853     904.1138     904.2424     904.3710     904.4995     904.6281     904.7566
 904.8852     905.0137     905.1423     905.2709     905.3994     905.5923     905.7851     906.1708
 906.6207     907.1349     907.7777     908.5491     909.3204     910.0918
   1.0000
   0.0000       0.4596       0.9193       1.3789       1.8385       2.2215       2.4513       2.6812
   2.9110       3.1408       3.3706       3.6004       3.8302       4.0600       4.2899       4.4431
   4.5963       4.7495       4.9027       5.0559       5.2091       5.3623       5.5155       5.6687
   5.8219       5.9752       6.1284       6.2816       6.4348       6.6646       6.8944       7.3540
   7.8903       8.5031       9.2691      10.1884      11.1076      12.0269
   1.0000
   0.0000       0.0000       0.0000       0.0000       0.0000       0.0000       0.0000       0.0000
   0.0000       0.0000       0.0000       0.0000       0.0000       0.0000       0.0000       0.0000
   0.0000       0.0000       0.0000       0.0000       0.0000       0.0000       0.0000       0.0000
   0.0000       0.0000       0.0000       0.0000       0.0000       0.0000       0.0000       0.0000
   0.0000       0.0000       0.0000       0.0000       0.0000       0.0000
   1.0000
   0.0000       0.0000       0.0000       0.0000       0.0000       0.0000       0.0000       0.0000
   0.0000       0.0000       0.0000       0.0000       0.0000       0.0000       0.0000       0.0000
   0.0000       0.0000       0.0000       0.0000       0.0000       0.0000       0.0000       0.0000
   0.0000       0.0000       0.0000       0.0000       0.0000       0.0000       0.0000       0.0000
   0.0000       0.0000       0.0000       0.0000       0.0000       0.0000
   1.0000
```

```
    901.8425    902.2281    902.6138    902.9985    903.2589    903.4091    903.5114    903.6347
    903.7818    903.9504    904.1345    904.3269    904.5238    904.7255    904.9327    905.0743
    905.2188    905.3664    905.5172    905.6712    905.8284    905.9886    906.1514    906.3166
    906.4835    906.6515    906.8198    906.9877    907.1542    907.4000    907.6389    908.0909
    908.5743    909.0930    909.7358    910.5072    911.2785    912.0499
   1004.6400      1.4000      0.3000      0.0200      0.0000      0.0000      0.0080      1.7000
     25.0000      0.0000      0.2500      1.0000      0.0000
 110000.0000 110000.0000 108000.0000 108000.0000      0.0000      0.0000
 135000.0000 135000.0000 135000.0000 135000.0000 135000.0000 135000.0000 135000.0000 135000.0000
 135000.0000 135000.0000 135000.0000
    300.0000    300.0000    300.0000    300.0000    300.0000    300.0000    300.0000    300.0000
    300.0000    300.0000    300.0000
      0.0000      0.0000      0.0000      0.0000      0.0000      0.0000      0.0000      0.0000
      0.0000      0.0000      0.0000
    200.0000    200.0000    200.0000    200.0000    200.0000    200.0000    200.0000    200.0000
    200.0000    200.0000    200.0000
      0.0000      0.0000      0.0000      0.0000      0.0000      0.0000      0.0000      0.0000
      0.0000      0.0000      0.0000
     40.0000     40.0000     40.0000     40.0000     40.0000     40.0000     40.0000     40.0000
     40.0000     40.0000     40.0000
      1.0000      1.0000      1.0000      1.0000      1.0000      1.0000      1.0000      1.0000
      1.0000      1.0000
      1.0000      1.0000      1.0000
 5000 5000 5000 5000 5000
0 1 0 1 1 0 1 0 0 1 1 1 0
1 1 1 1 1 1 1 1 1 1 1
    0    0    0    1   16
```

Input File for Straight Cascade

```
10   25    4   22 1000    6   19    4     0     0     0
 1    2    1    1    1    0    0    0
 3    4    3
   0.3048
   0.0000      0.0300      0.0600      0.0900      0.1200      0.1500      0.1800      0.2100
   0.2400      0.2700      0.3000      0.3300      0.3600      0.3900      0.4200      0.4500
   0.4800      0.5100      0.5400      0.5700      0.6000      0.6300      0.6600      0.6900
   0.7200
   0.3048
   0.0000      0.0000      0.0000      0.0000      0.0000      0.0000      0.0033      0.0050
   0.0069      0.0081      0.0090      0.0096      0.0099      0.0096      0.0086      0.0071
   0.0050      0.0025      0.0000      0.0000      0.0000      0.0000      0.0000      0.0000
   0.0000
   0.3048
   0.0000      0.0000      0.0000      0.0000      0.0000      0.0000      0.0066      0.0106
   0.0137      0.0162      0.0180      0.0192      0.0199      0.0191      0.0171      0.0141
   0.0101      0.0050      0.0000      0.0000      0.0000      0.0000      0.0000      0.0000
   0.0000
   0.3048
   0.1829      0.1829      0.1829      0.1829      0.1829      0.1829      0.1829      0.1829
   0.1829      0.1829      0.1829      0.1829      0.1829      0.1829      0.1829      0.1829
   0.1829      0.1829      0.1829      0.1829      0.1829      0.1829      0.1829      0.1829
   0.1829
   0.3048
   0.0000      0.0300      0.0600      0.0900      0.1200      0.1500      0.1800      0.2100
   0.2400      0.2700      0.3000      0.3300      0.3600      0.3900      0.4200      0.4500
   0.4800      0.5100      0.5400      0.5700      0.6000      0.6300      0.6600      0.6900
   0.7200
   0.3048
   0.0000      0.0000      0.0000      0.0000      0.0000      0.0000      0.0033      0.0050
   0.0069      0.0081      0.0090      0.0096      0.0099      0.0096      0.0086      0.0071
   0.0050      0.0025      0.0000      0.0000      0.0000      0.0000      0.0000      0.0000
   0.0000
   0.3048
   0.0000      0.0000      0.0000      0.0000      0.0000      0.0000      0.0066      0.0106
   0.0137      0.0162      0.0180      0.0192      0.0199      0.0191      0.0171      0.0141
   0.0101      0.0050      0.0000      0.0000      0.0000      0.0000      0.0000      0.0000
   0.0000
   0.3048
   0.1859      0.1859      0.1859      0.1859      0.1859      0.1859      0.1859      0.1859
   0.1859      0.1859      0.1859      0.1859      0.1859      0.1859      0.1859      0.1859
   0.1859      0.1859      0.1859      0.1859      0.1859      0.1859      0.1859      0.1859
   0.1859
   0.3048
   0.0000      0.0300      0.0600      0.0900      0.1200      0.1500      0.1800      0.2100
   0.2400      0.2700      0.3000      0.3300      0.3600      0.3900      0.4200      0.4500
   0.4800      0.5100      0.5400      0.5700      0.6000      0.6300      0.6600      0.6900
```

```
 0.7200
 0.3048
 0.0000      0.0000      0.0000      0.0000      0.0000      0.0000      0.0033      0.0050
 0.0069      0.0081      0.0090      0.0096      0.0099      0.0096      0.0086      0.0071
 0.0050      0.0025      0.0000      0.0000      0.0000      0.0000      0.0000      0.0000
 0.0000
 0.3048
 0.0000      0.0000      0.0000      0.0000      0.0000      0.0000      0.0066      0.0106
 0.0137      0.0162      0.0180      0.0192      0.0199      0.0191      0.0171      0.0141
 0.0101      0.0050      0.0000      0.0000      0.0000      0.0000      0.0000      0.0000
 0.0000
 0.3048
 0.1890      0.1890      0.1890      0.1890      0.1890      0.1890      0.1890      0.1890
 0.1890      0.1890      0.1890      0.1890      0.1890      0.1890      0.1890      0.1890
 0.1890      0.1890      0.1890      0.1890      0.1890      0.1890      0.1890      0.1890
 0.1890
 0.3048
 0.0000      0.0300      0.0600      0.0900      0.1200      0.1500      0.1800      0.2100
 0.2400      0.2700      0.3000      0.3300      0.3600      0.3900      0.4200      0.4500
 0.4800      0.5100      0.5400      0.5700      0.6000      0.6300      0.6600      0.6900
 0.7200
 0.3048
 0.0000      0.0000      0.0000      0.0000      0.0000      0.0000      0.0033      0.0050
 0.0069      0.0081      0.0090      0.0096      0.0099      0.0096      0.0086      0.0071
 0.0050      0.0025      0.0000      0.0000      0.0000      0.0000      0.0000      0.0000
 0.0000
 0.3048
 0.0000      0.0000      0.0000      0.0000      0.0000      0.0000      0.0066      0.0106
 0.0137      0.0162      0.0180      0.0192      0.0199      0.0191      0.0171      0.0141
 0.0101      0.0050      0.0000      0.0000      0.0000      0.0000      0.0000      0.0000
 0.0000
 0.3048
 0.1920      0.1920      0.1920      0.1920      0.1920      0.1920      0.1920      0.1920
 0.1920      0.1920      0.1920      0.1920      0.1920      0.1920      0.1920      0.1920
 0.1920      0.1920      0.1920      0.1920      0.1920      0.1920      0.1920      0.1920
 0.1920
1004.5080      1.4000      0.2000      0.0000      0.0000      0.0000      0.0200      1.7000
  35.0000      0.0020      0.1000      4.0000      0.0000
85440.0000  85440.0000  85440.0000  85440.0000      0.0000      0.0000
101352.9000 101352.9000 101352.9000      0.0000
  288.1670    288.1660    288.1660      0.0000
    0.0000      0.0000      0.0000      0.0000
  150.0000    150.0000    150.0000      0.0000
    0.0000      0.0000      0.0000      0.0000
    0.0000      0.0000      0.0000      0.0000
    1.0000      1.0000      1.0000
    1.0000      1.0000      1.0000      1.0000      1.0000      1.0000      1.0000      1.0000
    1.0000
 5000 5000 5000 5000 5000
0 1 1 1 1 0 0 0 0 0 1 0 0
1 1 1 1
    0    0    0    0    0
```

Input File for Curved Cascade

```
10   25    4   22 1000    6   19    4    0    0    0
 1    2    1    1    1    0    0    0
 3    4    3
   0.3048
   0.0000      0.0300      0.0600      0.0900      0.1200      0.1500      0.1800      0.2100
   0.2400      0.2700      0.3000      0.3300      0.3600      0.3900      0.4200      0.4500
   0.4800      0.5100      0.5400      0.5700      0.6000      0.6300      0.6600      0.6900
   0.7200
   0.3048
   0.0000      0.0000      0.0000      0.0000      0.0000      0.0000      0.0030      0.0043
   0.0046      0.0043      0.0027      0.0005     -0.0025     -0.0066     -0.0119     -0.0183
  -0.0256     -0.0340     -0.0429     -0.0510     -0.0590     -0.0671     -0.0751     -0.0831
  -0.0912
   0.3048
   0.0000      0.0000      0.0000      0.0000      0.0000      0.0000      0.0066      0.0106
   0.0137      0.0162      0.0180      0.0192      0.0199      0.0191      0.0171      0.0141
   0.0101      0.0050      0.0000      0.0000      0.0000      0.0000      0.0000      0.0000
   0.0000
   0.3048
   0.1829      0.1829      0.1829      0.1829      0.1829      0.1829      0.1829      0.1829
   0.1829      0.1829      0.1829      0.1829      0.1829      0.1829      0.1829      0.1829
   0.1829      0.1829      0.1829      0.1829      0.1829      0.1829      0.1829      0.1829
   0.1829
   0.3048
   0.0000      0.0300      0.0600      0.0900      0.1200      0.1500      0.1800      0.2100
   0.2400      0.2700      0.3000      0.3300      0.3600      0.3900      0.4200      0.4500
   0.4800      0.5100      0.5400      0.5700      0.6000      0.6300      0.6600      0.6900
   0.7200
   0.3048
   0.0000      0.0000      0.0000      0.0000      0.0000      0.0000      0.0030      0.0043
   0.0046      0.0043      0.0027      0.0005     -0.0025     -0.0066     -0.0119     -0.0183
  -0.0256     -0.0340     -0.0429     -0.0510     -0.0590     -0.0671     -0.0751     -0.0831
  -0.0912
   0.3048
   0.0000      0.0000      0.0000      0.0000      0.0000      0.0000      0.0066      0.0106
   0.0137      0.0162      0.0180      0.0192      0.0199      0.0191      0.0171      0.0141
   0.0101      0.0050      0.0000      0.0000      0.0000      0.0000      0.0000      0.0000
   0.0000
   0.3048
   0.1859      0.1859      0.1859      0.1859      0.1859      0.1859      0.1859      0.1859
   0.1859      0.1859      0.1859      0.1859      0.1859      0.1859      0.1859      0.1859
   0.1859      0.1859      0.1859      0.1859      0.1859      0.1859      0.1859      0.1859
   0.1859
   0.3048
   0.0000      0.0300      0.0600      0.0900      0.1200      0.1500      0.1800      0.2100
   0.2400      0.2700      0.3000      0.3300      0.3600      0.3900      0.4200      0.4500
   0.4800      0.5100      0.5400      0.5700      0.6000      0.6300      0.6600      0.6900
```

```
 0.7200
 0.3048
 0.0000      0.0000      0.0000      0.0000      0.0000      0.0000      0.0030      0.0043
 0.0046      0.0043      0.0027      0.0005     -0.0025     -0.0066     -0.0119     -0.0183
-0.0256     -0.0340     -0.0429     -0.0510     -0.0590     -0.0671     -0.0751     -0.0831
-0.0912
 0.3048
 0.0000      0.0000      0.0000      0.0000      0.0000      0.0000      0.0066      0.0106
 0.0137      0.0162      0.0180      0.0192      0.0199      0.0191      0.0171      0.0141
 0.0101      0.0050      0.0000      0.0000      0.0000      0.0000      0.0000      0.0000
 0.0000
 0.3048
 0.1890      0.1890      0.1890      0.1890      0.1890      0.1890      0.1890      0.1890
 0.1890      0.1890      0.1890      0.1890      0.1890      0.1890      0.1890      0.1890
 0.1890      0.1890      0.1890      0.1890      0.1890      0.1890      0.1890      0.1890
 0.1890
 0.3048
 0.0000      0.0300      0.0600      0.0900      0.1200      0.1500      0.1800      0.2100
 0.2400      0.2700      0.3000      0.3300      0.3600      0.3900      0.4200      0.4500
 0.4800      0.5100      0.5400      0.5700      0.6000      0.6300      0.6600      0.6900
 0.7200
 0.3048
 0.0000      0.0000      0.0000      0.0000      0.0000      0.0000      0.0030      0.0043
 0.0046      0.0043      0.0027      0.0005     -0.0025     -0.0066     -0.0119     -0.0183
-0.0256     -0.0340     -0.0429     -0.0510     -0.0590     -0.0671     -0.0751     -0.0831
-0.0912
 0.3048
 0.0000      0.0000      0.0000      0.0000      0.0000      0.0000      0.0066      0.0106
 0.0137      0.0162      0.0180      0.0192      0.0199      0.0191      0.0171      0.0141
 0.0101      0.0050      0.0000      0.0000      0.0000      0.0000      0.0000      0.0000
 0.0000
 0.3048
 0.1920      0.1920      0.1920      0.1920      0.1920      0.1920      0.1920      0.1920
 0.1920      0.1920      0.1920      0.1920      0.1920      0.1920      0.1920      0.1920
 0.1920      0.1920      0.1920      0.1920      0.1920      0.1920      0.1920      0.1920
 0.1920
1004.5080    1.4000      0.2000      0.0000      0.0000      0.0000      0.0200      1.7000
  35.0000    0.0020      0.1000      4.0000      0.0000
85440.0000  85440.0000  85440.0000  85440.0000  0.0000      0.0000
101352.9000 101352.9000 101352.9000 0.0000
 288.1670    288.1660    288.1660    0.0000
   0.0000      0.0000      0.0000    0.0000
 150.0000    150.0000    150.0000    0.0000
   0.0000      0.0000      0.0000    0.0000
   0.0000      0.0000      0.0000    0.0000
   1.0000      1.0000      1.0000
   1.0000      1.0000      1.0000    1.0000      1.0000      1.0000      1.0000      1.0000
   1.0000
 5000 5000 5000 5000 5000
0 1 1 1 1 0 0 0 0 0 1 0 0
1 1 1 1
   0    0    0    0    0
```

Input File for Inlet Guide Vane

```
22   95    5 1800 1000   35   81    2    0    0    0
 1    2    0    1    1    0    0    0
 3    5    2
   1.0000
  -0.2163     -0.2099     -0.2035     -0.1972     -0.1908     -0.1845     -0.1781     -0.1717
  -0.1654     -0.1590     -0.1527     -0.1463     -0.1399     -0.1336     -0.1272     -0.1209
  -0.1145     -0.1081     -0.1018     -0.0954     -0.0890     -0.0827     -0.0763     -0.0700
  -0.0636     -0.0573     -0.0509     -0.0445     -0.0382     -0.0318     -0.0254     -0.0191
  -0.0127     -0.0064      0.0000      0.0064      0.0127      0.0191      0.0254      0.0318
   0.0382      0.0445      0.0509      0.0573      0.0636      0.0700      0.0763      0.0827
   0.0890      0.0954      0.1018      0.1081      0.1145      0.1209      0.1272      0.1336
   0.1399      0.1463      0.1527      0.1590      0.1654      0.1717      0.1781      0.1845
   0.1908      0.1972      0.2035      0.2099      0.2163      0.2226      0.2290      0.2354
   0.2417      0.2481      0.2544      0.2608      0.2672      0.2735      0.2799      0.2862
   0.2926      0.2990      0.3053      0.3117      0.3180      0.3244      0.3308      0.3371
   0.3435      0.3498      0.3562      0.3626      0.3689      0.3753      0.3817
   1.0000
   0.0692      0.0692      0.0692      0.0692      0.0692      0.0692      0.0692      0.0692
   0.0692      0.0692      0.0692      0.0692      0.0692      0.0692      0.0692      0.0692
   0.0692      0.0692      0.0692      0.0692      0.0692      0.0692      0.0692      0.0692
   0.0692      0.0692      0.0692      0.0692      0.0692      0.0692      0.0692      0.0692
   0.0692      0.0692      0.0692      0.0782      0.0822      0.0853      0.0877      0.0896
   0.0911      0.0925      0.0936      0.0944      0.0951      0.0956      0.0960      0.0962
   0.0962      0.0961      0.0958      0.0953      0.0947      0.0939      0.0930      0.0918
   0.0904      0.0889      0.0871      0.0852      0.0830      0.0805      0.0778      0.0747
   0.0714      0.0678      0.0638      0.0595      0.0550      0.0502      0.0452      0.0400
   0.0349      0.0298      0.0249      0.0201      0.0156      0.0114      0.0074      0.0038
   0.0000     -0.0035     -0.0070     -0.0105     -0.0140     -0.0175     -0.0210     -0.0245
  -0.0280     -0.0315     -0.0350     -0.0385     -0.0420     -0.0455     -0.0490
   1.0000
   0.0000      0.0000      0.0000      0.0000      0.0000      0.0000      0.0000      0.0000
   0.0000      0.0000      0.0000      0.0000      0.0000      0.0000      0.0000      0.0000
```

0.0000	0.0000	0.0000	0.0000	0.0000	0.0000	0.0000	0.0000
0.0000	0.0000	0.0000	0.0000	0.0000	0.0000	0.0000	0.0000
0.0000	0.0000	0.0000	0.0163	0.0232	0.0283	0.0324	0.0358
0.0387	0.0412	0.0434	0.0453	0.0468	0.0481	0.0493	0.0502
0.0510	0.0516	0.0520	0.0523	0.0525	0.0525	0.0523	0.0519
0.0513	0.0506	0.0496	0.0485	0.0472	0.0456	0.0438	0.0418
0.0395	0.0369	0.0341	0.0310	0.0278	0.0245	0.0211	0.0177
0.0144	0.0114	0.0086	0.0061	0.0041	0.0024	0.0013	0.0006
0.0000	0.0000	0.0000	0.0000	0.0000	0.0000	0.0000	0.0000
0.0000	0.0000	0.0000	0.0000	0.0000	0.0000	0.0000	
0.9980							
49.9000	49.9000	49.9000	49.9000	49.9000	49.9000	49.9000	49.9000
49.9000	49.9000	49.9000	49.9000	49.9000	49.9000	49.9000	49.9000
49.9000	49.9000	49.9000	49.9000	49.9000	49.9000	49.9000	49.9000
49.9000	49.9000	49.9000	49.9000	49.9000	49.9000	49.9000	49.9000
49.9000	49.9000	49.9000	49.9000	49.9000	49.9000	49.9000	49.9000
49.9000	49.9000	49.9000	49.9000	49.9000	49.9000	49.9000	49.9000
49.9000	49.9000	49.9000	49.9000	49.9000	49.9000	49.9000	49.9000
49.9000	49.9000	49.9000	49.9000	49.9000	49.9000	49.9000	49.9000
49.9000	49.9000	49.9000	49.9000	49.9000	49.9000	49.9000	49.9000
49.9000	49.9000	49.9000	49.9000	49.9000	49.9000	49.9000	49.9000
49.9000	49.9000	49.9000	49.9000	49.9000	49.9000	49.9000	49.9000
49.9000	49.9000	49.9000	49.9000	49.9000	49.9000	49.9000	
1.0000							
-0.2163	-0.2099	-0.2035	-0.1972	-0.1908	-0.1845	-0.1781	-0.1717
-0.1654	-0.1590	-0.1527	-0.1463	-0.1399	-0.1336	-0.1272	-0.1209
-0.1145	-0.1081	-0.1018	-0.0954	-0.0890	-0.0827	-0.0763	-0.0700
-0.0636	-0.0573	-0.0509	-0.0445	-0.0382	-0.0318	-0.0254	-0.0191
-0.0127	-0.0064	0.0000	0.0064	0.0127	0.0191	0.0254	0.0318
0.0382	0.0445	0.0509	0.0573	0.0636	0.0700	0.0763	0.0827
0.0890	0.0954	0.1018	0.1081	0.1145	0.1209	0.1272	0.1336
0.1399	0.1463	0.1527	0.1590	0.1654	0.1717	0.1781	0.1845
0.1908	0.1972	0.2035	0.2099	0.2163	0.2226	0.2290	0.2354
0.2417	0.2481	0.2544	0.2608	0.2672	0.2735	0.2799	0.2862
0.2926	0.2990	0.3053	0.3117	0.3180	0.3244	0.3308	0.3371
0.3435	0.3498	0.3562	0.3626	0.3689	0.3753	0.3817	
1.0000							
0.0692	0.0692	0.0692	0.0692	0.0692	0.0692	0.0692	0.0692
0.0692	0.0692	0.0692	0.0692	0.0692	0.0692	0.0692	0.0692
0.0692	0.0692	0.0692	0.0692	0.0692	0.0692	0.0692	0.0692
0.0692	0.0692	0.0692	0.0692	0.0692	0.0692	0.0692	0.0692
0.0692	0.0692	0.0692	0.0782	0.0822	0.0853	0.0877	0.0896
0.0911	0.0925	0.0936	0.0944	0.0951	0.0956	0.0960	0.0962
0.0962	0.0961	0.0958	0.0953	0.0947	0.0939	0.0930	0.0918
0.0904	0.0889	0.0871	0.0852	0.0830	0.0805	0.0778	0.0747
0.0714	0.0678	0.0638	0.0595	0.0550	0.0502	0.0452	0.0400
0.0349	0.0298	0.0249	0.0201	0.0156	0.0114	0.0074	0.0038
0.0000	-0.0035	-0.0070	-0.0105	-0.0140	-0.0175	-0.0210	-0.0245
-0.0280	-0.0315	-0.0350	-0.0385	-0.0420	-0.0455	-0.0490	
1.0000							
0.0000	0.0000	0.0000	0.0000	0.0000	0.0000	0.0000	0.0000
0.0000	0.0000	0.0000	0.0000	0.0000	0.0000	0.0000	0.0000
0.0000	0.0000	0.0000	0.0000	0.0000	0.0000	0.0000	0.0000
0.0000	0.0000	0.0000	0.0000	0.0000	0.0000	0.0000	0.0000

```
      0.0000      0.0000      0.0000      0.0163      0.0232      0.0283      0.0324      0.0358
      0.0387      0.0412      0.0434      0.0453      0.0468      0.0481      0.0493      0.0502
      0.0510      0.0516      0.0520      0.0523      0.0525      0.0525      0.0523      0.0519
      0.0513      0.0506      0.0496      0.0485      0.0472      0.0456      0.0438      0.0418
      0.0395      0.0369      0.0341      0.0310      0.0278      0.0245      0.0211      0.0177
      0.0144      0.0114      0.0086      0.0061      0.0041      0.0024      0.0013      0.0006
      0.0000      0.0000      0.0000      0.0000      0.0000      0.0000      0.0000      0.0000
      0.0000      0.0000      0.0000      0.0000      0.0000      0.0000      0.0000
      1.0020
     50.1000     50.1000     50.1000     50.1000     50.1000     50.1000     50.1000     50.1000
     50.1000     50.1000     50.1000     50.1000     50.1000     50.1000     50.1000     50.1000
     50.1000     50.1000     50.1000     50.1000     50.1000     50.1000     50.1000     50.1000
     50.1000     50.1000     50.1000     50.1000     50.1000     50.1000     50.1000     50.1000
     50.1000     50.1000     50.1000     50.1000     50.1000     50.1000     50.1000     50.1000
     50.1000     50.1000     50.1000     50.1000     50.1000     50.1000     50.1000     50.1000
     50.1000     50.1000     50.1000     50.1000     50.1000     50.1000     50.1000     50.1000
     50.1000     50.1000     50.1000     50.1000     50.1000     50.1000     50.1000     50.1000
     50.1000     50.1000     50.1000     50.1000     50.1000     50.1000     50.1000     50.1000
     50.1000     50.1000     50.1000     50.1000     50.1000     50.1000     50.1000     50.1000
     50.1000     50.1000     50.1000     50.1000     50.1000     50.1000     50.1000     50.1000
     50.1000     50.1000     50.1000     50.1000     50.1000     50.1000     50.1000
   1004.0000      1.4000      0.3500      0.0050      0.0000      0.0000      0.0200      0.9500
     25.0000      0.0000      0.0000      0.0000      0.0000
  99000.0000  99000.0000  98315.0000  98315.0000      0.0000      0.0000
 101325.0000 101325.0000 101325.0000 101325.0000      0.0000
    288.1500    288.1500    288.1500    288.1500      0.0000
      0.0000      0.0000      0.0000      0.0000      0.0000
     60.0000     60.0000     60.0000     60.0000      0.0000
      0.0000      0.0000      0.0000      0.0000      0.0000
      0.0000      0.0000      0.0000      0.0000      0.0000
      1.0000      1.0000      1.0000      1.0000
      0.1000      0.1100      0.1200      0.1300      0.1400      0.1500      0.1600      0.1700
      0.1800      0.1900      0.1800      0.1700      0.1600      0.1500      0.1400      0.1300
      0.1200      0.1100      0.1000      0.0900      0.0900
 5000 5000 5000 5000 5000
0 1 1 1 1 1 0 0 1 0 0 1 0
1 0 1 0 1
    0     0     0     1    95
```

CONTENTS: PART 2

1-D STABILITY ANALYSIS OF DENSITY-PRESSURE RELATIONS USED IN THE COMPUTATION OF TRANSONIC FLOW

NOMENCLATURE FOR PART 2

A	area
a_0, a_1, a_2	pressure interpolation coefficients, Eq. 51
c	speed of sound
e	=0 for pressure update method =1 for density update method
i	grid index
M	Mach number
$\dot{m}$	mass flow rate
p	static pressure
R	gas constant
T	static temperature
u, $\underline{u}$	velocity in x direction, velocity vector
Vol	volume
x	1-d coordinate
δt	time step
δt_c	time step for continuity
ρ	density
γ	ratio of specific heats, c_p/c_v

PART 2
1-D STABILITY ANALYSIS OF DENSITY-PRESSURE RELATIONS
USED IN THE COMPUTATION OF TRANSONIC FLOW

2.1 Background

When calculations of 1-d or 2-d choked flow with a shock were attempted* with equations that were relaxed to perfect gas (i.e. so that when converged, the ideal gas equation of state would be satisfied with the same density and pressure as used in the momentum and continuity equations) convergence was not obtained. Eventually, as more and more iterations were taken wobbles appeared in the pressure solution which grew and continuity errors grew worse instead of better.

The following analysis explains the cause of the instability. Further analysis then shows the stability of the 3 point interpolation scheme used for the calculation of effective pressure. Still further analysis suggests a Mach number dependent interpolation scheme.

2.2 1-D Flow Example

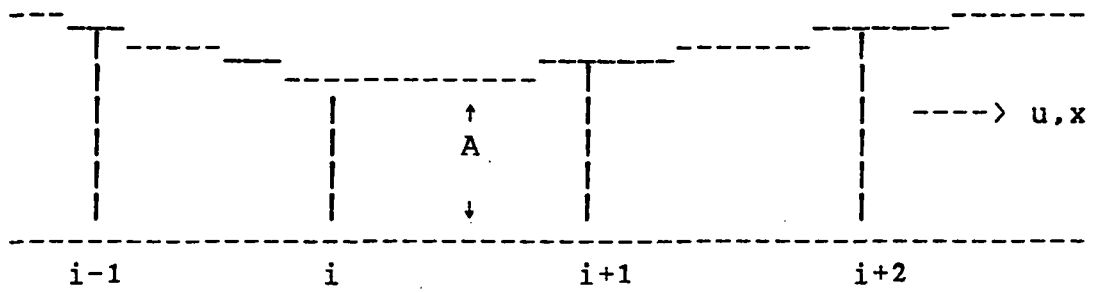

We are seeking a 1-d steady flow solution for continuity and momentum

$$\nabla \cdot \rho \underline{u} = 0 \qquad (1)$$

$$\nabla \cdot \rho \underline{u}\,\underline{u} = -\nabla p \qquad (2)$$

for a perfect gas with constant total temperature.

---

* Using either an effective pressure (Denton) or an effective density (Nicholson/Moore) finite-volume time marching method.

2.3 Continuity

Continuity between grid points i and i+1, in discretized form, when a converged solution is obtained, is simply

$$\rho^f_{i+1} u^f_{i+1} A_{i+1} - \rho^f_i u^f_i A_i = 0 \qquad (3)$$

where superscript f stands for final.

Now consider an intermediate solution, ρ and u, which does not satisfy continuity and changes, $\delta\rho$ and δu, so that continuity is satisfied. Then

$$(\rho_{i+1}+\delta\rho_{i+1})(u_{i+1}+\delta u_{i+1})A_{i+1} - (\rho_i+\delta\rho_i)(u_i+\delta u_i)A_i = 0 \qquad (4)$$

Rearranging,

$$\rho_{i+1}A_{i+1}\delta u_{i+1} - \rho_i A_i \delta u_i + u_{i+1}A_{i+1}\delta\rho_{i+1} - u_i A_i \delta\rho_i$$

$$= \rho_i u_i A_i - \rho_{i+1}u_{i+1}A_{i+1} + \delta\rho_i \delta u_i A_i - \delta\rho_{i+1}\delta u_{i+1}A_{i+1} \qquad (5)$$

The first two terms on the right hand side represent the current continuity error and the last two are of order δ^2 and so will be negligible when the computation is nearly converged and $\delta\rho \ll \rho$ and $\delta u \ll u$. Therefore we may write this equation as

$$\rho_{i+1}A_{i+1}\delta u_{i+1} - \rho_i A_i \delta u_i + u_{i+1}A_{i+1}\delta\rho_{i+1} - u_i A_i \delta\rho_i$$

$$= \dot{m}_{error,i} + \text{small} \qquad (6)$$

In the density update time marching calculation procedure (Denton), when there is a continuity error, the density on the <u>downstream</u> side of the control volume is changed.

$$\delta\rho_{i+1} = \dot{m}_{error,i}\delta t/Vol_i \qquad (7)$$

The density change affects continuity directly, but it also acts through the perfect gas equation to change the pressure which acts through the momentum equation to change the velocity.

In the pressure update time marching calculation procedure (Nicholson/Moore), when there is a continuity error, the pressure on the <u>upstream</u> side of the control volume is changed.

$$\delta p_i = \dot{m}_{error,i}\delta t_c RT/Vol_i \qquad (8)$$

This pressure change acts through the momentum equation to change the velocity and through the perfect gas equation to change the density.

2.4 Momentum

The steady state momentum equation discretized over the control volume between points i and i+1 is

$$(\rho uA)_{i+1}u_{i+1} - (\rho uA)_i u_i = -[p_{i+1}A_{i+1} - p_i A_i - p_s(A_{i+1}-A_i)] \qquad (9)$$

where p_s is the pressure acting on the sides of the control volume. Traditionally,

$$p_s = (p_{i+1}+p_i)/2 \qquad (10)$$

therefore,

$$(\rho uA)_{i+1}u_{i+1} - (\rho uA)_i u_i = -(p_{i+1} - p_i)(A_{i+1}+A_i)/2 \qquad (11)$$

We may write this as

$$\dot{m}_{i+1}u_{i+1} - \dot{m}_i u_i = - (p_{i+1} - p_i)Vol_i/\delta x_i \qquad (12)$$

where $\dot{m}=\rho uA$ is the mass flow rate, $Vol_i=\delta x_i(A_{i+1}+A_i)/2$ is the volume of the control volume and $\delta x_i=x_{i+1}-x_i$ is the grid spacing.

Eq. 12 may be rewritten as

$$(u_{i+1}-u_i)(\dot{m}_{i+1}+\dot{m}_i)/2 + (\dot{m}_{i+1}-\dot{m}_i)(u_{i+1}+u_i)/2 = -(p_{i+1}-p_i)Vol_i/\delta x_i \qquad (13)$$

or

$$\dot{m}(u_{i+1}-u_i) + u\,\dot{m}_{error,i} = -(p_{i+1}-p_i)Vol_i/\delta x_i \qquad (14)$$

In the Nicholson/Moore method the continuity error term is omitted and the change in velocity on the downstream side of the control volume is proportional to the momentum error,

$$\delta u_{i+1} = [\, - (p_{i+1}+\delta p_{i+1}-p_i-\delta p_i)Vol_i/\delta x_i - \dot{m}(u_{i+1}-u_i)\,]\,\delta t/(\rho_{i+1}Vol_i) \qquad (15)$$

where δp is the change in pressure calculated from the continuity error. In the Denton method, the continuity error is not omitted in the momentum equation and the change in ρu is calculated from

the momentum error,

$$\delta(\rho u)_{i+1} = u_{i+1}\delta\rho_{i+1} + \rho_{i+1}\delta u_{i+1}$$

$$= [\ -(p_{i+1}+\delta p_{i+1}-p_i-\delta p_i)Vol_i/\delta x_i$$

$$- \dot{m}(u_{i+1}-u_i) - u\,\dot{m}_{error,i}\ ]\ \delta t/Vol_i \qquad (16)$$

Taking the mean velocity u approximately equal to the velocity on the downstream side u_{i+1}, we may subtract u times Eq. 7 from Eq. 16 and so for the Denton method we get

$$\delta u_{i+1} = [\ -(p_{i+1}+\delta p_{i+1}-p_i-\delta p_i)Vol_i/\delta x_i$$
$$- \dot{m}(u_{i+1}-u_i)]\delta t/(\rho_{i+1}Vol_i) \qquad (17)$$

the same as for the Nicholson/Moore method.

If at the beginning of a time step the momentum equation is balanced except for the continuity error,

$$\dot{m}(u_{i+1}-u_i) = -(p_{i+1}-p_i)Vol_i/\delta x_i \qquad (18)$$

then for both methods we have

$$\delta u_{i+1} = (\delta p_i - \delta p_{i+1})\ \delta t/(\rho_{i+1}\delta x_i) \qquad (19)$$

In general , in the density update (Denton) method, the time step is calculated from the CFL condition

$$\delta t = \delta x/(u+c) \qquad (20)$$

where c is the speed of sound. In the pressure update method the time step for momentum is obtained from the coefficient of u_{i+1} in the steady flow equation so that

$$\delta t = \delta x/u. \qquad (21)$$

We may combine these two equations by saying

$$\delta t = \delta x/(u+ec) \qquad (22)$$

where e=1 for the density update method and e=0 for the pressure update method. Combining Eqs. 18 and 15 then gives

$$\rho_{i+1}\delta u_{i+1} = (\delta p_i - \delta p_{i+1})/(u+ec)_{i+1}. \qquad (23)$$

2.5 Change in Continuity for One Time Step

The left hand side of Eq. 6 may be used to evaluate the change in continuity for one time step. Substituting Eq. 23 into this expression to eliminate $\rho\delta u$ yields

$$A_{i+1}(\delta p_i-\delta p_{i+1})/(u+ec)_{i+1} - A_i(\delta p_{i-1}-\delta p_i)/(u+ec)_i$$

$$+ u_{i+1}A_{i+1}\delta\rho_{i+1} - u_iA_i\delta\rho_i = \dot{m}_{change,i}. \qquad (24)$$

Rearranging to order the coefficients of the δp's and $\delta\rho$'s

$$- A_i/(u+ec)_i \quad \delta p_{i-1}$$

$$+ [A_{i+1}/(u+ec)_{i+1}+A_i/(u+ec)_i] \quad \delta p_i \quad - u_iA_i \quad \delta\rho_i$$

$$- A_{i+1}/(u+ec)_{i+1} \quad \delta p_{i+1} \quad + u_{i+1}A_{i+1} \quad \delta\rho_{i+1}$$

$$= \dot{m}_{change,i} \qquad (25)$$

For stability we require that the change in continuity be of the same sign as the continuity error. Note that this is a necessary condition for stability but may not be a sufficient condition to ensure stability.

2.6 Stability of Density Update Method Using Perfect Gas

For an intermediate solution where there is a continuity error only between i and i+1, Eq. 7 yields

$$\delta\rho_{i+1} = \dot{m}_{error,i}\delta t/Vol_i \qquad (26a)$$

$$\delta\rho_i = 0 \qquad (26b)$$

$$\delta\rho_{i-1} = 0 \qquad (26c)$$

and from perfect gas, assuming temperature changes over the time step are negligible*,

$$\delta p_{i+1} = \delta \rho_{i+1} RT = \dot{m}_{error,i} RT\ \delta t/Vol_i \qquad (27a)$$

$$\delta p_i = \delta \rho_i RT = 0 \qquad (27b)$$

$$\delta p_{i-1} = \delta \rho_{i-1} RT = 0. \qquad (27c)$$

For this case then Eq. 25 reduces to

$$[\ - A_{i+1} RT/(u+c)_{i+1} + u_{i+1} A_{i+1}\ ]\ \dot{m}_{error,i} \delta t/Vol_i = \dot{m}_{change,i} \qquad (28)$$

Since for stability we require $\dot{m}_{error}$ and $\dot{m}_{change}$ to have the same sign, we must have

$$[\ - RT/(u+c)_{i+1} + u_{i+1}\ ]\ A_{i+1} > 0. \qquad (29)$$

Substituting c^2/γ for RT yields

$$- c^2/[\gamma(u+c)_{i+1}] + u_{i+1} > 0 \qquad (30)$$

or

$$\gamma\ u_{i+1}\ (u+c)_{i+1} > c^2. \qquad (31)$$

Evaluating for $\gamma = 1.4$ we need

$$u > 0.48\ c. \qquad (32)$$

Thus for low Mach number flow this density update method is unstable.

2.7 Stability of Pressure Update Method Using Perfect Gas

For a continuity error only between i and i+1, Eq. 8 yields

$$\delta p_i = \dot{m}_{error,i} \delta t_c RT/Vol_i \qquad (33a)$$

$$\delta p_{i+1} = 0 \qquad (33b)$$

---

* If at this point the alternative assumption was made that the changes were isentropic, then $\delta p = \gamma RT \delta \rho$ and less conservative stability criteria would be obtained, equivalent to setting $\gamma = 1.0$ in the following analysis.

$$\delta p_{i-1} = 0 \qquad (33c)$$

and from perfect gas assuming temperature changes over the step are negligible

$$\delta \rho_i = \delta p_i / RT \qquad (34a)$$

$$\delta \rho_{i+1} = \delta p_{i+1} / RT = 0. \qquad (34b)$$

Therefore, in this case, Eq. 21 becomes

$$(A_{i+1}/u_{i+1} + A_i/u_i - u_i A_i/RT)\dot{m}_{error,i}\delta t_c RT/Vol_i = \dot{m}_{change,i}. \qquad (35)$$

For $\dot{m}_{error}$ and $\dot{m}_{change}$ to have the same sign, we require

$$A_{i+1}/u_{i+1} + A_i/u_i - u_i A_i/RT > 0. \qquad (36)$$

Assuming the values at i are approximately the same as the values at i+1, and again using c^2/γ for RT yields

$$2/u - \gamma u/c^2 > 0 \qquad (37)$$

or

$$2c^2 > \gamma u^2. \qquad (38)$$

For $\gamma = 1.4$ then we need

$$u < 1.2\ c; \qquad (39)$$

thus for high Mach numbers this pressure update method is unstable.

2.8 A Downwind Effective Pressure or Upwind Effective Density

If an inconsistency in the pressure-density relation is introduced such that the pressure used in the momentum equation is offset by 1 grid point from the density used in the continuity equation, the equation of state may be written as

$$p_i = \rho_{i+1} RT \qquad (40)$$

In a density update method this may be viewed as an effective pressure evaluated downwind of its point of use in the momentum equation. Similarly, in a pressure update method the equation represents an effective density evaluated upstream of its point of use in the continuity equation.

For both the density and pressure update methods, Eq. 21 now becomes

$$
\begin{aligned}
&- (A_i/(u+ec)_i + u_i A_i/RT)(\delta tRT/Vol_{i-1}) && \hat{m}_{error,i-1} \\
&+ (A_{i+1}/(u+ec)_{i+1} + A_i/(u+ec)_i + u_{i+1}A_{i+1}/RT)(\delta tRT/Vol_i) && \hat{m}_{error,i} \\
&- (A_{i+1}/(u+ec)_{i+1})(\delta tRT/Vol_{i+1}) && \hat{m}_{error,i+1} \\
&= \hat{m}_{change,i} && (41)
\end{aligned}
$$

From this equation we can see that the coefficient of $\hat{m}_{error,i}$ is always positive and so this pressure-density relation passes the simple stability criterion ($\hat{m}_{change,i}$ same sign as $\hat{m}_{error,i}$) for all Mach numbers. Note also that the coefficients of $\hat{m}_{error,i-1}$ and $\hat{m}_{error,i+1}$ are of opposite sign to the coefficient of $\hat{m}_{error,i}$ and in general of smaller magnitude; this further assures the stability of Eq. 40.

While the pressure-density relation, Eq. 40, is stable, testing has shown that it results in poor shock capturing as the calculated shock is spread over numerous grid points. Fig. 1 shows the calculated and theoretical pressure distribution for a 1-d calculation with a nominal shock Mach number of 1.45.

2.9 Stability of 3-point Interpolation for Effective Pressure

One of the pressure-density relations used in the density update method is a three point interpolation of density to obtain the effective pressure. For approximately uniform T we may write this as

$$p_i = (\rho_{i+1} - (1/3)(\rho_{i+2} - \rho_{i-1})) RT \qquad (42)$$

so that for the change in p we have

$$\delta p_i = (\delta\rho_{i+1} - (1/3)\delta\rho_{i+2} + (1/3)\delta\rho_{i-1})RT. \qquad (43)$$

Substituting into Eq. 25 and neglecting variations of A, u and c with i, we obtain

$$\begin{aligned} &- (Ac^2/(\gamma(u+c)) (\delta\rho_i - (1/3)\delta\rho_{i+1} + (1/3)\delta\rho_{i-2}) \\ &+ (2Ac^2/(\gamma(u+c)) (\delta\rho_{i+1} - (1/3)\delta\rho_{i+2} + (1/3)\delta\rho_{i-1}) - uA\,\delta\rho_i \\ &- (Ac^2/(\gamma(u+c)) (\delta\rho_{i+2} - (1/3)\delta\rho_{i+3} + (1/3)\delta\rho_i) + uA\,\delta\rho_{i+1} \\ &\qquad = \dot{m}_{change,i} \end{aligned} \qquad (44)$$

Collecting terms and substituting the Mach number, M for u/c

$$\begin{aligned} &+ Ac/(3\gamma(M+1)) && \delta\rho_{i+3} \\ &- 5Ac/(3\gamma(M+1)) && \delta\rho_{i+2} \\ &+ Ac(7/(3\gamma(M+1))+M) && \delta\rho_{i+1} \\ &- Ac(4/(3\gamma(M+1))+M) && \delta\rho_i \\ &+ 2Ac/(3\gamma(M+1)) && \delta\rho_{i-1} \\ &- Ac/(3\gamma(M+1)) && \delta\rho_{i-2} \qquad = \dot{m}_{change,i} \end{aligned} \qquad (45)$$

we can see that the change in continuity for the control volume between i and i+1 is now dependent on the change in density at 6 grid points.

Eq. 45 passes the first simple test for stability; the coefficient of $\delta\rho_{i+1}$ is positive for all Mach numbers and so a continuity error, $\dot{m}_{error,i}$, will result in a change in continuity, $\dot{m}_{change,i}$, of the same sign. However, since the

coefficients of $\delta\rho_{i+3}$ and $\delta\rho_{i-1}$ are also positive, it is appropriate to apply a more sophisticated stability criterion. The criterion we will apply is:

> the center point coefficient must be greater than the sum of the other positive coefficients.

$$\text{Coef}_{\text{center}} > \text{Sum Coef}_{+} \tag{46}$$

Applying this to Eq. 45, we require

$$Ac(7/(3\gamma(M+1))+M) > 3Ac/(3\gamma(M+1)) \tag{47}$$

which is always true. Thus, Eq. 42 should be stable for all Mach numbers. The experience of Denton and other users of his code confirms this.

2.10 Stability of 3-point Interpolation for Effective Density

A similar analysis can be done for the pressure-update effective-density method using a three point interpolation of pressure to obtain the effective density.

$$\rho_{i+1} = [p_i + (1/3)(p_{i+1}-p_{i-2})]/RT \tag{48}$$

Substituting the change in density

$$\delta\rho_{i+1} = (\delta p_i + (1/3)\delta p_{i+1} - (1/3)\delta p_{i-2})/RT \tag{49}$$

into Eq. 25, gives

$$\begin{aligned} &+ (A/c)(-1/M + \gamma M/3)\ \delta p_{i+1} \\ &+ (A/c)(\ 2/M + 2\gamma M/3)\ \delta p_i \\ &- (A/c)(\ 1/M + \gamma M\ )\ \delta p_{i-1} \\ &- (A/c)(\ \ \ \ \ \gamma M/3)\ \delta p_{i-2} \\ &+ (A/c)(\ \ \ \ \ \gamma M/3)\ \delta p_{i-3} \end{aligned} = \dot{m}_{\text{change},i} \tag{50}$$

The center point coefficient is the coefficient of δp_i, since this is proportional to $\dot{m}_{\text{error},i}$ in the pressure update method. In Eq. 50, the coefficient of δp_i is positive and greater than the sum of the other positive coefficients; therefore Eq. 48 should be stable for all Mach numbers.

2.11 Mach Number Dependent Interpolation Formula for Effective Density

In section 2.7 it was indicated that when the Mach number is low, the pressure update method is stable with the ideal gas equation of state satisfied at each grid point. Since this is the correct pressure-density relation for ideal gases it should be used where feasible. In this section we will start with a generalized pressure interpolation equation for effective density

$$\rho_{i+1} = [p_i + a_o(p_{i+1}-p_i) + a_1(p_{i+1}-p_{i-1})/2 + a_2(p_{i+1}-p_{i-2})/3\ ]/RT \qquad (51)$$

and seek Mach number limitations to a_o, a_1 and a_2 using criterion (Eq.) 46. Comparing equations 40 and 51, the upwind effective density corresponds to $a_o=a_1=a_2=0$, the 3 point interpolation, Eq. 48, corresponds to $a_o=a_1=0$, $a_2=1$, and ideal gas to $a_o=1$, $a_1=a_2=0$.

Substituting

$$\delta\rho_{i+1} = [(1-a_o)\delta p_i + (a_o + a_1/2 + a_2/3)\delta p_{i+1} - (a_1/2)\delta p_{i-1} - (a_2/3)\delta p_{i-2}\ ]/RT \qquad (52)$$

into Eq. 25 and rearranging in terms of the ceofficients of each δp, a_o, a_1 and a_2, yields

$$\begin{aligned}(A/c)\ \{ &(-1/M + \gamma M a_o + (\gamma M/2)a_1 + (\gamma M/3)a_2)\ \delta p_{i+1} \\ &+(2/M +\gamma M - 2\gamma M a_o - (\gamma M/2)a_1 - (\gamma M/3)a_2)\ \delta P_i \\ &+(-1/M -\gamma M + \gamma M a_o - (\gamma M/2)a_1)\ \delta p_{i-1} \\ &+(+ (\gamma M/2)a_1 - (\gamma M/3)a_2)\ \delta p_{i-2} \\ &+(+ (\gamma M/3)a_2)\ \delta p_{i-3} \\ &= \dot{m}_{change,i}\end{aligned} \qquad (53)$$

Let us first consider the case when $a_1=a_2=0$ and find limiting values of a_o. From Eq. 51, it is obvious that we should consider only values in the range

$$0 \le a_o \le 1. \qquad (54)$$

The coefficient of δp_i is positive when

$$2/M + \gamma M - 2\gamma M a_o > 0. \qquad (55)$$

This gives a limit on a_o which is a function of Mach number,

$$a_o < 1/(\gamma M^2) + 1/2. \qquad (56)$$

But the coefficient of δp_{i+1} is positive when

$$-1/M + \gamma M a_o > 0, \quad \text{or} \quad M^2 > 1/(\gamma a_o) \qquad (57)$$

In this region, from Eq. 46, we require

$$2/M + \gamma M - 2\gamma M a_o > -1/M + \gamma M a_o \qquad (58)$$

or

$$a_o < 1/(\gamma M^2) + 1/3. \qquad (59)$$

Valid values of a_o based on these criteria are shown as a function of Mach number in Fig. 2.

Let us next consider limiting values of a_1 when a_o and a_2 are zero. From Eq. 53 the coefficient of δp_i

$$2/M + \gamma M - \gamma M a_1/2 > 0 \qquad (60)$$

is positive for all Mach numbers in the range

$$0 \leq a_1 \leq 1. \qquad (61)$$

The coefficient of δp_{i-2} is positive for all M and the coefficient of δp_{i+1} is positive when

$$-1/M + \gamma M a_1/2 > 0 \quad \text{or} \quad M^2 > 2/(\gamma a_1). \qquad (62)$$

For $M^2 < 2/(\gamma a_1)$ we then require the coefficient of δp_i to be greater than the coefficient of δp_{i-2},

$$2/M + \gamma M - \gamma M a_1/2 > \gamma M a_1/2. \qquad (63)$$

With $a_1 \leq 1$, this is always satisfied. For $M^2 > 2/(\gamma a_1)$ we require the coefficient of δp_i to be greater then the sum of the coefficients of δp_{i-2} and δp_{i+1},

$$2/M + \gamma M - \gamma M a_1/2 > \gamma M a_1 - 1/M \qquad (64)$$

or

$$a_1 < 2/(\gamma M^2) + 2/3. \qquad (65)$$

Thus we can have $a_1=1$ up to $M^2=6/\gamma$ or up to $M=2.07$ for $\gamma=1.4$. Fig. 3 shows the valid range of a_1 based on these criteria.

We now consider combinations of a_0, a_1 and a_2. In particular if

$$a_0 + a_1 + a_2 = 1. \qquad (66)$$

the interpolation scheme is second order accurate. (See Appendix A.)

For Mach numbers less than 2, $a_1=1$ is stable. Therefore, for $M \leq 2$, we will choose

$$a_2 = 0$$
$$a_0 + a_1 = 1. \qquad (67)$$

From similar stability analyses to those already given

$$a_0 < 2/(\gamma M^2) - 1/3 \qquad (68)$$

should be stable for $M \leq 2$.

For $M > 2$, we will choose

$$a_0 = 0$$
$$a_1 + a_2 = 1. \qquad (69)$$

The stability analysis suggests acceptable values of a_1 are

$$a_1 < 0.4 + 3.6/(\gamma M^2). \qquad (70)$$

The stability criteria, Eqs. 68 and 70, are shown on Fig. 4.

A set of equations for a_0, a_1 and a_2, which satisfy Eq. 66 and so give second order accurate interpolation, and which satisfy Eqs. 67-70 so that they satisfy the stability criteria, have been selected. These are:

$$\text{for } M \leq 2 \qquad a_0 = (0.8/3)(4/M^2 - 1)$$

$$a_1 = 1 - a_0 \qquad (71)$$

$$a_2 = 0;$$

$$\text{for } M > 2 \qquad a_0 = 0$$

$$a_1 = 4/M^2 \qquad (72)$$

$$a_2 = 1 - a_1.$$

These Mach number dependent formulations for a_0, a_1 and a_2 are shown in Fig 5. These equations are tested in Part 3 where they are referred to as the M&M formula.

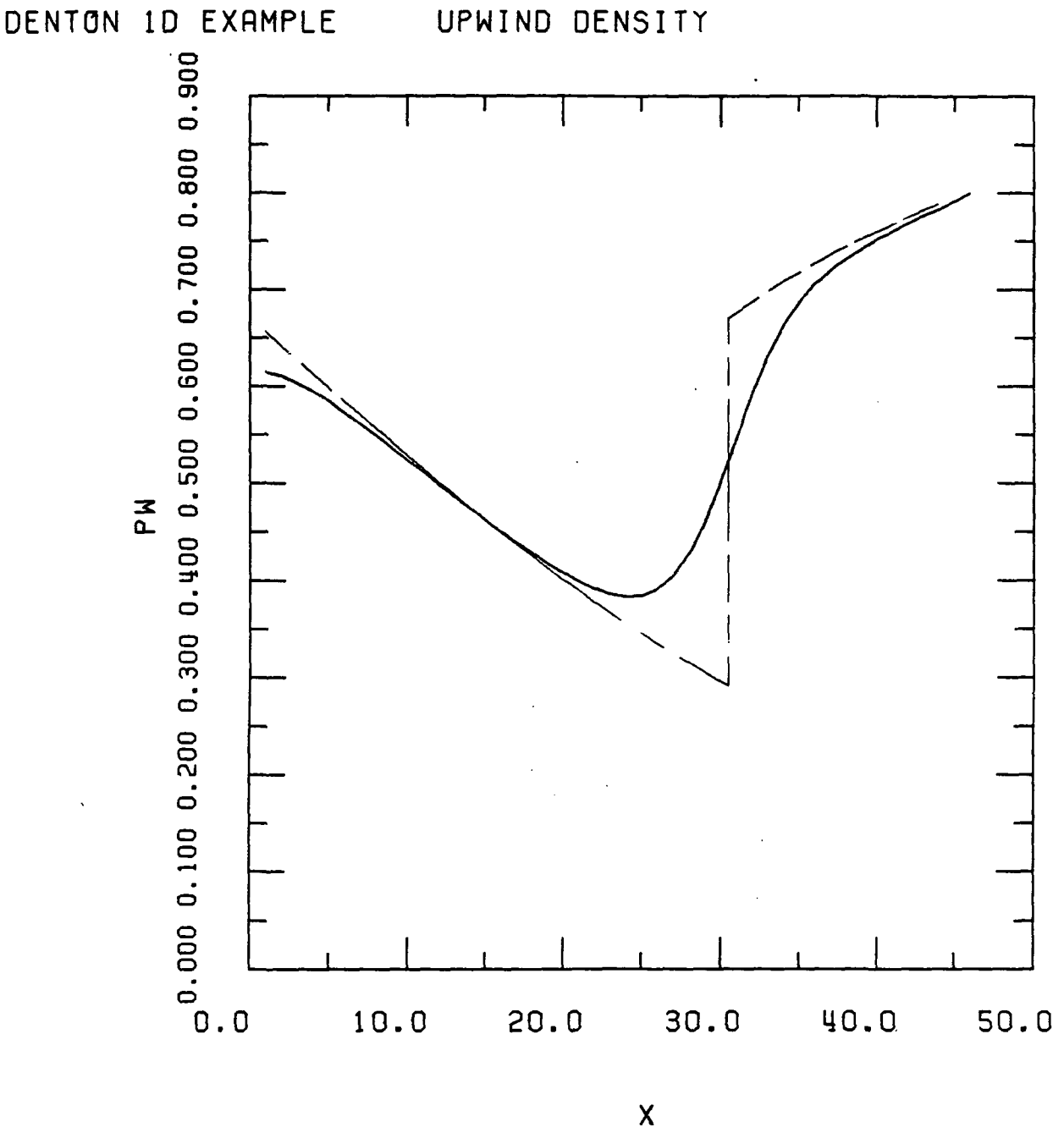

Fig. 1 Comparison of calculated and theoretical 1-D static pressure distributions, PW = $P/P_{t,inlet}$.

—— —— theoretical;

———— calculated using an upwind effective density, Eq. 40.

Grid spacing, $\delta x = 1$; $P_{exit}/P_{t,inlet} = 0.80$.

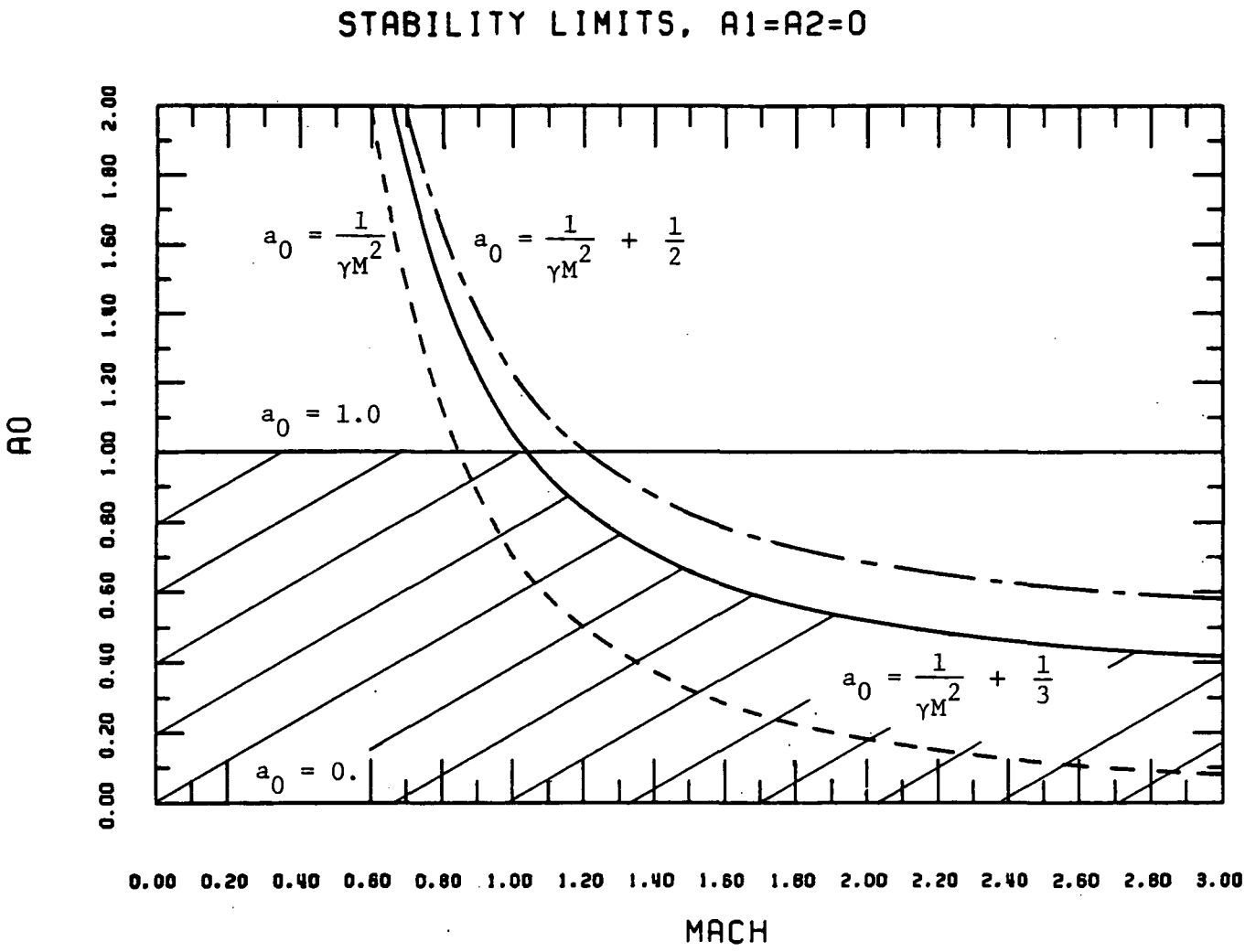

Fig. 2 Acceptable values of a_0 as a function of Mach number based on Eqs. 54, 56, 57, and 59 (for $\gamma = 1.4$).

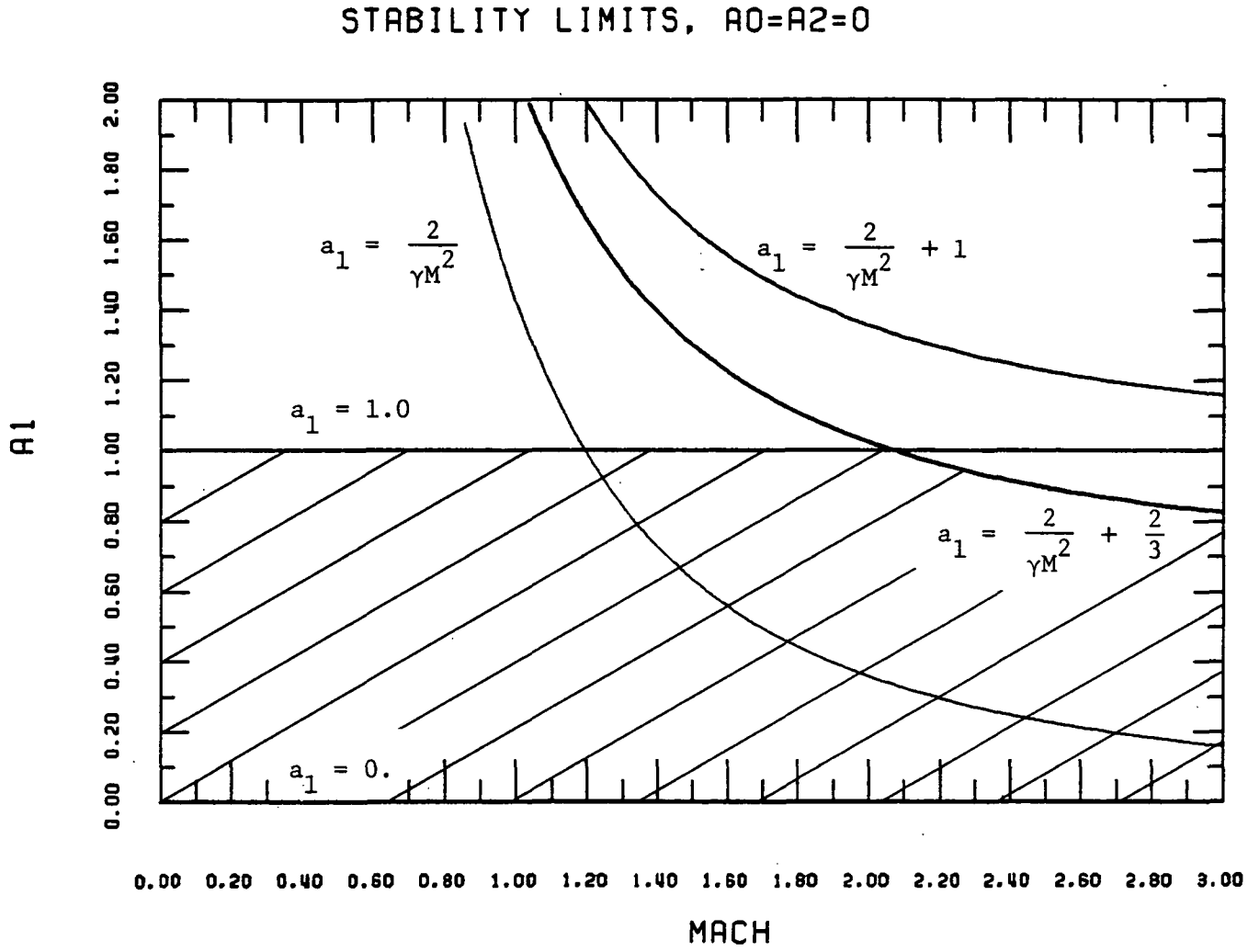

Fig. 3 Acceptable values of a_1 as a function of Mach number based on Eqs. 61, 62, 63, and 65 (for $\gamma = 1.4$).

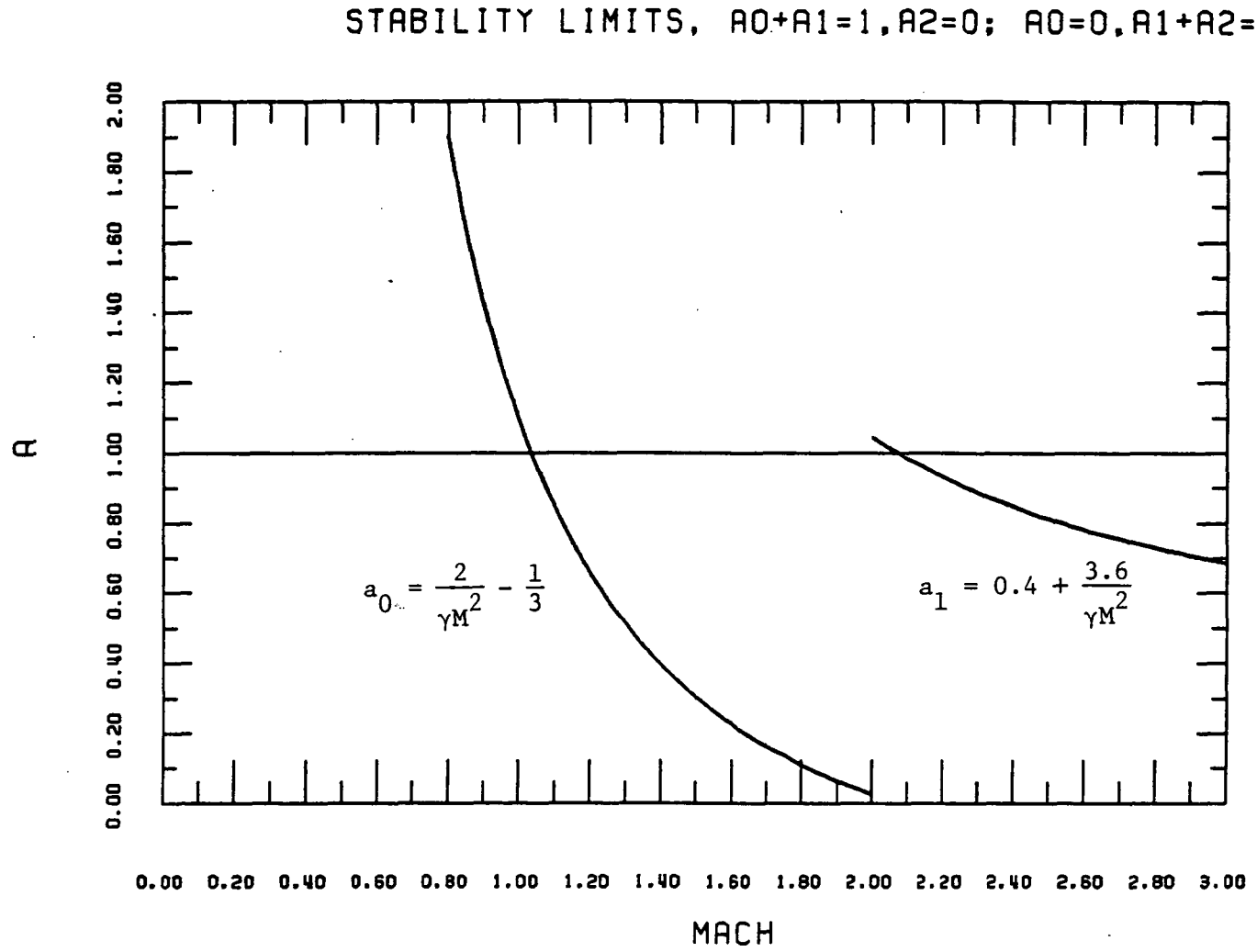

Fig. 4 Stability limits for a_0 when $a_2 = 0$ and $a_0 + a_1 = 1$, and for a_1 when $a_0 = 0$ and $a_1 + a_2 = 1$.

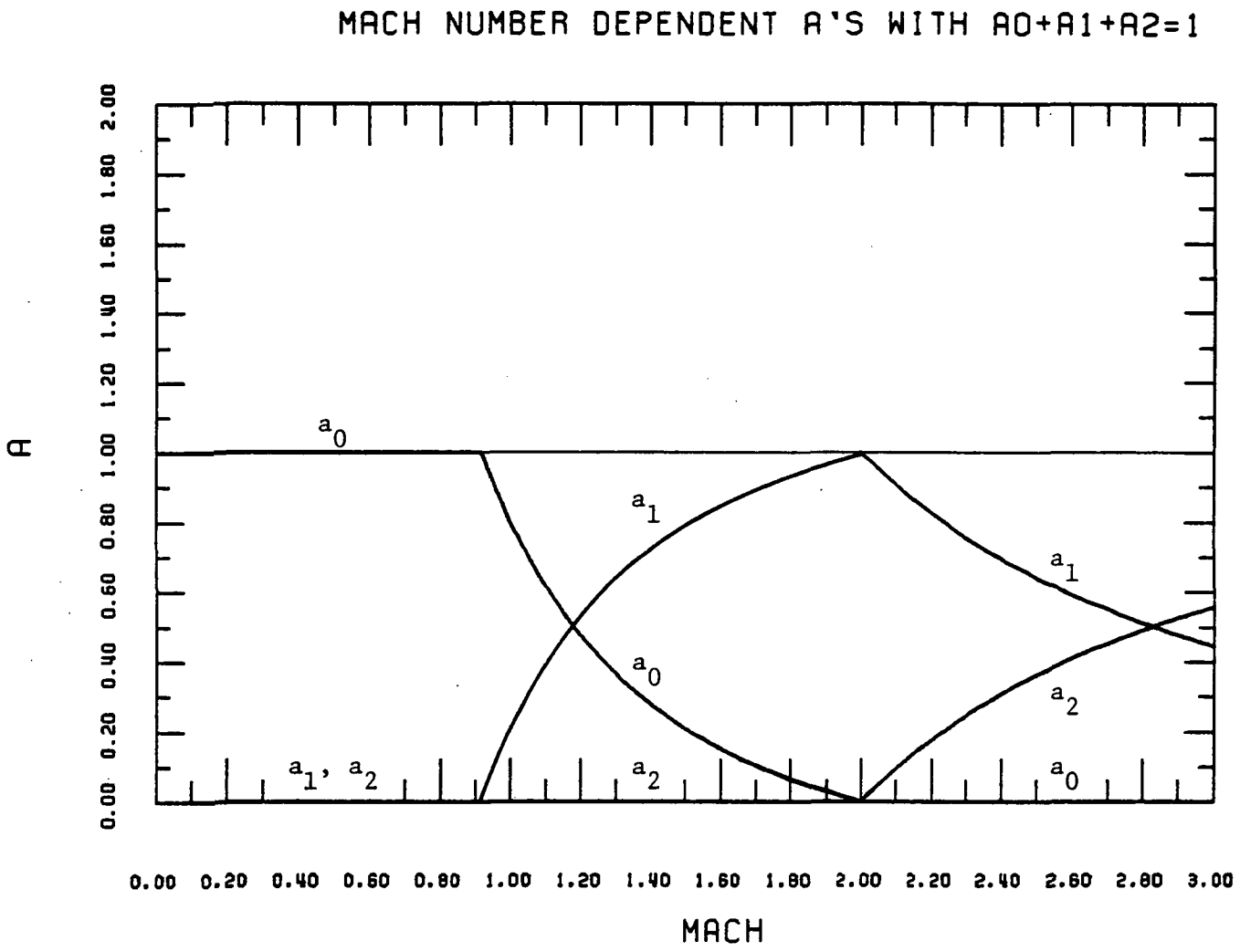

Fig. 5 M & M Mach number dependent values (Eqs. 71 and 72) for the coefficients in Eq. 51.

PART 2

APPENDIX A. TRUNCATION ERROR OF PRESSURE INTERPOLATION EQUATION

The truncation error of the interpolated pressure used to calculate the density in Eq. 51 may be determined using Taylor series analysis. The interpolated pressure p^e is given by

$$p^e_{i+1} = p_i + a_0(p_{i+1}-p_i) + a_1(p_{i+1}-p_{i-1})/2 + a_2(p_{i+1}-p_{i-2})/3$$

and to determine the accuracy of p^e we will look at the magnitude of $p^e_{i+1}-p_{i+1}$. With grid spacing h, and expanding about i+1, we have

$$p_{i-2} = p - 3hp' + 9(h^2/2)p'' - O(h^3)$$

$$p_{i-1} = p - 2hp' + 4(h^2/2)p'' - O(h^3)$$

$$p_i = p - hp' + (h^2/2)p'' - O(h^3)$$

$$p_{i+1} = p$$

Therefore,

$$p^e_{i+1}-p_{i+1} = h(a_0+a_1+a_2-1)p' - (h^2/2)(a_0+2a_1+3a_2-1)p'' + O(h^3).$$

And if

$$a_0 + a_1 + a_2 = 1,$$

then the difference between p_e and p is of the order of h^2, so that p^e is a second order accurate approximation for p.

CONTENTS: PART 3
1-D COMPUTATIONAL TESTS OF SHOCK CAPTURING
USING PRESSURE INTERPOLATION FORMULAE
TO CALCULATE EFFECTIVE DENSITY

Nomenclature for Part 3

a_o, a_1, a_2	pressure interpolation coefficients, Eq. 2
i	grid index in flow direction
$k = c_p/c_v$	ratio of specific heat capacities
M	Mach number
P	pressure
R	gas constant
T	static temperature
x	axial distance, Eq. 1
δx	grid spacing
ρ	density

Superscript

e	pressure used to evaluate the effective density

Subscript

t	total

PART 3
1-D COMPUTATIONAL TESTS OF SHOCK CAPTURING USING PRESSURE INTERPOLATION FORMULAE TO CALCULATE EFFECTIVE DENSITY

3.1 Denton's 1-D Nozzle for Testing Shock Capturing

Denton [1] has tested shock capturing with his finite-volume method in a convergent-divergent nozzle (see Fig. 1) designed to produce a linear variation of Mach number with distance for 1-D isentropic flow. The equation for the Mach number variation with distance is

$$x = 10. + 45. (M - 1) \tag{1}$$

Denton considered flow between x = 1, M = 0.8 and x = 46, M = 1.8; the throat, M = 1.0, is at x = 10. He used three back pressures with $P_{exit}/P_{t\ inlet}$ = 0.85, 0.80, and 0.75, respectively. The theoretical 1-D solutions for these three flows are shown in Fig. 2. The maximum Mach numbers, just upstream of the shock, are 1.267, 1.455, and 1.578, respectively; this is a range of shock Mach number typical of turbomachinery flows.

We have used these three pressure ratios for Denton's 1-D nozzle to test shock capturing with three of the pressure interpolation methods discussed in Part 2.

3.2 Effective Density Method

This annual report (Parts 1, 2, and 3) includes the results of calculations made with three different methods:

(a) The Effective Pressure Method as currently programmed in Denton's code at NASA Lewis.
(b) The Effective Density Method incorporated into Denton's code at NASA Lewis by S. Nicholson; this method uses the same time steps for the continuity and momentum equations.
(c) The Effective Density Method developed at VPI&SU with different time steps for continuity and momentum [2,3]; this is incorporated in the Nicholson/Moore time-marching codes at VPI&SU.

These methods are outlined to show their similarities and differences in Table 1.

In Part 1, results from methods a and b were presented and compared. The stability analysis in Part 2 was applied to methods a and c. Here in Part 3 the calculations are performed using method c.

3.3 Pressure Interpolation Schemes

The effective density methods (b and c in Section 3.2) use an interpolated approximation for the pressure in the evaluation of the density. A general form of the interpolation formula considered in this report is

$$P^e_{i+1} = P_i + a_o(P_{i+1} - P_i) + \frac{a_1}{2}(P_{i+1} - P_{i-1}) + \frac{a_2}{3}(P_{i+1} - P_{i-2}) \tag{2}$$

Table 1. Outline of Effective Pressure and Effective Density Calculation Methods.

UNKNOWNS (2 - DIMENSIONS)

$\rho, u, v, (\rho u), (\rho v), (\rho e_o), h_o, P, T$

OUTLINE OF METHODS

EFFECTIVE PRESSURE WITH THE SAME TIME STEPS	EFFECTIVE DENSITY WITH THE SAME TIME STEPS	EFFECTIVE DENSITY WITH DIFFERENT TIME STEPS
CONTINUITY		
$\frac{\partial \rho}{\partial t} + \nabla \cdot (\rho \underline{u}) = 0$ (1)		
$\delta\rho = (-\oint (\rho \underline{u}) \cdot d\underline{A})\ \delta t/Vol$	$\delta p = (-\oint (\rho \underline{u}) \cdot d\underline{A})\ RT\ \delta t/Vol$	$\delta p = (-\oint (\rho \underline{u}) \cdot d\underline{A})\ RT\ \delta t_c/Vol$
$\rho = \rho + \delta\rho$	$p = p + \delta p$	$p = p + \delta p$
ENERGY		
$\frac{\partial}{\partial t}(\rho e_o) + \nabla \cdot h_o \rho \underline{u} = 0$ (2)	h_o = constant	
$\delta(\rho e_o) = (-\oint h_o (\rho \underline{u}) \cdot d\underline{A})\ \delta t/Vol$	$T = (h_o - \frac{u^2+v^2}{2})/C_p$	
$(\rho e_o) = (\rho e_o) + \delta(\rho e_o)$		
$T = ((\rho e_o)/\rho - \frac{u^2+v^2}{2})/C_v$		
$P = \rho RT$	$\rho = P/RT$	
$h_o = (\rho e_o)/\rho + RT$		

Table 1 (cont.)

MOMENTUM (INVISCID)

$$\frac{\partial}{\partial t}(\rho \underline{u}) + \nabla \cdot (\rho \underline{u})\ \underline{u} = -\nabla p \qquad (3)$$

USING EQ. 3

$$\delta(\rho u) = (-\oint (u(\rho \underline{u}) \cdot d\underline{A} + p\underline{i} \cdot d\underline{A}) * \delta t/Vol$$

$$\delta(\rho v) = (-\oint (v(\rho \underline{u}) \cdot d\underline{A} + p\underline{i} \cdot d\underline{A}) * \delta t/Vol$$

$$(\rho u) = (\rho u) + \delta(\rho u)$$

$$(\rho v) = (\rho v) + \delta(\rho v)$$

$$u = (\rho u)/\rho$$

$$v = (\rho v)/\rho$$

USING EQ. 3

$$\delta(\rho u) = (-\oint (u(\rho \underline{u}) \cdot d\underline{A} + p\underline{i} \cdot d\underline{A}) * \delta t/Vol$$

$$\delta(\rho v) = (-\oint (v(\rho \underline{u}) \cdot d\underline{A} + p\underline{i} \cdot d\underline{A}) * \delta t/Vol$$

$$(\rho u) = (\rho u) + \delta(\rho u)$$

$$(\rho v) = (\rho v) + \delta(\rho v)$$

$$u = (\rho u)/\rho$$

$$v = (\rho v)/\rho$$

USING EQ. 3 - (u or v) TIMES EQ. 1

$$\rho \delta u = (-\oint (u(\rho \underline{u}) \cdot d\underline{A} + p\underline{i} \cdot d\underline{A}) + u \oint (\rho \underline{u}) \cdot dA)) * \delta t_m/Vol$$

$$\rho \delta v = (-\oint (v(\rho \underline{u}) \cdot d\underline{A} + p\underline{i} \cdot d\underline{A}) + v \oint (\rho \underline{u}) \cdot d\underline{A})) * \delta t_m/Vol$$

$$u = u + \delta u$$

$$v = v + \delta v$$

$$(\rho u) = \rho u$$

$$(\rho v) = \rho v$$

ENERGY

$$h_o = \text{constant}$$

$$T = (h_o - \frac{u^2+v^2}{2})/C_p$$

$$\rho = P/RT$$

and this is used to evaluate the density as

$$\rho_{i+1} = \frac{p^e_{i+1}}{RT_{i+1}} \quad . \tag{3}$$

This general form is a linear combination of a single-point interpolation, $P_{i+1} - P_i$, a 2-point interpolation, $P_{i+1} - P_{i-1}$, and a 3-point interpolation, $P_{i+1} - P_{i-2}$. The single-point interpolation, of course, really gives the correct perfect gas equation and involves no approximation.

The coefficients a_o, a_1, and a_2 are here taken to be constants or functions of Mach number. Combinations, including individual terms or pairs of terms, for which the sum of the coefficients

$$a_o + a_1 + a_2 = 1$$

are second order accurate, as shown in Appendix A, Part 2.

Correct Perfect Gas Equation ($a_o = 1$, $a_1 = 0$, $a_2 = 0$)

This scheme has the advantage that it involves no interpolation or approximation for the pressure. Experience has shown (see Part I) that it is stable for subsonic flow. But the stability analysis of Part 2 shows that for Mach numbers above about 1.2 this scheme becomes unstable. Thus it could not be used for the test cases of Denton's 1-D nozzle.

These observations about the use of the correct perfect gas equation are in agreement with Denton's findings for his scheme B [1]. In that method changes of density were sent to the upstream corners of the element, which is equivalent to our sending pressure changes upstream. The method "proved stable, without any correction factors or damping, at low Mach numbers but instability was found to develop at Mach numbers around unity and above."

2-Point Interpolation ($a_o = 0$, $a_1 = 1$, $a_2 = 0$)

The stability analysis of Part 2 shows the 2-point scheme to be stable for Mach numbers up to about 2.0. Use of a 2-point scheme or a 3-point scheme has been suggested by Denton in his recent ASME and AGARD Lecture Notes [4,5].

3-Point Interpolation ($a_o = 0$, $a_1 = 0$, $a_2 = 1$)

3-point schemes have been shown in Part 2 to be the most conservative (in terms of stability) of the schemes considered in this report. Perhaps for this reason, such a method is used to stabilize the current NASA version of the Denton code. Both 3-point and 2-point schemes provide second order accuracy for a continuously changing pressure; they give correct interpolated values for linear variations in pressure (assuming equally spaced grid points).

M&M Mach Number Dependent Interpolation

The advantages of the three schemes just considered are:

(1) the accuracy and stability of the perfect gas equation for subsonic flow;
(2) the stability of the 3-point interpolation at Mach numbers greater than 2.0;
(3) the stability and reduced smearing of properties of the 2-point interpolation at supersonic Mach numbers up to 2.0.

These advantages have been combined in a single Mach number dependent interpolation scheme in Part 2. In this method

$$\left.\begin{aligned} a_o &= \frac{0.8}{3}\left(\frac{4}{M^2} - 1\right) \quad ; \quad 0 \leq a_o \leq 1 \\ a_1 &= 1 - a_o \\ a_2 &= 0 \end{aligned}\right\} \quad M < 2.0 \qquad (4)$$

$$\left.\begin{aligned} a_o &= 0 \\ a_1 &= \frac{4}{M^2} \\ a_2 &= 1 - a_1 \end{aligned}\right\} \quad M \geq 2.0$$

The values of the three coefficients are shown graphically in Fig. 3. Note, once again, that the sum of the coefficients is equal to one for all Mach numbers, so that this scheme is also second order accurate. For the calculations presented here M was taken as the larger of M on the upstream side or downstream side of the control volume.

3.4 Computational Tests of Three Pressure Interpolation Schemes

Of the four schemes just considered, three are stable in the Mach number range 1.0 to 2.0. These are the 2-point, 3-point, and M&M interpolation methods. In this section, results of shock capturing with these three methods are presented and compared for Denton's 1-D nozzle.

Calculation Details

Number of Axial Grid Points = 46 , $\delta x = 1$
At inlet i = 1 , M = 0.80
For air k = 1.4 , R = 287. J/kg K
$P_{exit}/P_{t\ inlet}$ = 0.85 , 0.80 , 0.75

Figures

The variations of static pressure, Mach number, and total pressure are plotted for each interpolation scheme using the same scales as for the theoretical solutions, Fig. 2. Fig. 4 shows the results for the 3-

C-2

point scheme, Fig. 5 for the 2-point scheme, and Fig. 6 for the M&M method. The results from the 3-point and M&M schemes are shown together with the theoretical solution on Fig. 7 for the pressure ratio of 0.80.

Table

The calculated values of maximum Mach number upstream of the shock and total pressure ratio are compared with the values from the theoretical 1-D solutions in Table 2.

Shock Losses

The total pressure ratios across the shocks are well calculated by all three interpolation formulae as shown in Table 2b. This is in spite of the fact that the calculated values for the maximum Mach numbers upstream of the shocks are significantly different from the theoretical values. For example, at the lowest back pressure, the theoretical Mach number upstream of the shock is 1.578 while the 3-point interpolation formula gives 1.502, the 2-point formula gives 1.528, and the M&M formula gives 1.534. For this case the calculated values of total pressure ratio are all in the range 0.9027 to 0.9028, compared with the theoretical value of 0.9032. In general the M&M formula gives the closest agreement with the upstream Mach number while the 3-point formula gives the worst results. Based on the maximum calculated upstream Mach number for these cases, the M&M formula would give shock losses from 16 to 42 percent too small, while the 3-point formula would give values from 27 to 62 percent too small. Interestingly the agreement for shock losses based on maximum upstream Mach number improves (for all three formulae) as the Mach number increases. However, these results show that peak calculated Mach number should not be used to predict shock losses and that the calculated total pressure loss across the shock is accurate to better than 0.1% and it should be used.

Smoothing Upstream of Shock

The results in Figs. 4, 5, and 6 show that the interpolation formulae all act to smooth properties upstream of the shocks. The smoothing is most noticeable in the static pressure and Mach number distributions, especially with the 3-point interpolation scheme. The 2-point scheme gives less smoothing while the M&M formula gives the sharpest and most accurate upstream distributions.

Overshoots and Undershoots Downstream of Shock

Both the 3-point and 2-point interpolation schemes give overshoots in static pressure and undershoots in Mach number downstream of the shocks. Only the M&M interpolation formula shows no noticeable overshoots and undershoots and this is because it has a better formulation for subsonic flow; in fact, from Eq. 4, it can be seen that the M&M formula reduces to the correct perfect gas equation for Mach numbers less than 0.918.

Table 2. Results of Calculations for Denton's 1-D Nozzle.

Table 2a: Maximum Mach number upstream of shock

$\frac{P_{exit}}{P_{t\ inlet}}$	Interpolation Formula			
	Theoretical	3-Point	2-Point	Mach Number Dependent
0.85	1.267	1.173	1.193	1.216
0.80	1.455	1.375	1.395	1.408
0.75	1.578	1.502	1.528	1.534

Table 2b: Total pressure ratio, $P_{t\ exit}/P_{t\ inlet}$

$\frac{P_{exit}}{P_{t\ inlet}}$	Interpolation Formula			
	Theoretical	3-Point	2-Point	Mach Number Dependent
0.85	0.9847	0.98487	0.98492	0.98494
0.80	0.9433	0.94331	0.94335	0.94338
0.75	0.9032	0.90271	0.90277	0.90281

Shock Location

The M&M formula captures the shocks over about four grid points centered around the theoretical shock locations. This is seen for the pressure ratio of 0.8 in Fig. 7. In contrast, Fig. 7 shows the 3-point scheme smearing the shock over about ten grid points with the shock displaced slightly downstream due to inadequate resolution of the subsonic flow. Once again the 2-point scheme gives results intermediate between those of the M&M and 3-point schemes.

3.5 Conclusions - Progress in Shock Capturing

Significant improvements have been made in the finite-volume time-marching method to allow more accurate calculations of the distributions of flow properties through shocks. In Part 1, the Effective Density Method was introduced to reduce undershoots and overshoots in total pressure in the region of the shock. A stability analysis in Part 2 was then used to develop a Mach number dependent interpolation scheme for pressure which combines the advantages of the correct perfect gas equation for subsonic flow with the stability of 2-point and 3-point interpolation schemes for supersonic flow. The M&M interpolation formula, representing this new scheme, when used in the Effective Density Method, further removes the overshoot in static pressure in the subsonic flow downstream of a shock.

References

1. Denton, J. D., "An Improved Time Marching Method for Turbomachinery Calculations," ASME Paper 82-GT-239.

2. Nicholson, S., "Development of a Finite Volume Time Marching Method," VPI&SU Turbomachinery Research Group Report No. JM/85-3, February 1985.

3. Nicholson, S., and J. Moore, "Extension of a Finite Volume Explicit Time Marching Method to Laminar and Turbulent Flow," VPI&SU Turbomachinery Research Group Report No. JM/85-6, June 1985.

4. Denton, J. D., "A Method of Calculating Fully Three Dimensional Inviscid Flow through Any Type of Turbomachine Blade Row," Lecture Notes for ASME Short Course on 3-D Flows in Turbomachinery Blade Rows, Phoenix, AZ, March 1983.

5. Denton, J. D., "The Calculation of Fully Three Dimensional Flow through Any Type of Turbomachine Blade Row," Lecture Notes for ASME Short Course on 3-D Flows in Turbomachinery Blade Rows, Houston, TX, March 1985, and AGARD Lecture Series No. 140 on 3-D Computation Techniques Applied to Internal Flows in Propulsion Systems, Rome, Italy, Cologne, West Germany, and Paris, France, June 1985.

DENTON 1D EXAMPLE 12/85

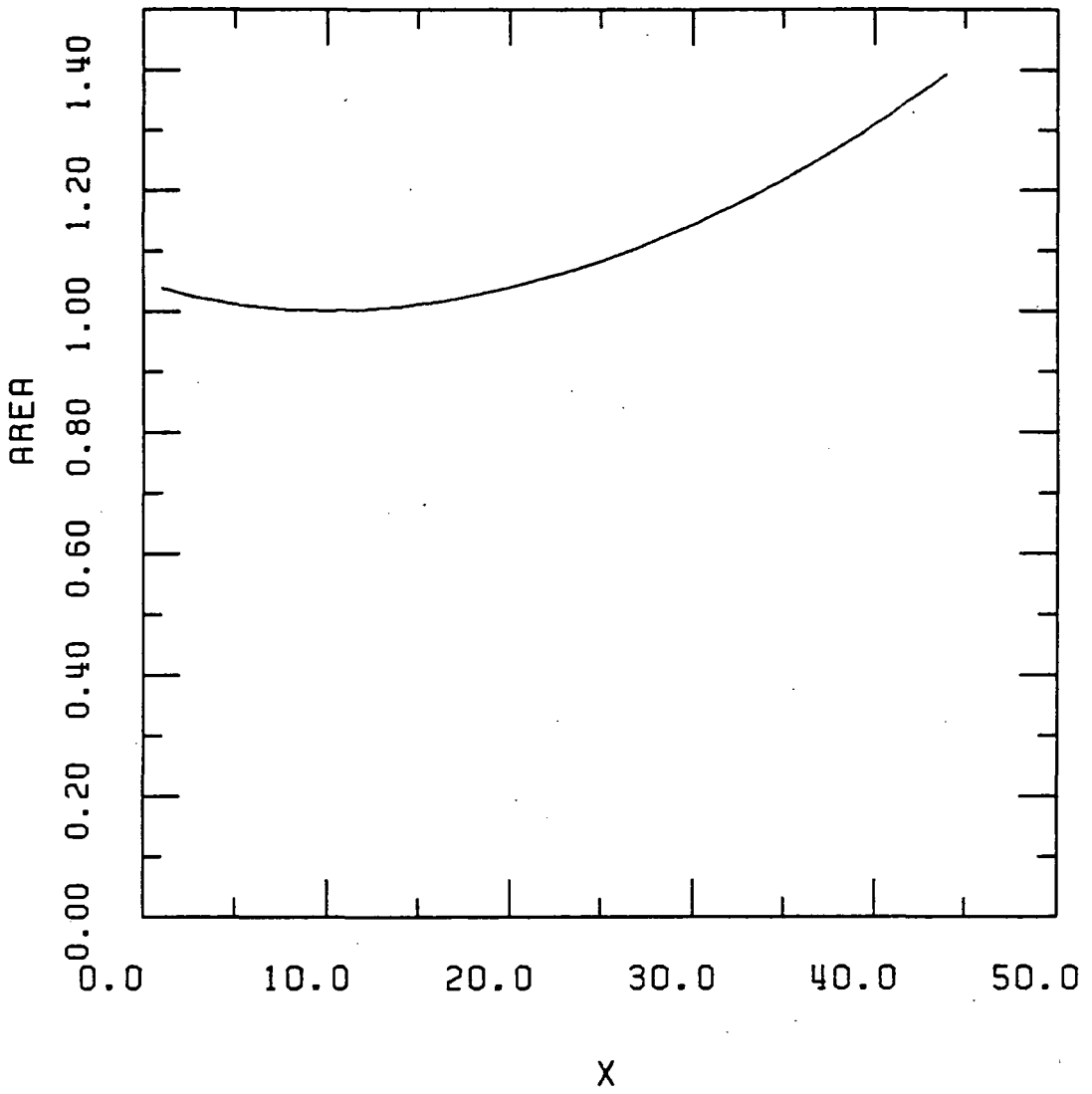

Fig. 1 Denton's convergent-divergent nozzle with a linear variation of Mach number with distance for 1-D isentropic flow, $x = 10. + 45.(M - 1.)$.

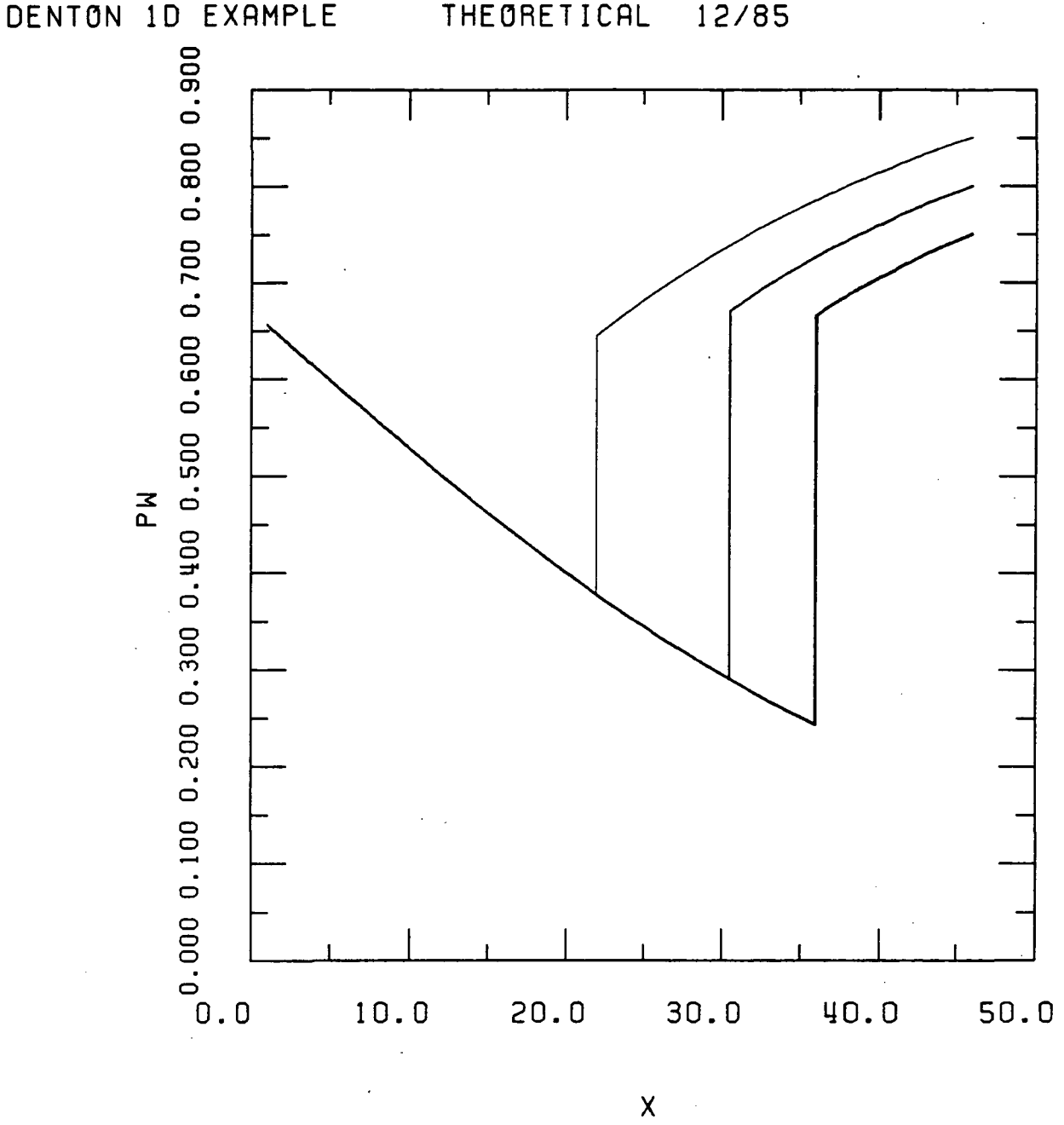

Fig. 2 Theoretical 1-D solutions for Denton's nozzle for three exit static pressures at x = 46., $P_{exit}/P_{t,inlet}$ = 0.85, 0.80, and 0.75.

Fig. 2a $PW = P/P_{t,inlet}$.

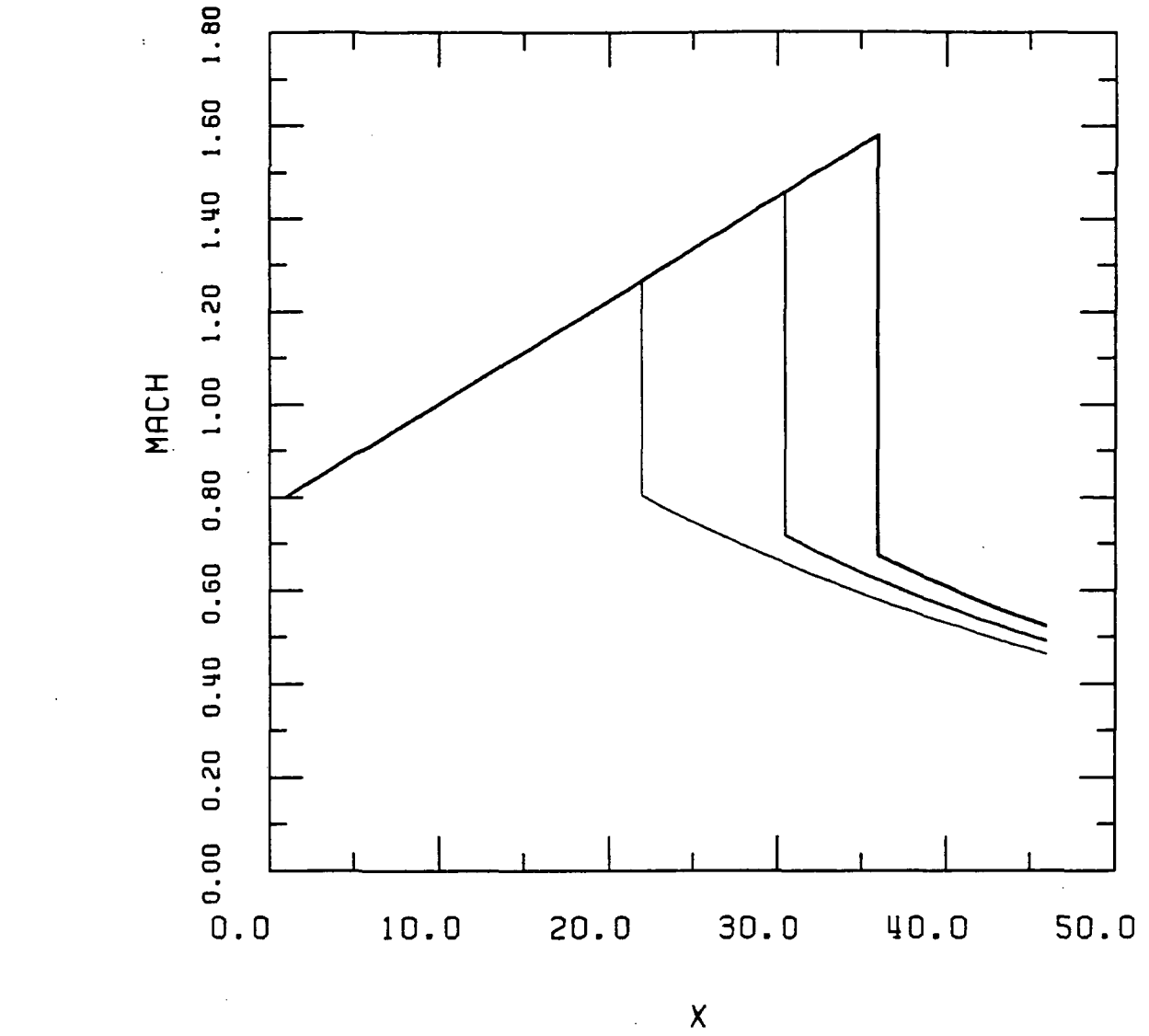

Fig. 2b Mach number.

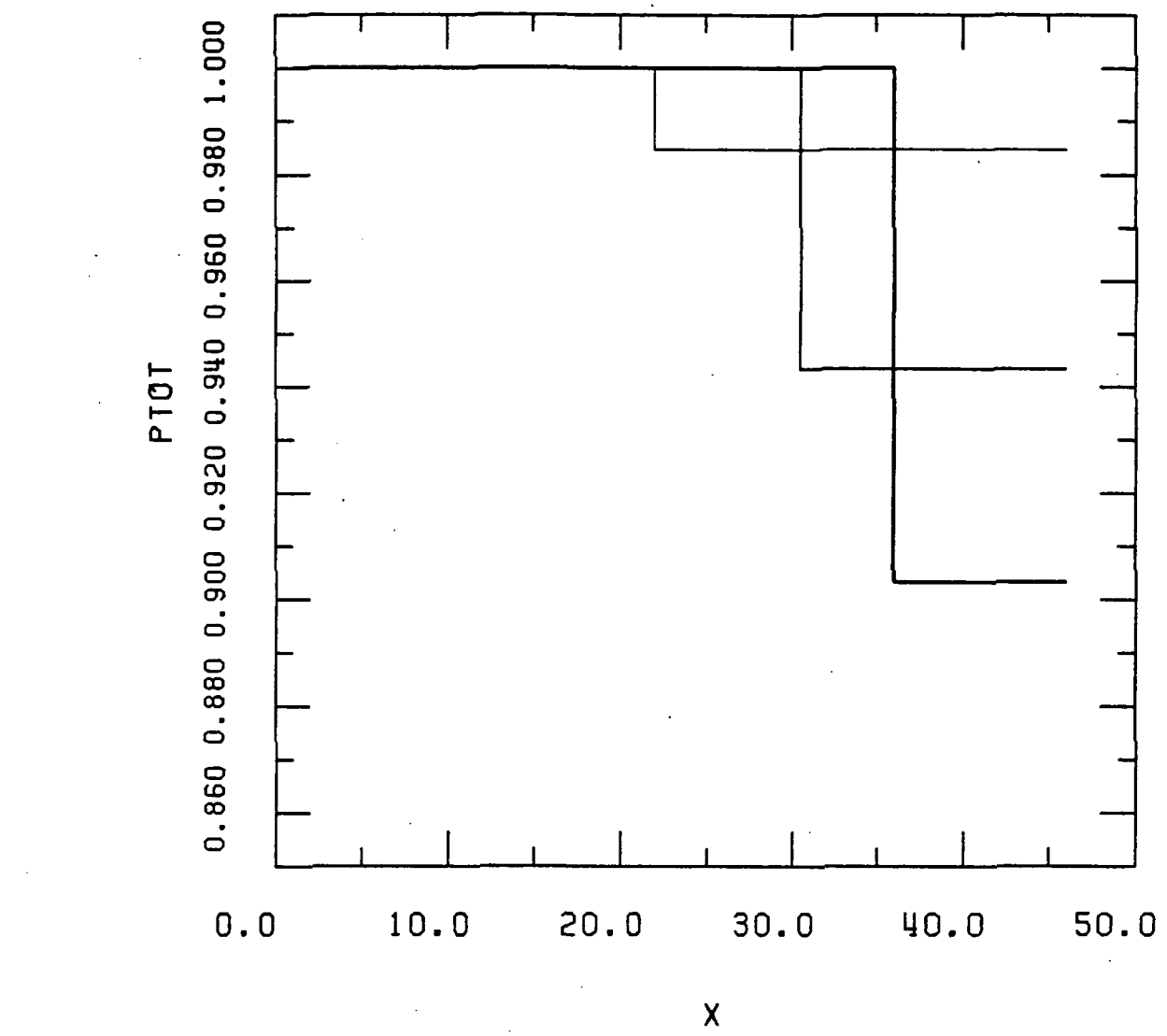

Fig. 2c PTOT = $P_t/P_{t,inlet}$.

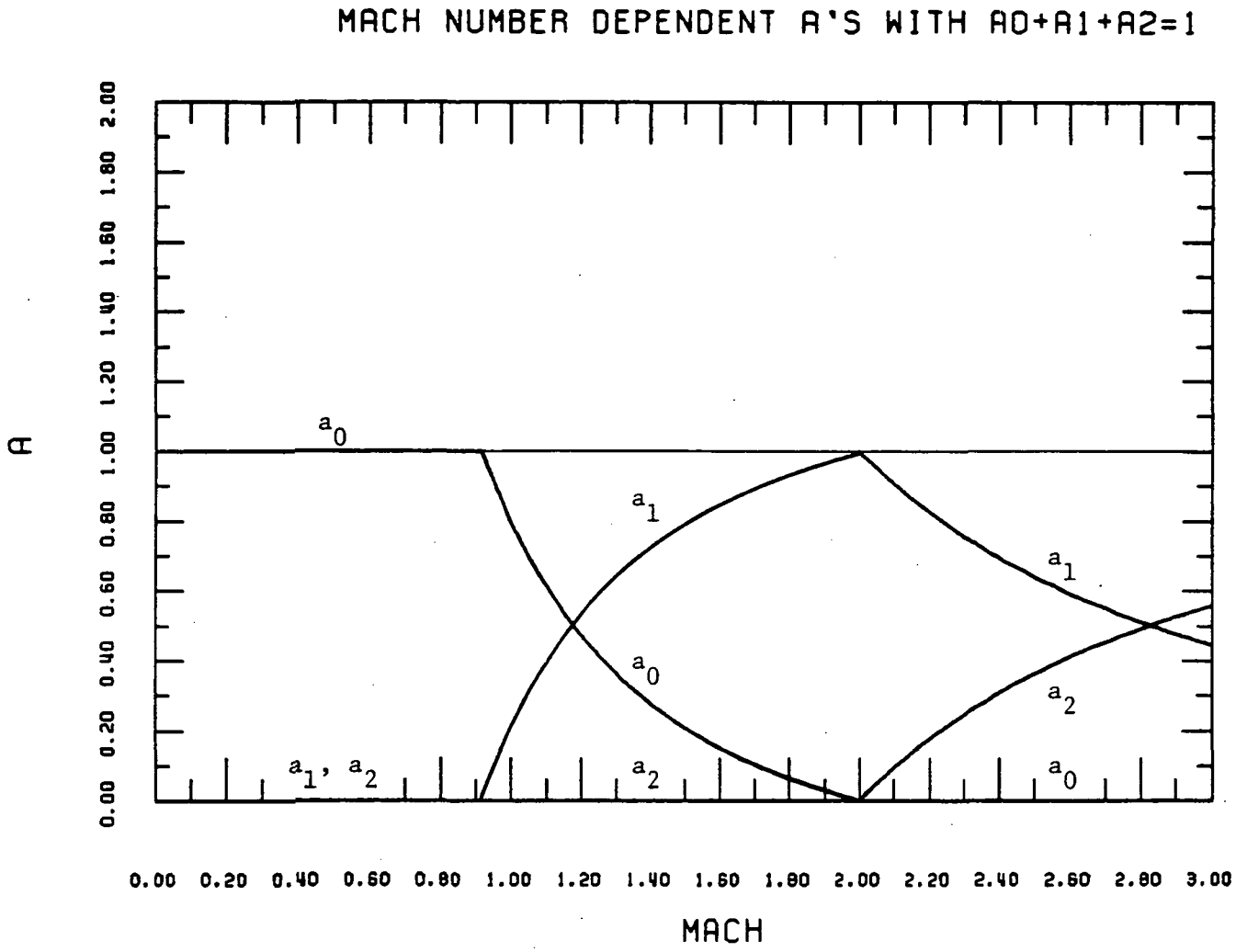

Fig. 3 M & M Mach number dependent values (Eq. 4) for the coefficients in Eq. 2.

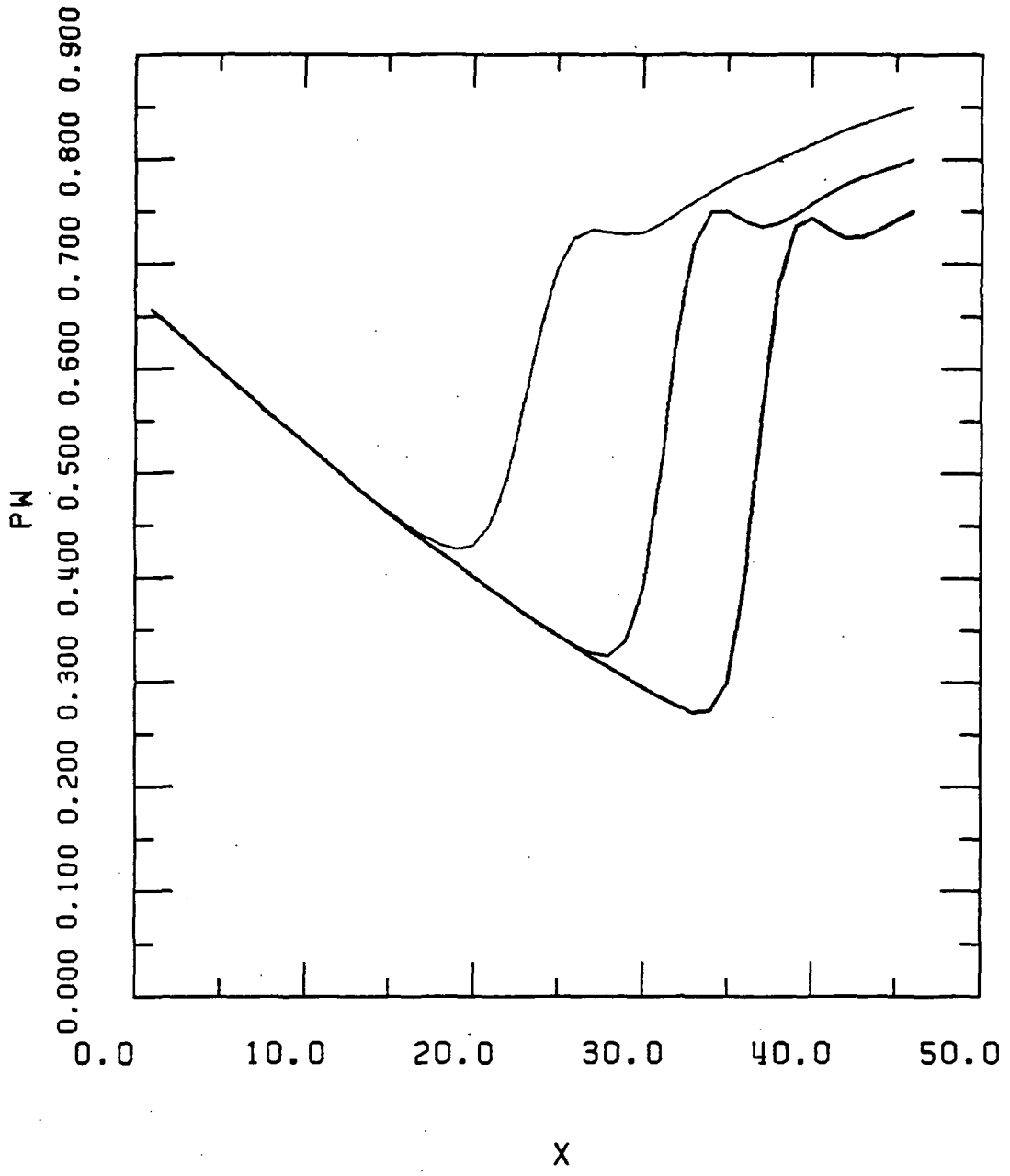

Fig. 4 Calculated 1-D solution for Denton's nozzle using 3-point interpolation, Eq. 2 with $a_0 = a_1 = 0$ and $a_2 = 1$.

Calculations for three exit static pressures at x = 46., $P_{exit}/P_{t,inlet}$ = 0.85, 0.80, and 0.75.

Fig. 4a $PW = P/P_{t,inlet}$.

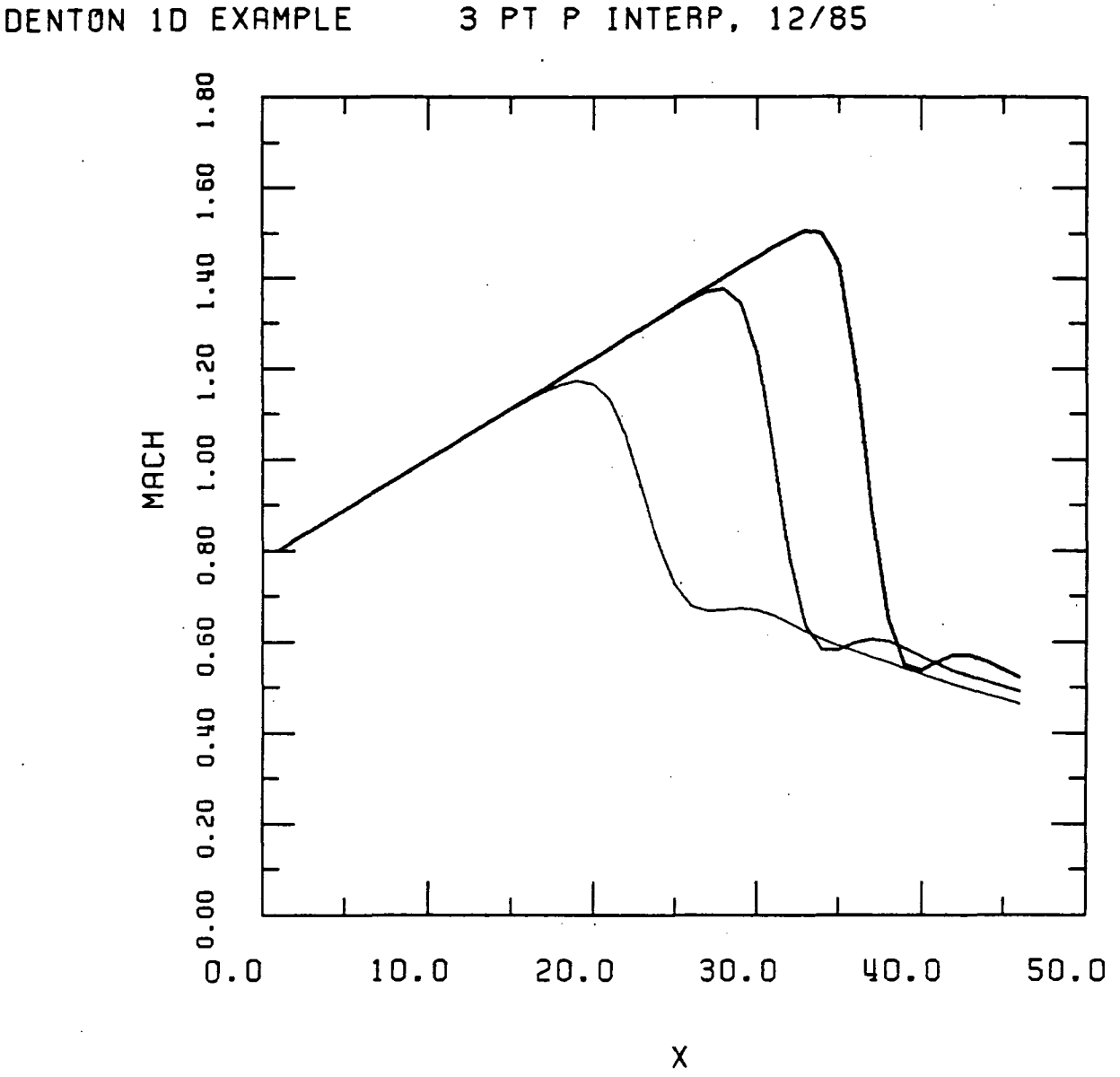

Fig. 4b Mach number.

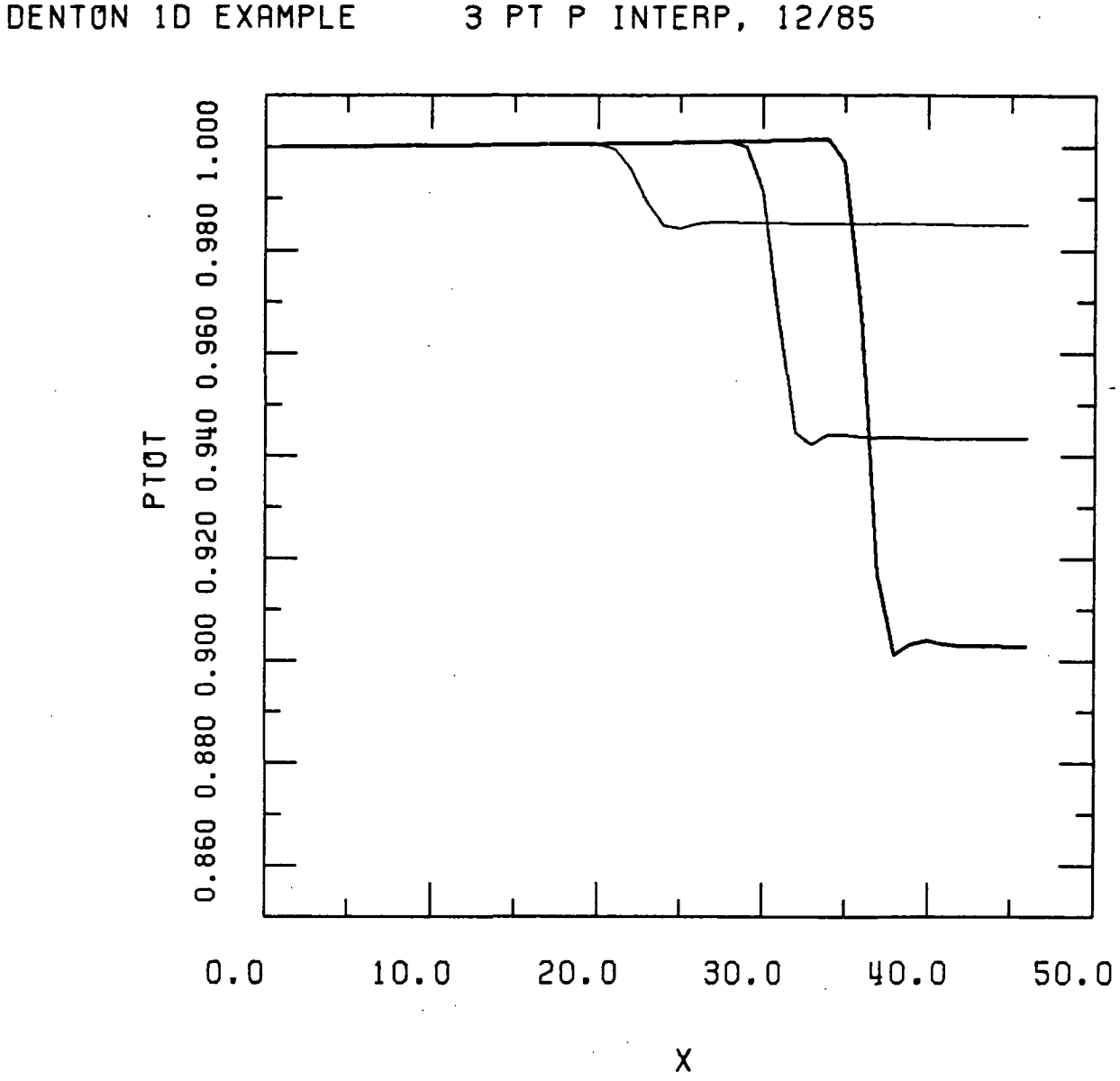

Fig. 4c PTOT = $P_t/P_{t,inlet}$.

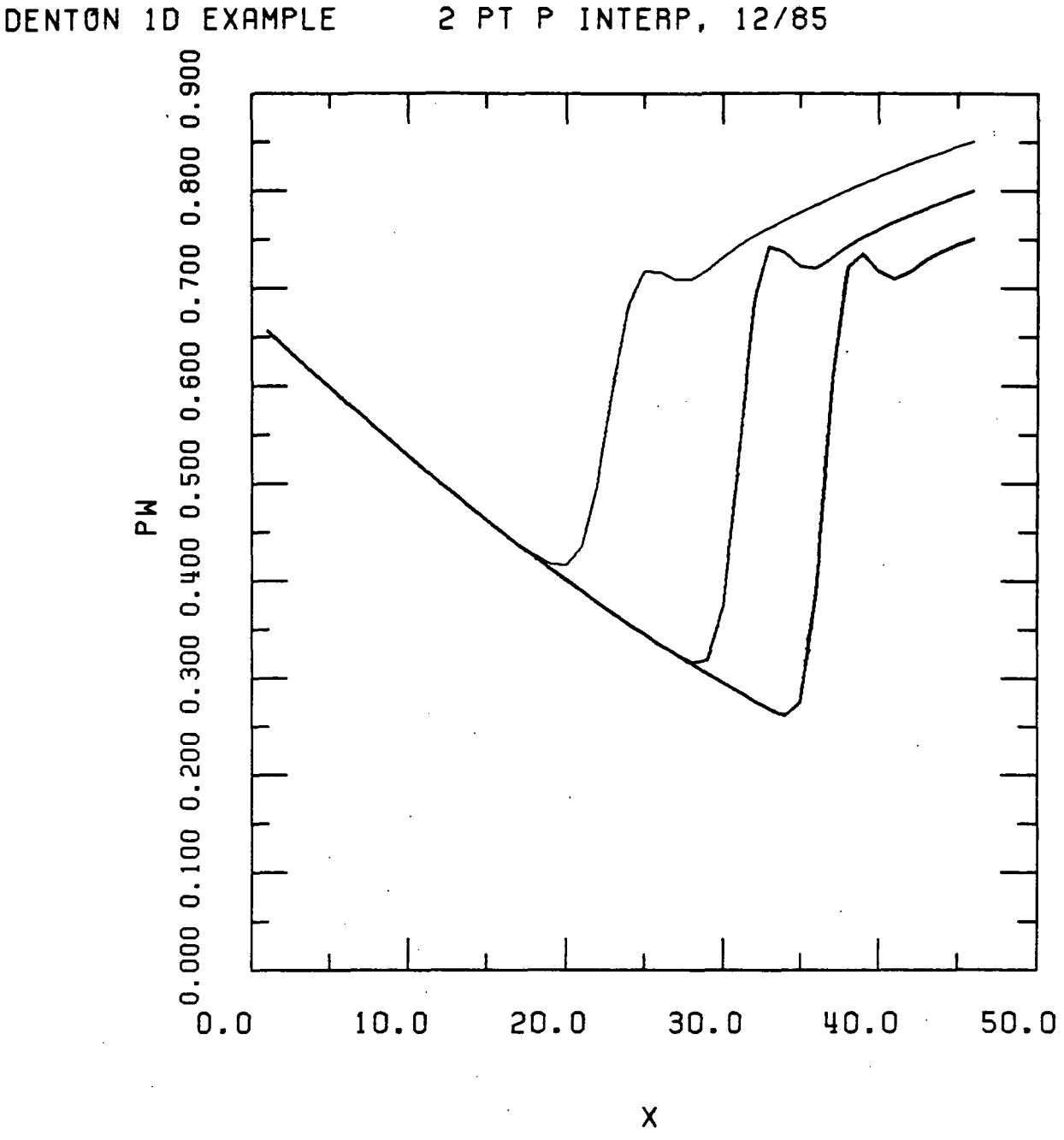

Fig. 5 Calculated 1-D solution for Denton's nozzle using 2-point interpolation, Eq. 2 with $a_0 = a_2 = 0$ and $a_1 = 1$.
Calculations for three exit static pressures at x = 46., $P_{exit}/P_{t,inlet}$ = 0.85, 0.80, and 0.75.

Fig. 5a $PW = P/P_{t,inlet}$.

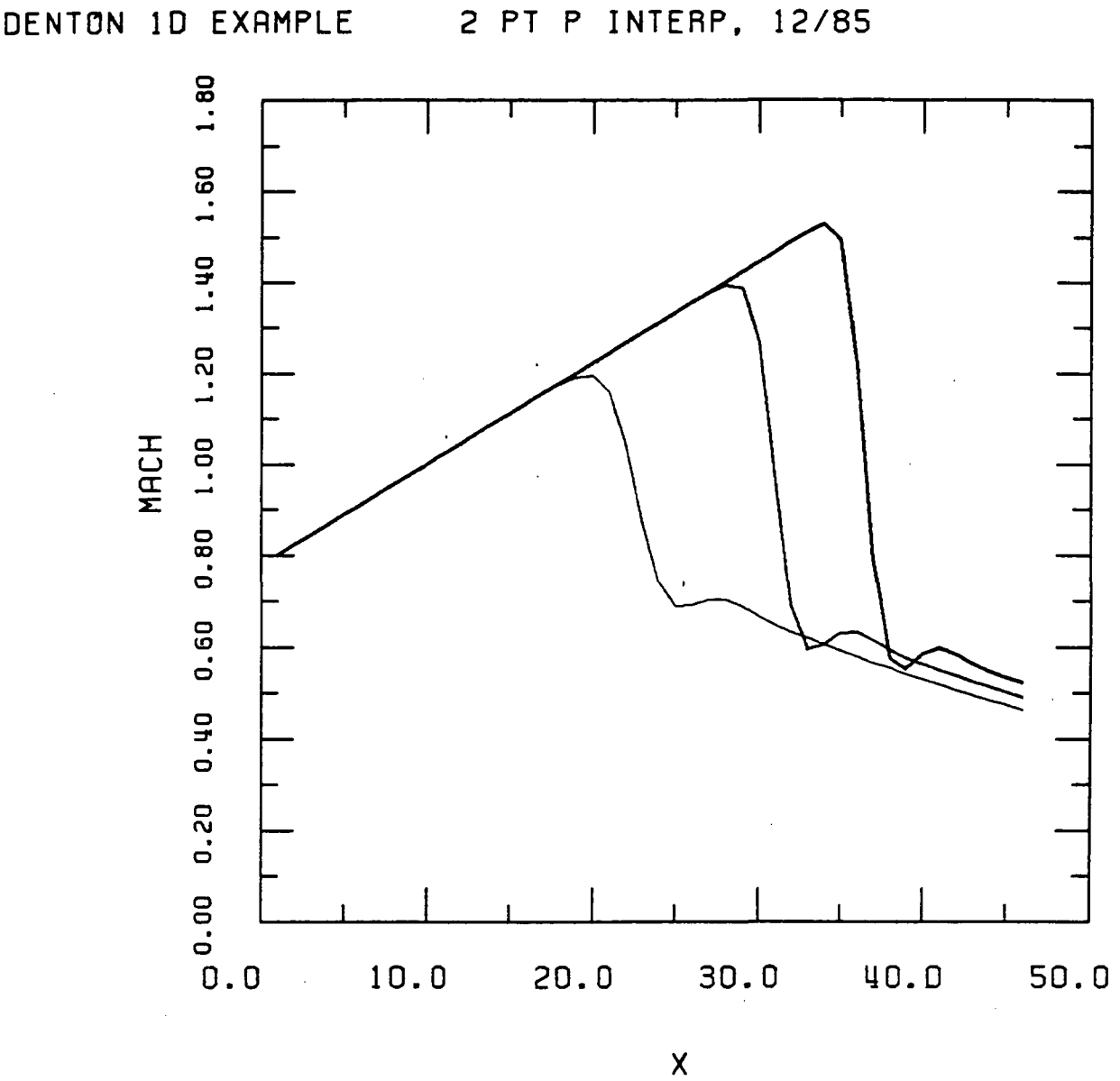

Fig. 5b Mach number.

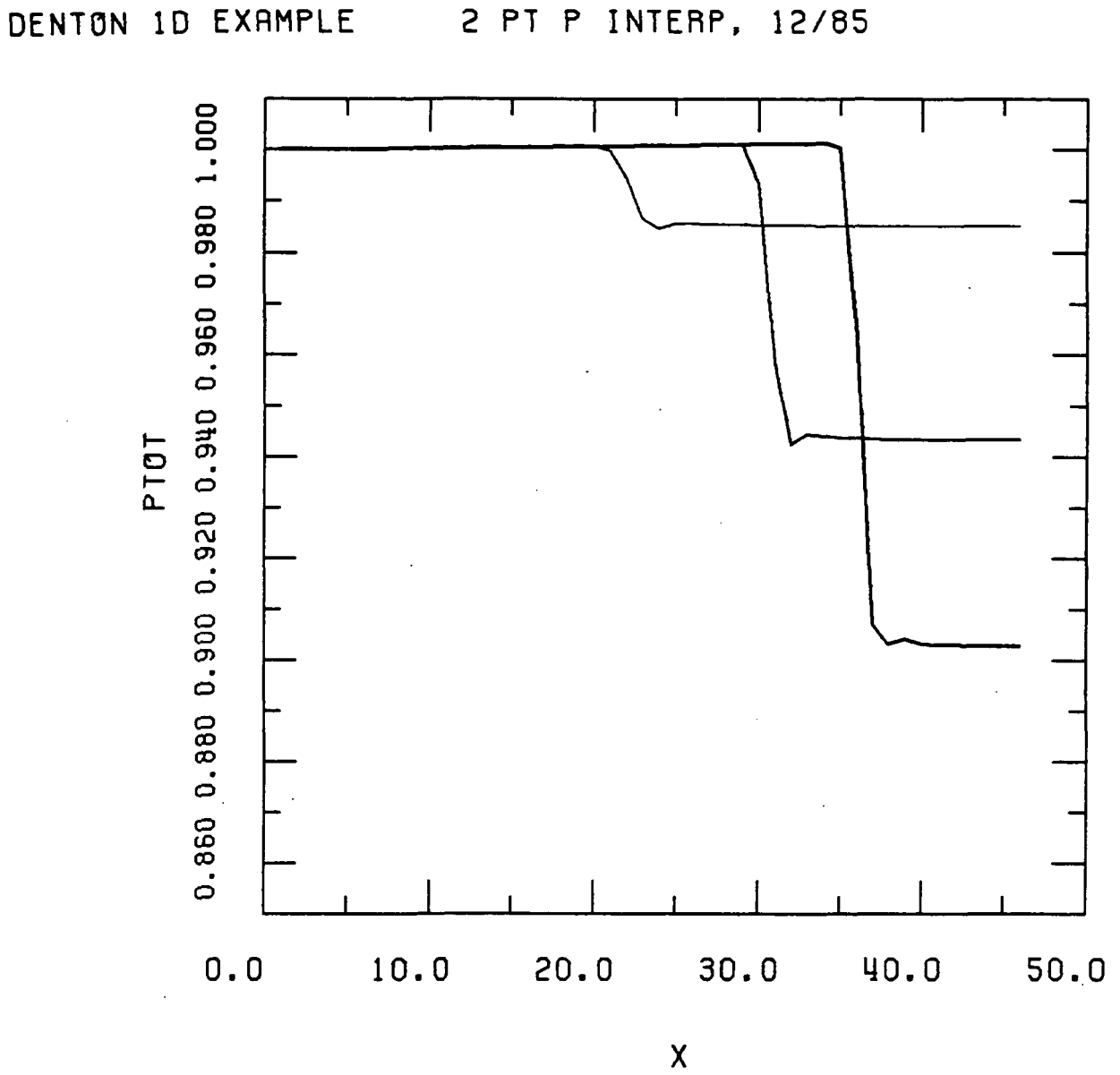

Fig. 5c PTOT = $P_t/P_{t,inlet}$.

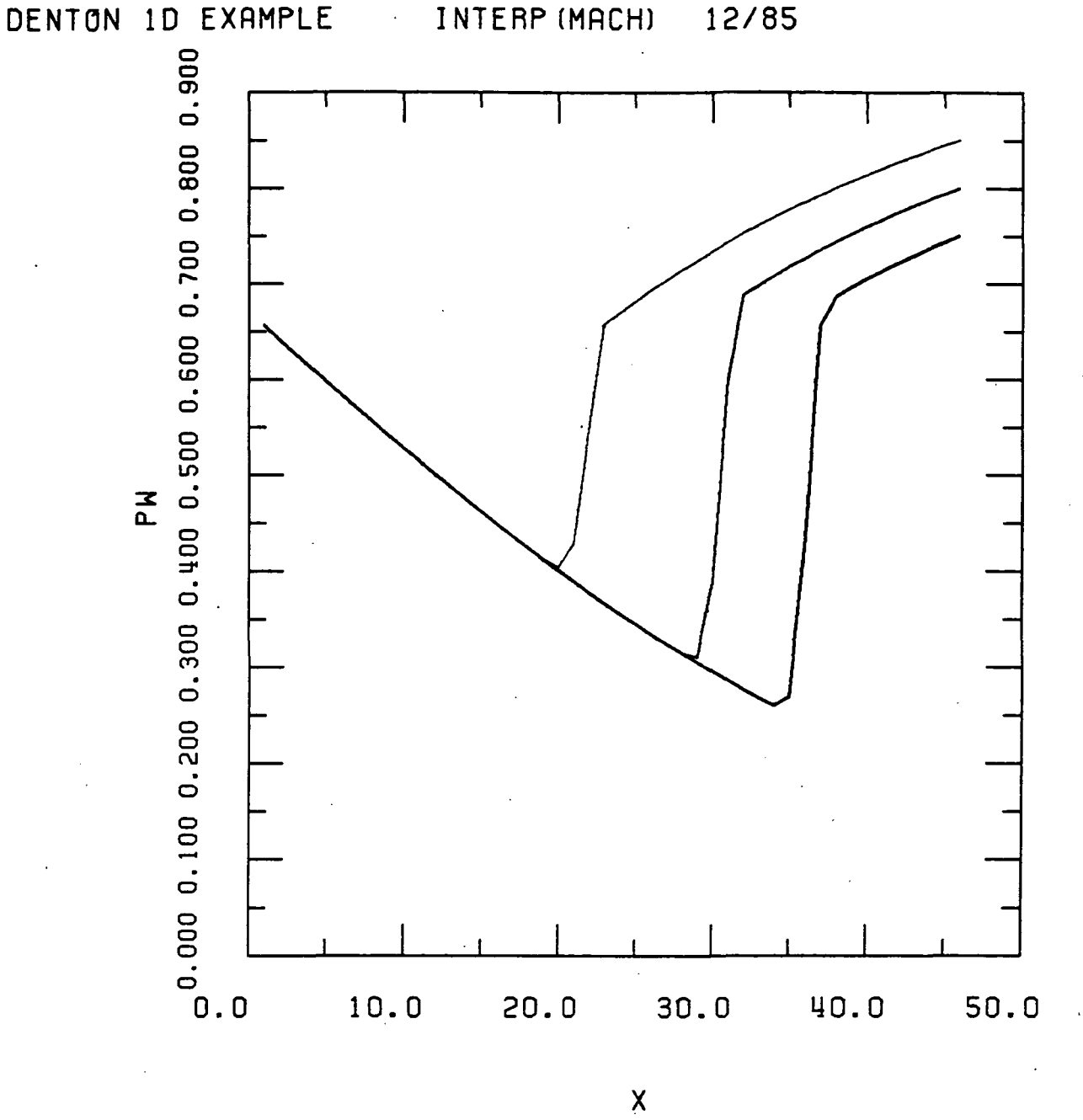

Fig. 6 Calculated 1-D solution for Denton's nozzle using M & M formula, Eq. 4.
Calculations for three exit static pressures at x = 46., $P_{exit}/P_{t,inlet}$ = 0.85, 0.80, and 0.75.

Fig. 6a $PW = P/P_{t,inlet}$.

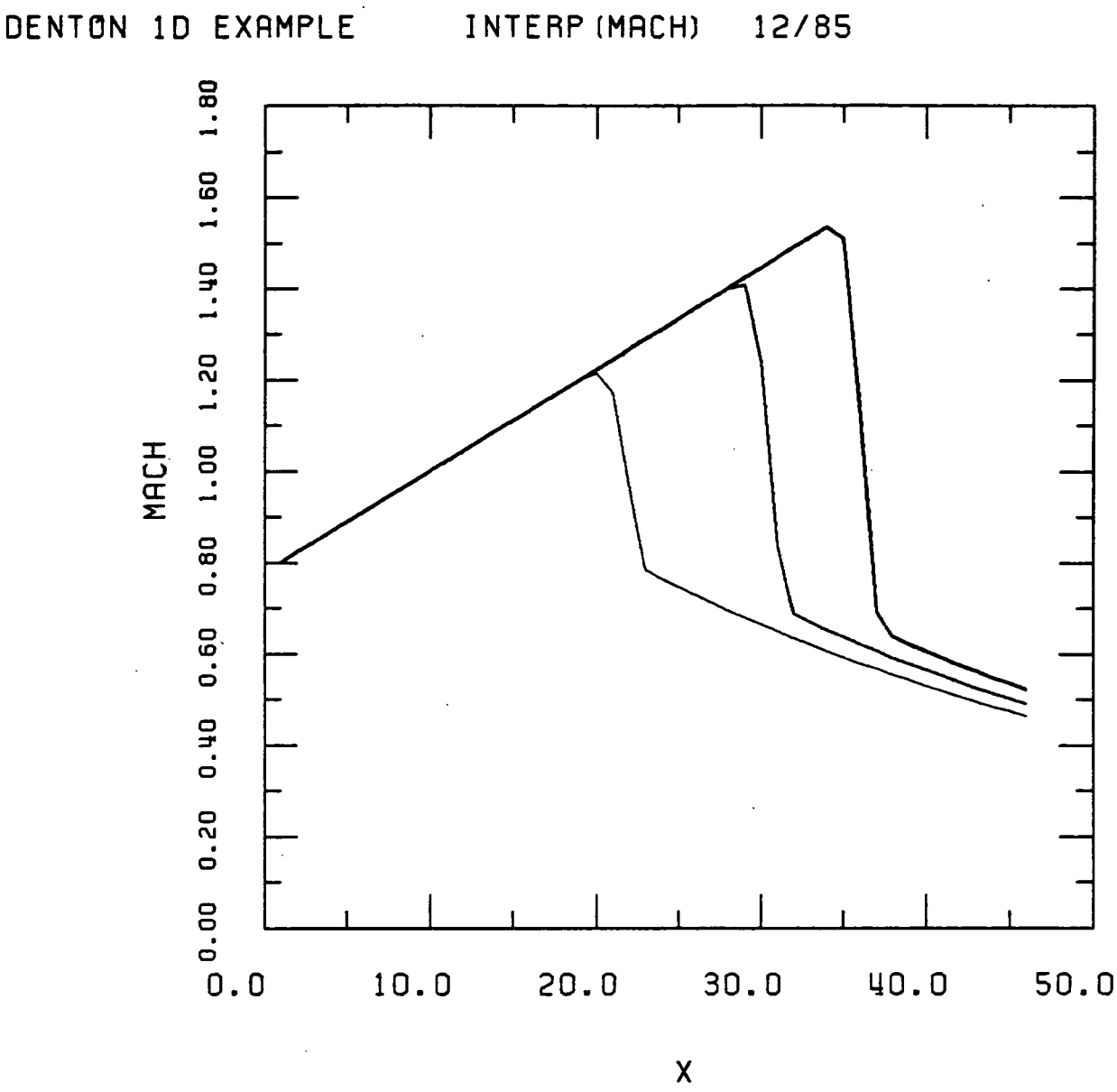

Fig. 6b Mach number.

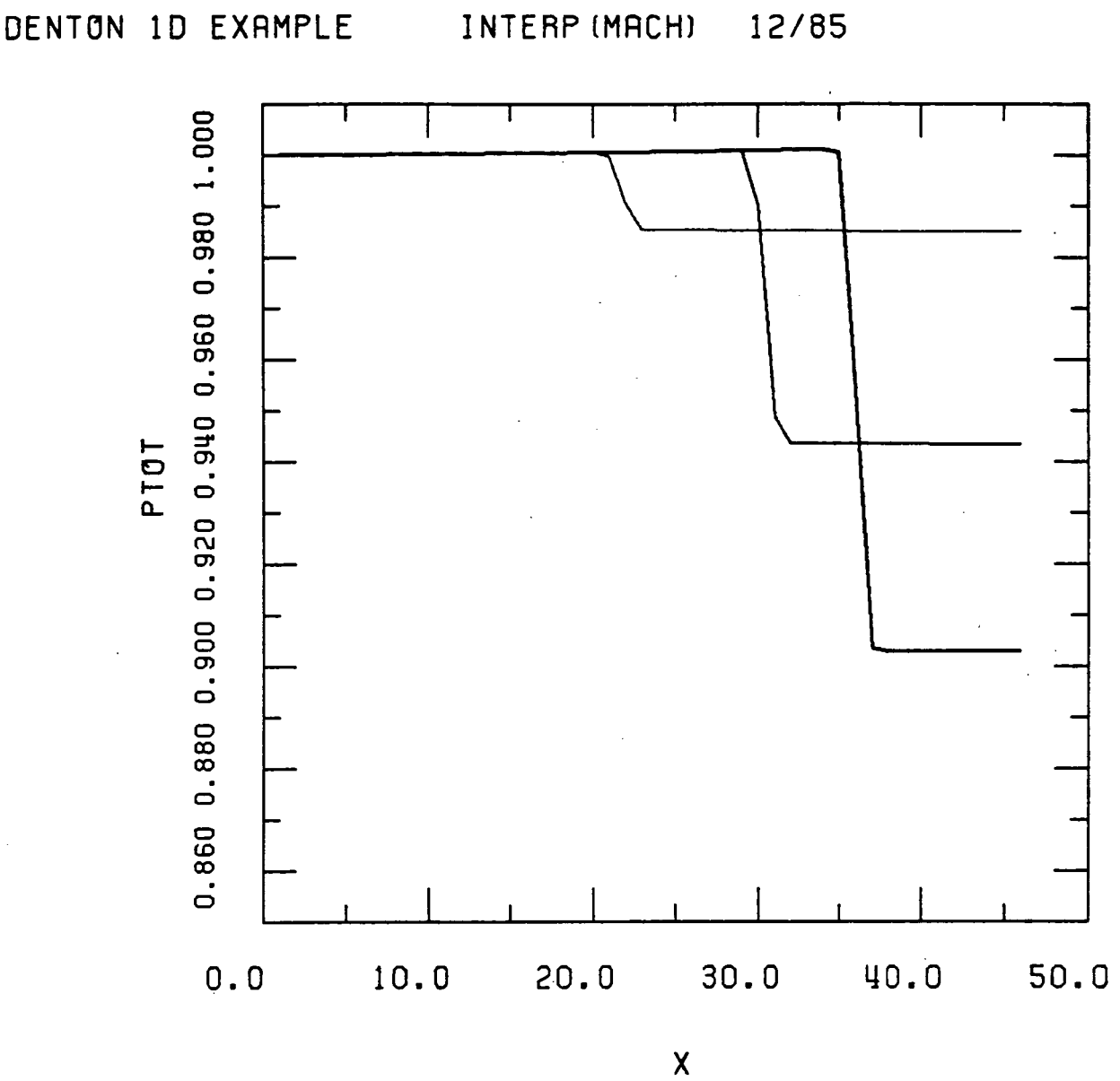

Fig. 6c PTOT = $P_t/P_{t,inlet}$.

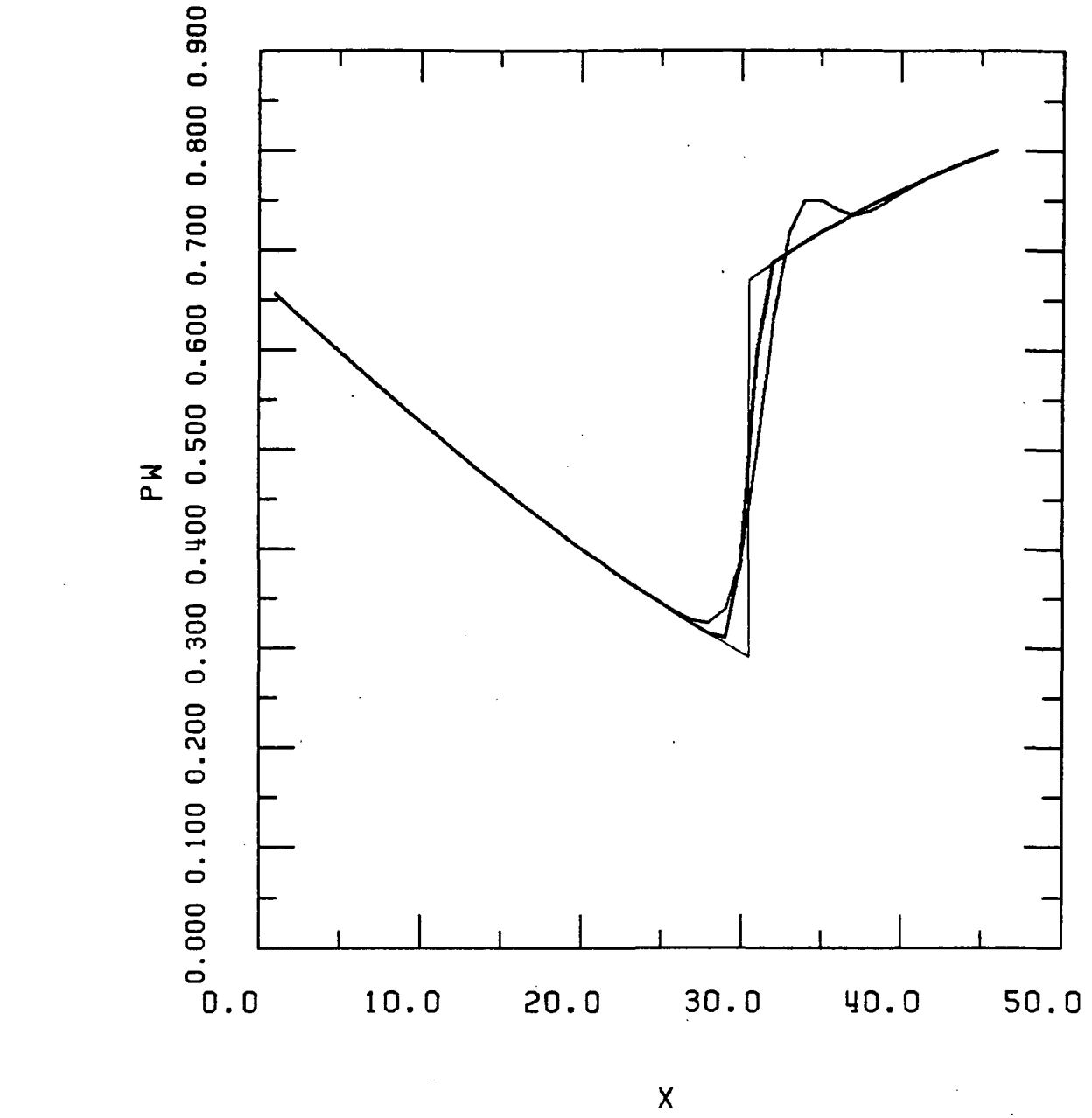

Fig. 7 Comparison of calculated results with the theoretical 1-D solution for $P_{exit}/P_{t,inlet} = 0.80$.

Thin line - theoretical solution:

Medium line - calculated using 3-point interpolation:

Thick line - calculated using M & M formula.

Fig. 7a $PW = P/P_{t,inlet}$.

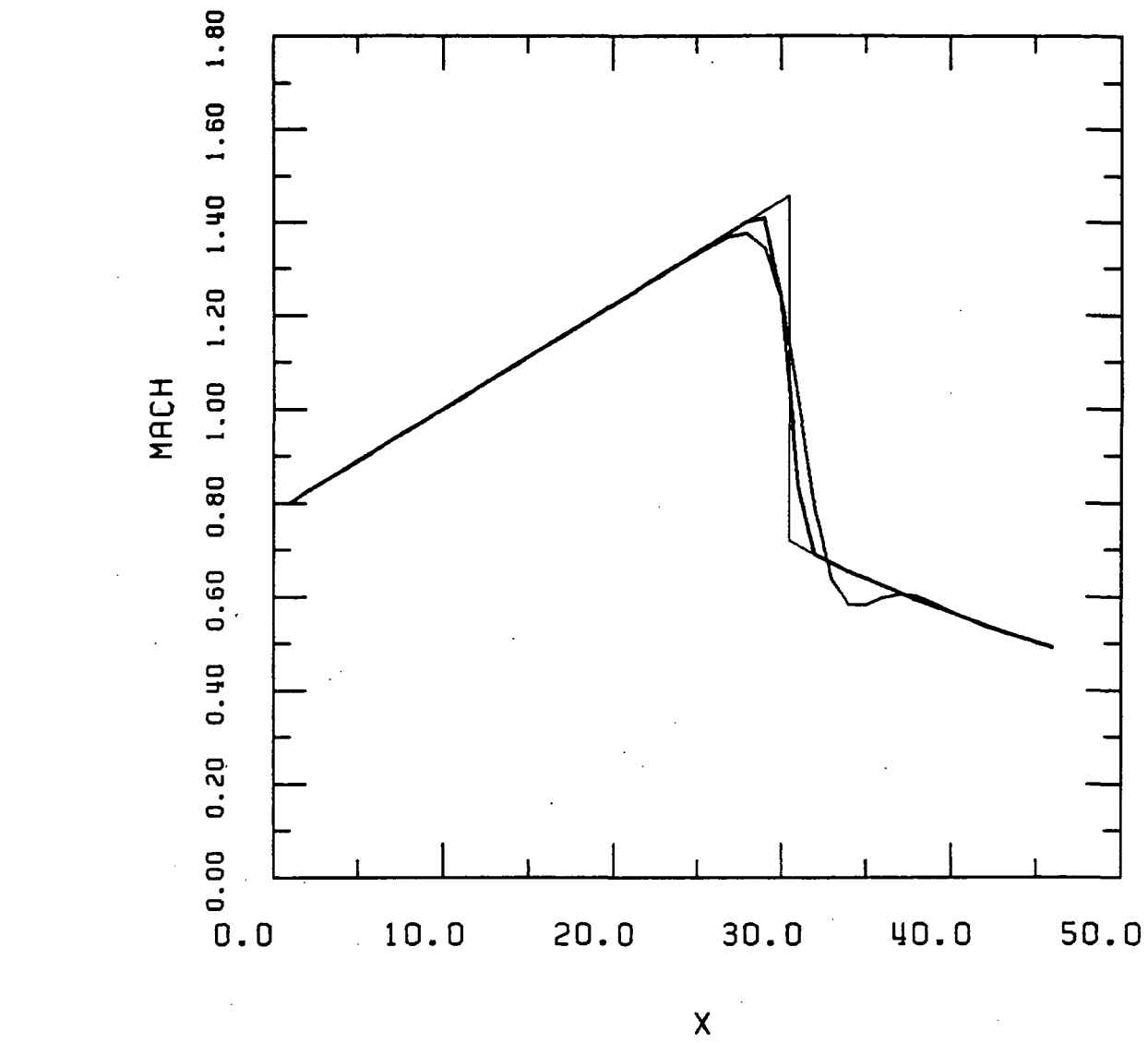

Fig. 7b Mach number.

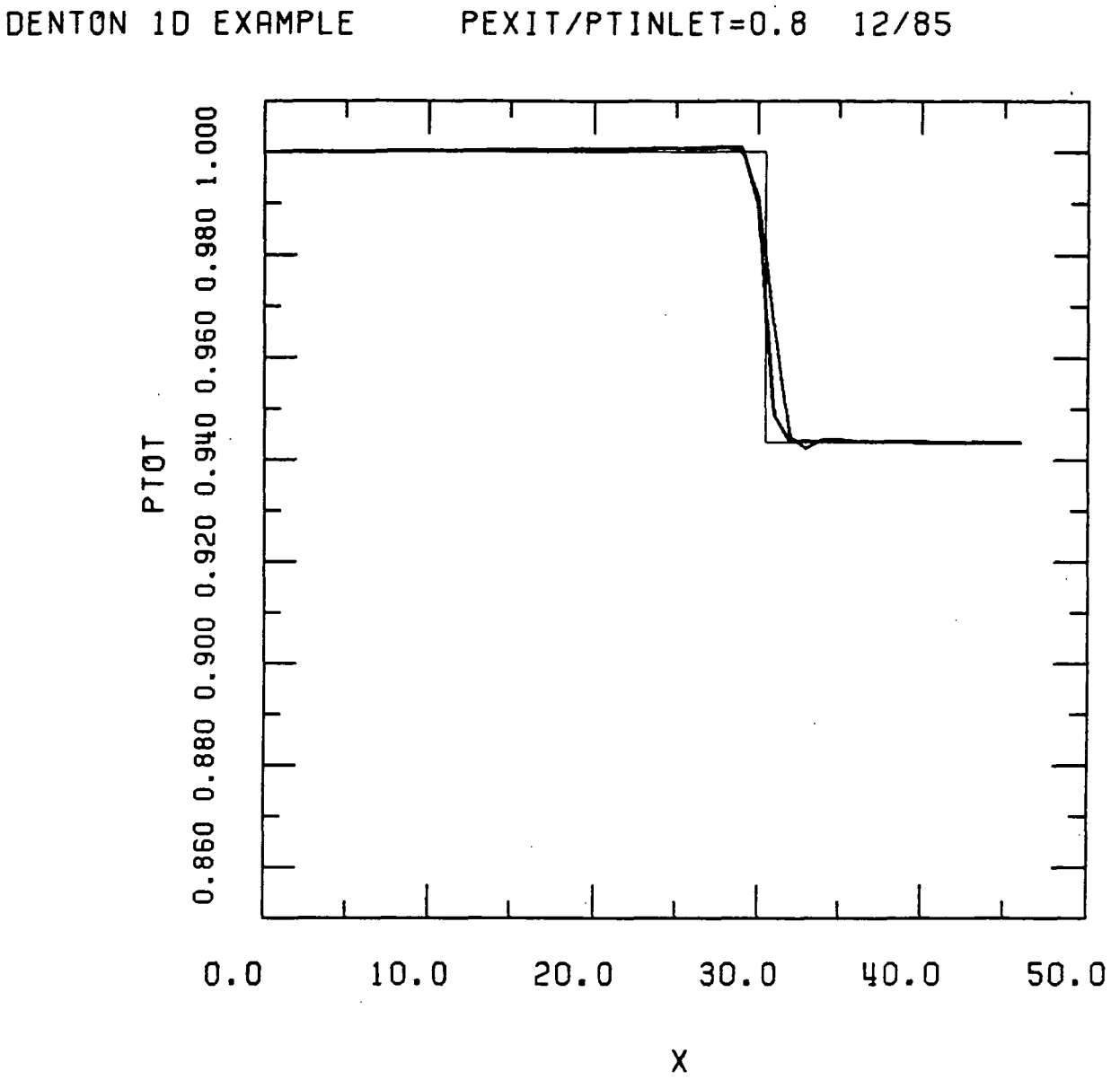

Fig. 7c PTOT = $P_t/P_{t,inlet}$.